UNIVERSITY OF CALIFORNIA
Santa Barbara

The role of fluctuating food supply on recruitment, survival and population dynamics in the sea

A Dissertation submitted in partial satisfaction
of the requirements for the degree of

Doctor of Philosophy

in

Ecology, Evolution and Marine Biology

by

Daniel Kenji Okamoto

Committee in Charge:

Professor Sally J. Holbrook, Chair

Dr Daniel C. Reed

Professor Russell J. Schmitt

Professor Cherie J. Briggs

December 2014

The Dissertation of
Daniel Kenji Okamoto is approved:

_____

Dr Daniel C. Reed

_____

Professor Russell J. Schmitt

_____

Professor Cherie J. Briggs

_____

Professor Sally J. Holbrook, Committee Chair

September 2014

for Christian

& A.E. Taylor

Acknowledgements

Throughout my tenure at this University, I've had the blessing of a committee invested in and dedicated to my success. Watching friends and colleagues float in the wake of advisors' absentia always made me appreciate my own mentors. Dan Reed, Sally Holbrook, and Russ Schmitt let me follow my own curiosity and pursuits, and provided direction, time, criticism (and data) to keep me focused and productive. Cherie Briggs too provided critical and and remarkable discussions that led to moments of redirection in my research.

Many groups financially supported my research and graduate career. Foremost among these was the National Science Foundation in support of the Santa Barbara Coastal Long Term Ecological Research (LTER) site. The Department of Ecology, Evolution and Marine Biology provided several quarters of support. The Worster award, UC Affiliates Nancy Brown Graduate Dissertation Fellowship, UCSB Graduate Division Dissertation Fellowship and the Charles A. Storke Award also provided funding that was essential in completing this work.

The community at UCSB should consider themselves lucky to have the indispensable team of Clint Nelson and Shannon Harrer. The research of graduate students and many faculty would sink without their contributions. Steve Schroeter is an essential collaborator for my fourth chapter, with whom I look forward to our ongoing collaborations. I also must thank all those countless others with whom I shared days on boats, hours

Daniel Kenji Okamoto

Ecology, Evolution and Marine Biology
University of California, Santa Barbara
okamoto@lifesci.ucsb.edu

Research Interests

Quantitative population dynamics of marine fish, invertebrates and algae; kelp forest & benthic marine community ecology; reproductive ecology; statistical ecology, ecological time series analysis

Education

Fall - 2014	PhD:	UC Santa Barbara - Ecology, Evolution & Marine Biology
2009	MS:	University of Alaska Fairbanks - School of Fisheries and Ocean Sciences
2005	BS:	University of Washington - Biology/Aquatic and Fishery Sciences

Peer Reviewed Publications:

Okamoto, DK, GL Eckert & MS Stekoll. 2013. Recruitment inhibition and coexistence between subtidal algal crusts and kelps. Marine Ecology-Progress Series. 493:103-112

Okamoto, DK, RJ Schmitt, SJ Holbrook, & DC Reed. 2012. Fluctuations in food supply drive recruitment dynamics in a marine fish. Proceedings of the Royal Society B: Biological Sciences: 279: 4542-4550

Britton-Simmons, KH, B Pister, I Sánchez, **DK Okamoto**. 2011. Response of a native, herbivorous snail to the introduced seaweed *Sargassum muticum*. Hydrobiologia. 66: 187-196

Britton-Simmons, KH, GR Foley, **DK Okamoto**. 2009. Spatial subsidy in the subtidal zone: utilization of drift algae by a deep subtidal sea urchin. Aquatic Biology. 5: 233-243

Quantitative Graduate Level Coursework:

UCSB: Dept of Stats & Appl Probability
Bootstrap and Resampling Methodology
Time Series Analysis
Bayesian Inference
Linear and Nonlinear Mixed Effects Models
Advanced Statistical Methods

UAF: School of Fisheries & Ocean Sciences
Quantitative Fisheries Population Dynamics
Bioeconomic Modeling
Bayesian Decision Theory
Natural Resource Modeling
Modern Applied Statistics

Regression & ANOVA

EMPLOYMENT

2009 - current	SBC - LTER (Santa Barbara Coastal Long Term Ecological Research) program: Graduate Research Assistant, Diver & Graduate Representative
2011	Monterey Bay Aquarium Seafood Watch: Contract Analyst
2006 - 2009	University of Alaska Fairbanks: Graduate Research Assistant
	Designed two subtidal artificial reefs in Southeast Alaska, oversaw installation and currently co-manage ongoing annual surveys (*http://www.fakr.noaa.gov/habitat/reef/lynncanal/default.htm*)
2009 - current	National Marine Fisheries Service: Alaska Fisheries Science Center Contract Research Diver:
2004 - 2006	UW Friday Harbor Laboratories: Research Diver & Technician
2005	Washington Dept. Fish & Wildlife: Scientific Technician II
2004 - 2005	University of Washington: Research Technician for Alan Kohn
2002	Deckhand: Commercial purse seine fishing (salmon), Southeast Alaska

INTERNSHIPS

2006	Marine Molecular Ecology, UW Friday Harbor Laboratories.
2005	Boersma Lab, University of Washington.
2004	Univ. of Washington Alaska Salmon Program, Bristol Bay, AK.

ACADEMIC HONORS:

2014   Best Student Presentation (Hon. Mention)
                        - International Temperature Reefs Symposium
2013   Worster Summer Research Award
2013   UCSB Graduate Division Dissertation Fellowship
2013   Charles A. Storke Graduate Fellowship
2013   UC Affiliates Nancy Brown Graduate Dissertation Fellowship
2013   UCSB Block Grant fellowship (tuition, stipend and fees)
2011   UCSB Block Grant fellowship
2009   UCSB Block Grant fellowship
2008   Dr. H. Richard Carlson Scholarship – University of Alaska Fairbanks
2006   Howard Hughes Medical Institute Scholarship, UW Friday Harbor Laboratories
2005   Kappa Sigma Endowment Fund Scholarship-Leadership Award
2001   Michelson Scholarship (Gig Harbor High School)

TEACHING ASSISTANTSHIPS:

2011 & 2012	Applied Marine Ecology	*-UC Santa Barbara*
2010, 2011, 2012	Introduction to Ecology	*-UC Santa Barbara*
2009	Applied Marine Ecology Lab	*-UC Santa Barbara*
2009	Aquatic Community Ecology	*-UC Santa Barbara*
2009	Multivariate Data Analysis	*-University of Alaska*
2009	Fisheries Population Dynamics	*-University of Alaska*
2008	Marine Ecology	*-University of Alaska*
2008	Regression & ANOVA	*-University of Alaska*

MENTORING EXPERIENCE:

2013-2014	Stephanie Saccardi	*-UCSB undergraduate*
	Evan Barba	*-UCSB undergraduate*
2007	Michael Pantalos	*-Cornell undergraduate* via *University of Alaska*)

PROFESSIONAL PRESENTATIONS

2013	Guest Lecture: "Statistical Power Analysis" - Florida State University
2008	Guest Lecture: "Marine Ecology" - University of Alaska Southeast
2014	International Temperate Reefs Symposium, Perth, Australia
2012	American Fisheries Society - St. Paul, MN, USA (both invited & submitted)
2011-2013	UCSB EEMB Graduate Student Symposium - Santa Barbara, CA, USA
2011	American Fisheries Society - Seattle, WA, USA
2009	Western Society of Naturalists - Seaside, CA, USA
2008	Western Society of Naturalists - Vancouver, BC, Canada
2008	International Temperate Reef Symposium - Adelaide, Australia
2007, 2008	American Fisheries Society, Alaska Chapter - Juneau, AK, USA

INVITED WORKING GROUP PARTICIPATION

2013	Kelp Forests and Climate Change, Santa Barbara, CA, USA
	(NCEAS - National Center for Ecological Analysis & Synthesis)

Abstract

The role of fluctuating food supply on recruitment, survival and population dynamics in the sea

Daniel Kenji Okamoto

This collection of work focuses on dynamics of two marine taxa with very different life histories, both of whom are sensitive to changes in food supply. Chapters 1 and 2 focus on black surfperch (*Embiotoca jacksoni*), a direct developer with internal reproduction while chapters 3 and 4 focus on the purple sea urchin (*Strongylocentrotus purpuratus*) a broadcast spawner with pelagic larvae. Chapter 1 was published in Proceedings of the Royal Society: B in 2012, and is co-authored by Russ Schmitt, Sally Holbrook and Dan Reed. In this chapter I used long-term data on surfperch and their prey to illustrate how variability food for surpferch corresponds to changes in the number of young that adults produce and how well those young survive. Chapter 2 provides evidence that survival in adult surfperch responded to both prey availability and competition among adults. This work is a collaboration with Russ Schmitt and Sally Holbrook. Chapter 3 focuses on fertilization dynamics in sea urchins and the role that varying egg concentrations during spawning can have on the rate of fertilization when mixed with sperm. I conducted laboratory experiments and developed new models to show that the per capita rate of interactions among eggs and sperm slow down as egg concentrations increase. Finally, in chapter 4 I used a 23-year dataset of larval settlement of purple urchins at seven sites to investigate whether settlement patterns were related to major climatic and biological

variables including food supply and temperature. This chapter is an ongoing collaboration with Steve Schroeter, Dan Reed and several others. These analyses show a strong, negative relationship between settlement and El Niño cycles as well as temperature in southern California, indicating that multi-year fluctuations in climate may regulate the patterns of settlement that are highly variable in time. Collectively, these chapters highlight the importance of considering complex interactions and nonlinearities in dynamics of marine species.

Contents

List of Figures

List of Tables

Chapter 1

Fluctuations in food supply drive recruitment variation in a marine fish

Abstract

Reproductive rates and survival of young in animal populations figure centrally in generating management and conservation strategies. Model systems suggest food supply can drive these often highly variable properties, yet for many wild species, quantifying such effects and assessing their implications have been challenging. I used spatially explicit time series of a well-studied marine reef fish (black surfperch *Embiotoca jacksoni*) and its known prey resources to evaluate the extent to which fluctuations in food supply influenced production of young by adults and survival of young to subadulthood. My analyses reveal: 1) variable food available to both adults and to their offspring directly produced an order of magnitude variation in the number of young-of-year (YOY) produced per adult, and 2) food available to YOY produced a similar magnitude of variation in their subsequent survival. I then show that such large natural variation in vital rates can significantly alter decision thresholds (biological reference points) important for precautionary management. These findings reveal how knowledge of food resources can improve understanding of population dynamics and reduce risk of overharvest by more accurately identifying periods of low recruitment.

Key Words: population dynamics; stock-recruitment; food limitation; marine fish; population regulation; biological reference points.

Introduction

Properties governing reproductive rates and survival of young help shape a population's risk of extinction (Coulson et al. 2001) and resilience to perturbation or harvest (Mace 1994). As a result, understanding how environmental change alters these properties remains a fundamental but elusive challenge that has direct implications to conservation (Shaffer 1981) and resource management (Myers 2001). A large body of evidence suggests that food supply can influence population dynamics by, for example, altering reproductive performance of adults and/or survival of young. This has been documented for a range of vertebrates, including terrestrial mammalian herbivores (e.g. Koskela et al. 1998, Mduma et al. 1999), marine mammals (e.g. Reid and Croxall 2001), passerine birds (e.g. Newton 1998), seabirds (e.g. Ashbrook et al. 2010, Reid and Croxall 2001) and freshwater (Mason 1976) and marine fish (e.g. Hjermann et al. 2007, Maunder and Deriso 2011, Olsen et al. 2011). Although fluctuations in food supply are ubiquitous in nature, conservation and management strategies frequently assume populations have constant mean vital rates through time. Such constancy typically is assumed for population viability analyses based on life tables or matrix projection models (Morris and Doak 2002), as well as for many stock-recruit models in fisheries (Quinn and Deriso 1999). In marine fishes, for example, basic stock-recruitment models are expected to perform well only where there is comparatively low temporal variability in recruitment (Koslow 1992), which could be a major reason why many stock-recruit models account

for little variation in the data (Wootton 1998). If externally driven temporal variation in vital rates is high, then the application of such simplistic models could lead to severe mismanagement, particularly if periods of recruitment failure are underestimated.

One solution to better predict or understand risk of recruitment failure has been to map variation in fecundity or survival onto physical environmental variables (Quinn and Deriso 1999). However, this correlative approach (Hilborn and Walters 1992) appears best supported when species occupy harsh physical environments (Myers 1998). In stock-recruitment models of marine fish, difficulty in assessing food supply and other more direct drivers at appropriate scales has resulted in the use of environmental indices (Mueter et al. 2002) or regime metrics ("good" vs. "poor") (Kitaysky et al. 2010) to account for variation in adult reproduction and survival of young. Thus, even when there is strong environmental correlation with demographic rates, the descriptor variables (e.g., sea surface temperature (Mantua and Hare 2002)) usually are far removed from the underlying biological mechanism. As a result, such correlations often have not proved especially useful (McClatchie et al. 2010, Myers 2001).

The growing availability of appropriate long-term data is enabling more direct assessments of the roles of food and other such drivers of dynamics for marine fishes and other species (Beaugrand and Kirby 2010, Maunder and Deriso 2011, Olsen et al. 2011). However, even when food has been considered explicitly, few empirical studies have addressed the dynamical consequences of the cumulative effect of fluctuations in food across multiple life stages over time. The replenishment of adult stock may not

be limited by a bottleneck at a single life history stage; rather a cohort may be susceptible to food stressors at multiple stages (Maunder and Deriso 2011). For example, low food availability to adults during the reproductive period may yield few offspring, but subsequent high food availability for those offspring may offset such effects due to above normal survival. In contrast, successive years of low food may lead to low adult fecundity and poor offspring survivorship that collectively result in recruitment failure. Thus, identifying the effect of food resources on multiple life stages may substantially improve predictions of recruitment failure in managed populations.

Here I investigated 1) the extent to which food supply explained observed variation in reproduction and survival of a common marine reef fish (the black surfperch *Embiotoca jacksoni*), and 2) how refined estimates of vital rates for this species altered a common decision threshold (i.e., a biological reference point) used for precautionary management of fisheries. I formulated a priori hypotheses from detailed knowledge of black surfperch feeding and reproductive ecology (Baltz 1984, Holbrook and Schmitt 1984, 1986, Schmitt and Holbrook 1986, 2007) and evaluated those using spatially explicit time series data on age-structure and food availability. I first constructed several basic models for two important dynamical processes: production of young-of-year (age 0, YOY) by mature adults (age 2+ (Baltz 1984)); and subsequent survival of YOY to subadulthood (age 1, immature subadults). I then compared these basic models to those that incorporated food available to one or more age classes in the model (adults, YOY, subadults). In this manner, my model construction and selection framework served to quantitatively

evaluate and describe functional relationships between availability of food known to be important and recruitment dynamics. This yielded insight regarding the circumstances under which incorporating such information can alter a common biological reference point used to forecast impaired recruitment (i.e., the adult stock size required to produce 50% of maximum recruitment (Mace 1994)).

Methods

Study system

Black surfperch occupy shallow temperate reefs. Females are viviparous and annually produce well developed, locally retained young (for more details see (Holbrook and Schmitt 1986, Schmitt and Holbrook 1986). This quality facilitates tracking of adults and offspring on a reef over multiple years. Young consume the same general taxa as adults (Holbrook and Schmitt 1984), with diets dominated by caprellid and gammarid amphipods and other small crustaceans living within benthic, reef dwelling macroalgae (Schmitt and Holbrook 2007).

Time series data

Data on age-specific abundance of black surfperch, the amount of foraging habitat and the availability of their food were collected at 11 sites on the north side of Santa Cruz Island, CA annually in autumn (when fish copulate (Froeschke et al. 2007)) inter-

mittently from 1982 - 1992 and annually from 1993 - 2008. At each site, three fixed 40 m transects at 3, 6, and 9 m depth contours (the typical depth range) were surveyed annually for black surfperch (in a 40 x 2 m swath), their foraging habitat and principal food using SCUBA. Counts of fish were always made by the same observer (R. Schmitt) and included the number of YOY, subadults and mature adults. In this study prey were identified as caprellid and gammarid amphipods that were within the gape limitation of black surfperch since they composed the majority of prey biomass in algal samples (84%) and in diets of black surfperch (Ebeling and Laur 1986, Schmitt and Holbrook 1984). The index of food availability for a given year was calculated as the mean biomass of each prey taxon within suitable foraging habitats in that year multiplied by the cover of appropriate habitat at each site in each year. For further details see Appendix A:S1. Data used in analyses are available from http://metacat.lternet.edu/knb/metacat/knb-lter-sbc.60.

Young-of-year production

To examine the extent to which food availability influenced the production of young-of-year (YOY), I incorporated into stock-recruit (S-R) models: 1) availability of food in the year that females became pregnant and 2) availability of food in the following year when their newly produced YOY feed. I used three typical S-R models (Beverton-Holt, Cushing, Ricker) (Quinn and Deriso 1999) as well as a density independent (linear) form (Figure 1.1a-c). I hypothesized that increasing food available to adults and/or YOY

directly modified the YOY-per-adult relationship; thus the S-R function was multiplied by the food variables (see Appendix A:S2 for model construction). Because the food effect may taper with increasing food, I added a shape parameter in the exponent of each food variable that allowed this behavior. The general structure of the full models used was:

$$YOY_{t+1,i} = \alpha f(A_{t,i})e^{[\gamma_1 \ln(F_{t,i})+\gamma_2 \ln(F_{t+1,i})+\epsilon_{t,i}]}$$

$$= e^{\psi} f(A_{t,i})(F_{t,i})^{\gamma_1}(F_{t+1,i})^{\gamma_2} e^{\epsilon_{t,i}} \tag{1.1}$$

Where $\alpha = e^{\psi}$ is the density-independent productivity parameter, $A_{t,i}$ is adult density in year t at site i, $f(A_{t,i})$ is one of the stock-recruit relationships in Figure 1.1, $F_{t,i}$ is food available to those adults, $F_{t+1,i}$ is food available to the YOY they produce, γ_1 and γ_2 are shape parameters for the food variables, and $\epsilon_{i,t}$ is an error term. ψ was allowed to vary randomly among sites to account for site variation, avoid pitfalls of pseudoreplication and induce correlation among multiple observations within a site among years. I fit the relationships as non-linear mixed effects models (NLMMs) (Pinheiro et al. 2011) using a Gaussian likelihood after natural log transformation. Stock-recruit relationships tend to exhibit lognormal error structure so the models were natural log-transformed, with a small constant added to YOY (1/9, the minimum, non-zero mean density observed). By convention both sides of the model were divided by the number of adults to fit models on a per capita basis (YOY per adult). Model predictions (in log-space) were back-

transformed to the original scale using a bias correction (by adding $\sigma^2_{residual}/2$ before taking the antilog, where $\sigma^2_{residual}$ is the estimated within-site error variance (Baskerville 1972)), which is necessary because back transforming the mean of log transformed data otherwise yields the median on the original scale which will be biased low.

To test hypotheses, I compared models with 1) no food information, 2) food information for either adults or YOY, and 3) food information for both adults and YOY. All model comparisons in this study were performed using corrected Akaike Information Criterion (AICc). AICc values were compared using the following criteria: 1) the simplest model(s) within 2 units of the minimum is (are) favored, 2) models 4+ units from the minimum are rejected with caution, and 3) models 10+ units greater than the minimum effectively have no statistical support and are rejected with confidence (Burnham and Anderson 2002). Comparing models with different fixed effects requires use of Maximum Likelihood (ML), yet comparing models with different random effects requires Restricted Maximum Likelihood (REML) (Pinheiro and Bates 2000, Zuur et al. 2009). Thus I first confirmed that parameters other than ψ should not vary randomly by site by comparing models fit using REML (see Appendix A:S2), then compared models with different fixed effects fit using ML, and finally refit models using REML to get unbiased parameter estimates. In the best-fit models I detected no significant effect of residual autocorrelation using AICc (Appendix A:S3).

Young-of-year survival

I evaluated the effect of food on indices of YOY survival to subadulthood by including food available to YOY in year (t) at the ith site and food available to subadults in year $(t+1)$ in models of YOY survival. Note that I use the term survival to mean an index of survival, not a true estimate of survival per se because YOY are cryptic in comparison to subadults. As a result, YOY densities are assumed to be underestimated, particularly at low densities and therefore the ratio of subadults in year $(t+1)$ and YOY in year (t) can exceed 1 when YOY are scarce. In the same fashion as for YOY production, I used a general relationship for YOY survivorship:

$$S_{t+1,i} = \delta f(YOY_{t,i})e^{[\gamma_1 \ln(F_{t,i}) + \gamma_2 \ln(F_{t+1,i}) + \epsilon_{t,i}]}$$

$$= e^{\zeta} f(YOY_{t,i})(F_{t,i})^{\gamma_1}(F_{t+1,i})^{\gamma_2} e^{\epsilon_{t,i}} \tag{1.2}$$

Where $\delta = e^{\zeta}$ is the density independent subadult-YOY ratio, $F_{t,i}$ is food available to YOY in year (t) at the ith site, $F_{t+1,i}$ is food available to subadults in year $(t+1)$ at the ith site, γ_1 and γ_2 are shape parameters for the food variables, and $f(YOY_{t,i})$ is either: 1) a linear relationship between YOY and subsequent subadults (Figure 1.1, constant survival) or 2) an accelerating to linear function (Figure 1.1d); this accommodates subadult/YOY ratios >1 caused by low biased YOY estimates (see Appendix A:S4). NLMMs were fit in log-space (fit as subadults + 1/9 per YOY, with 1/9 again

being the smallest non-zero value) using a Gaussian likelihood (after log-transformation) and back-transformed predictions were bias-corrected. Only δ was allowed to vary by site (see Appendix A:S2 for results for comparison of random effect structures). For model selection I used the same process as outlined for YOY production models. For precautionary purposes I used a first order autoregressive model [AR(1)] to account for potential autocorrelation as its inclusion allowed the model to conform to residual normality (see Appendix A:S3) and slightly modified model parameter estimates.

Subadult abundance predicted by reproductive adults and food availability

I combined the most statistically supported YOY production and YOY survival models into a single, parameterized model to assess how well these models together explained variation in subadult abundance. I compared the predictions of this best combined model to those that combined the previously-parameterized standard Beverton-Holt, Cushing or Ricker models with the standard linear YOY survival models (each lacking food information) hereafter referred to as the standard (non-food) combined models. For each I estimated variance explained in subadult densities as well as mean bias of the predictions (predicted-observed) for each combined model.

Impact of food information on the biological reference point B50%R

To explore how explicit information on food might alter biological reference points (BRP), I examined a major BRP used to indicate stock thresholds for impaired re-

cruitment. The adult stock size required to produce 50% of the maximum estimated recruitment produced at high biomass (B50%R) is a generally reliable threshold (Mace 1994). Ricker and Beverton-Holt models have estimable theoretical maximum recruitment levels, while the Cushing model requires estimating recruitment at historical adult mean-maximum densities (13 adults per 80 m2 in this case). I solved the best-fit YOY production model with food to estimate how proportional reductions in mean food availability would alter B50%R in comparison to that from the corresponding model without food and used residual bootstraps to calculate 95% confidence intervals (999 iterations) whereby I 1) added randomly sampled residuals (with replacement) to the fitted values, 2) re-estimated model parameters using these data and 3) calculated 2.5 and 97.5% quantiles.

Results

Temporal variation in the study system

Abundances of adult black surfperch and their foraging habitat were highest in the early years of the study and declined substantially during the late 1980s and early 1990s (Figure 1.2a, b). From 1993-2008 the densities of all age classes exhibited an increase (Figure 1.2b, Figure 1.3a). Food availability showed substantial inter-annual variability (Figure 1.3b, SD of site means= 3.714) with much smaller inter-site variability (SD of annual means = 0.940).

Young-of-year production

The Cushing model that included food levels for both adults and YOY explained 41 percent of the variance and was strongly supported as the best of the models tested (AICc value 7.7 to 50.0 units less than all other models, Table 1). The model indicated that YOY production was positively influenced by adult density ($A_{t,i}$), food available to adults (Figure 1.4a, b) and food available to YOY. In the model, the food effect decreased as food became more available, indicated by shape parameters with values <1 ($\gamma_1 = 0.68$ 0.12 SE, P <0.001; $\gamma_2 = 0.46$ 0.11 SE, P <0.001). Random site effects for ψ varied substantially ($\psi = -1.70$ 0.20 SE, P <0.001, = 0.43 [SD of random effects]), suggesting substantial variation by site not accounted for by my measure of food (Appendix A:S2). The best model fit did not violate normality assumptions for residuals or random effects (Appendix A:S5). Removing the effects of food availability to either adults or YOY significantly reduced the quality of the fit of the Cushing model. Variance explained dropped to 16 to 31% for models with food information for one life stage and to 1 to 4% for traditional models lacking food information altogether (Table 1). The Beverton-Holt and Ricker models that included food levels for both adults and YOY were both improvements over models with no food information, but nonetheless had little statistical support when compared with the full Cushing model (Table 1).

Young-of-year survival

The model for young-of-year survival with the best statistical support included an accelerating to linear YOY to subadult function, and positive effects of food available to YOY in year (t) and food available to subadults in year (t+1) (Table 2; Figure 1.5a, b). This model explained 72 percent of the variance. The effect of food decreased as food became more available, as indicated by shape parameters with values <1 (γ_1 = 0.57 0.10 SE, P <0.001; γ_2 = 0.26 0.11 SE, P = 0.019). There was substantial variation in survival by site (ζ= -1.73 0.29 SE, P <0.001, σ_z= 0.61 [SD of random effects]). The best model fit did not violate normality assumptions for residuals or random effects (Appendix A:S5).

Removing food components of the model structure significantly reduced explanatory power, but the far more important one was food available to YOY (indicated by an increase in AICc of only 3.0 when food to subadults was removed in contrast to an increase of 20.2 when food to YOY was removed; Table 2). However, food variables only became statistically significant when the nonlinear functional relationship between YOY and subadults was incorporated (Table 2). Subadult abundance predicted by reproductive adults and food availability

The best combined model (predicting subadult densities from adult densities two years prior and food covariates from lags 0, 1, and 2 years using parameter estimates shown above) far outperformed the standard (non-food) combined models that did not include food as explanatory variables. The best combined model explained much more

of the variation in subadult densities ($R^2 = 0.68$, Figure 1.6) than the standard combined models,($R^2 = 0.31$-0.36). Furthermore, the best combined model did not exhibit significant bias (bias = 0.07, $t_{129} = 1.02$, P = 0.31, Figure 1.6) whereas the standard (non-food) combined models showed significant, positive bias (overprediction) ranging from 0.66 to 0.69 (Appendix A:S5).

Impact of food information on the biological reference point B50%R

When reductions in mean annual food availability were greater than 35%, the estimated number of adults required to produce 50% of maximum mean-recruitment (B50%R) by the best model significantly exceeded B50%R estimated by the model without food information (Figure 1.7). For black surfperch, such reductions in mean annual food availability may be due to either changes in availability of foraging habitat or density of prey within such habitat. Once food is reduced by >40%, the number of adults required to produce sufficient recruitment is equal to or greater than the historical mean maximum (indicated by the arrow in Figure 1.7). In contrast, with no or modest change in food availability, the number of adults is less than or equal to that estimated by the model without food information because of stronger density dependence in the full model (a smaller β).

Discussion

My findings not only show that fluctuations in food to a marine fish can substantially shape both the production of young and their subsequent survival, more importantly they demonstrate the serious consequences that can arise from failing to account for such food limitation in models used to describe population dynamics or guide management decisions. Relatively simple models are still the dominant choice to characterize complex population dynamics and at times can prove to be as effective as models with more biological realism (Adkison 2009). In the realm of such realism, food limitation remains a central research frontier in fisheries science and population dynamics, particularly of marine vertebrates. Although a plethora of research demonstrates direct and often cascading roles of predators in regulating populations in both marine and terrestrial systems (2010), top-down influences do not necessary render bottom-up forcing unimportant, including for marine fishes (Anderson 2001, Anderson and Sabado 1995). In the case of black surfperch, whose individual and population attributes indeed are affected by predators (Holbrook and Schmitt 1988, Schmitt and Holbrook 1985), I found that more than an order of magnitude of natural variation in several vital rates was driven by natural fluctuations in the amount of food available to multiple life stages. In systems exhibiting such food limitation, knowledge of food supply can substantially alter estimates of useful biological reference points, particularly when reductions in food are severe.

Food-driven variability in the number of young black surfperch produced by adults challenges traditional assumptions made by many population models that fecundity and survival of young is purely intrinsic. Such effects result from either increased survival of newly produced offspring or increased reproductive output. The latter may result from increased size-specific fecundity in response to food (Kjesbu et al. 1998) or increased growth rates of adults when food availability is high, allowing higher fecundity via a consistent length-fecundity relationship. Species such as surfperch that exhibit the capacity to abort or resorb embryos in response to stress (Schultz 2008), show plasticity in their size-fecundity relationship (Behrens 1977), or exhibit increased growth rates in response to food (Anderson and Sabado 1995, Holbrook and Schmitt 1986) may be especially susceptible to such size-specific fecundity effects when either foraging habitat or the density of food therein changes substantially through time. In either case, I found strong effects of food in all model forms, with the most pronounced in the Cushing. The strong fit in the Cushing model may have resulted from the fact that adult densities were seldom at or above historically high levels throughout the period of this study, limiting the opportunity for asymptotic recruitment or overcompensation to occur. Like production of young by adults, the effect of food availability on survival of juveniles has been widely suspected, especially for marine fish (Olsen et al. 2011, Shelbourne 1957), and was also strongly supported by my analyses.

For black surfperch, the large effect of food on production and survival of young diminished as food supply increased. Since fecundity must have an upper limit, survival

cannot exceed 100% and fish are likely to become food satiated at some point, it is bio-logically sensible that their positive relationships with food decelerate and they become increasingly influenced by other factors. While black surfperch is not a fished species, my analyses do not include the effects of other factors that affect demographic rates such as the density of their main predator (kelp bass *Paralabrax clathratus*) (Holbrook and Schmitt 1988), structural complexity of refuge habitat (Schmitt and Holbrook 1985), and competition with other species (e.g., *Embiotoca lateralis* (Schmitt and Holbrook 1990)). Because the best combined model (which included food) explained 68 percent of observed variation in subadult density, these types of external factors could account for some portion of the unexplained variance. Furthermore, for a given supply of food, pro-duction of young and survival to subadulthood varied substantially among study sites, suggesting the potential importance of external factors. As young-of-year and, to a lesser extent, subadults are subject to predation, variation in predator densities and/or the abundance of foliose algae that provide refuge may account for some of the unexplained variation. However, my analyses cover population trends of black surfperch during a period when both predator densities (California Department of Fish and Game 2006) and foliose algae (Figure 1.2) were consistently low. I expect that large fluctuations in predator densities, although not seen since the late 1980's, may give rise to synchronous changes in survival of young.

Given that food rarely will be the sole constraint of populations, an approach such as ours that focuses on food resources is perhaps best suited to predict recruitment failure

(via low reproductive or survival rates) rather than to predict production of banner year classes. Models that incorporate only food resource information are likely to be less accurate in predicting high recruitment events because other factors likely increase in importance as food availability increases. In contrast, large reproductive output or high survival of young is not expected when food is scarce regardless of predator densities or other external factors. Thus management decisions and conservation measures should carefully consider resource driven predictions when conditions are poor, but place less confidence in such predictions when food is abundant. Such conclusions are evident from my analyses of the biological reference point (BRP) based on the adult stock that produces 50% of the maximum number of recruits (i.e., B50%R). Inclusion of food information had no substantive effect on estimates of B50%R when food availability remained constant, but a large decline in food supply, such as observed in the black surfperch system in the 1980's, predicted such dramatic reductions in productivity that the stock would be considered impaired with respect to recruitment even if the stock was at its historical mean maximum density. Thus, basing inference upon models and associated BRPs that ignore food information can be imprudent. While calculations as performed here require high quality food information that is often unavailable, adaptive BRPs could be estimated in the absence of such data where annual demographic vital rates such as adult survival, adult fecundity, and mortality of young can be measured in season. Such measurements may in some cases provide better estimates of BRPs than those provided by resource informed models, but would lack abilities to anticipate

and evaluate environmental vs. anthropogenic effects on demographic rates. For species subject to changes in foraging habitat, such as black surfperch, evaluating the subsequent effect on vital rates and BRPs has the potential to substantially alter recruitment-based management policies in an adaptive setting.

It is reasonable to infer that, for many fishes and other taxa, adult fecundity and survival can exhibit strong plasticity to the availability of food in a manner similar to black surfperch. I suggest that populations exposed to highly variable environments may be more likely to exhibit recruitment dynamics that fluctuate as a result of substantial changes in food availability to a host of life-history stages. Moreover, the history of environmental forcing matters; multiple years of low food will likely lead to recruitment failure in such systems. In contrast, alternating years of high food may buffer a cohort against a single low food year. The surprising lack of definitive evidence for such phenomena stems historically from logistical and analytical limitations and because high quality, long-term data series of food information are often unavailable. However, accrual of more long-term data and continued advancement of our understanding of ecological systems should lessen such constraints. Tandem investment in time-series estimates of population abundance, age structure and known food resources coupled with experimentation and modeling should improve our ability to assess and manage populations whose food resources vary through time.

Acknowledgements

References

Adkison, M. 2009. Drawbacks of complex models in frequentist and Bayesian approaches to natural-resource management. Ecological Applications 19:198–205.

Anderson, T. 2001. Predator responses, prey refuges, and density-dependent mortality of a marine fish. Ecology 82:245–257.

Anderson, T., and B. Sabado. 1995. Correspondence between food availability and growth of a planktivorous temperate reef fish. Journal of Experimental Marine Biology and Ecology 189:65–76.

Ashbrook, K., S. Wanless, M. Harris, and K. Hamer. 2010. Impacts of poor food availability on positive density dependence in a highly colonial seabird. Proceedings of the Royal Society B: Biological Sciences 277:2355–2360.

Baltz, D. 1984. Life history variation among female surfperches (Perciformes: Embiotocidae). Environmental Biology of Fishes 10:159–171.

Baskerville, G. 1972. Use of logarithmic regression in the estimation of plant biomass. Canadian Journal of Forest Research 2:49–53.

Beaugrand, G., and R. Kirby. 2010. Climate, plankton and cod. Global Change Biology 16:1268–1280.

Behrens, D. 1977. Fecundity and reproduction of the viviparous perches *Hypsurus caryi* (Agassiz) and *Embiotoca jacksoni* Agassiz. Calif. Fish Game 63:234–252.

Burnham, K., and D. Anderson. 2002. Model selection and multimodel inference: a practical information-theoretic approach. 2nd ed. Springer Verlag, New York.

California Department of Fish and Game. 2006. Compilation and analysis of CIAP nearshore survey data. http://www.dfg.ca.gov/marine/fir/crane.asp.

Coulson, T., G. Mace, E. Hudson, and H. Possingham. 2001. The use and abuse of population viability analysis. Trends in Ecology & Evolution 16:219–221.

Ebeling, A., and D. Laur. 1986. Foraging in surfperches: resource partitioning or individualistic responses? Environmental Biology of Fishes 16:123–133.

Froeschke, B., L. Allen, and D. Pondella. 2007. Life History and courtship behavior of black perch, Embiotoca jacksoni (Teleostomi: Embiotocidae), from Southern California. Pacific Science 61:521–531.

Hilborn, R., and C. Walters. 1992. Quantitative fisheries stock assessment: choice, dynamics, and uncertainty, vol. 2. 1st ed. Chapman & Hall, New York.

Hjermann, D., B. Bogstad, A. Eikeset, G. Ottersen, H. Gjøsaeter, and N. Stenseth. 2007. Food web dynamics affect Northeast Arctic cod recruitment. Proceedings of the Royal Society B: Biological Sciences 274:661–669.

Holbrook, S., and R. Schmitt. 1984. Experimental analyses of patch selection by foraging black surfperch (*Embiotoca jacksoni* Agazzi). Journal of Experimental Marine Biology and Ecology 79:39–64.

———. 1986. Food acquisition by competing surfperch on a patchy environmental gradient. Environmental biology of fishes 16:135–146.

———. 1988. The combined effects of predation risk and food reward on patch selection. Ecology 69:125–134.

Kitaysky, A., J. Piatt, S. Hatch, E. Kitaiskaia, Z. Benowitz Fredericks, M. Shultz, and J. Wingfield. 2010. Food availability and population processes: severity of nutritional stress during reproduction predicts survival of long lived seabirds. Functional Ecology 24:625–637.

Kjesbu, O., P. Witthames, P. Solemdal, and M. Greer Walker. 1998. Temporal variations in the fecundity of Arcto-Norwegian cod (*Gadus morhua*) in response to natural changes in food and temperature. Journal of Sea Research 40:303–321.

Koskela, E., P. Jonsson, T. Hartikainen, and T. Mappes. 1998. Limitation of reproductive success by food availability and litter size in the bank vole, *Clethrionomys glareolus*. Proceedings of the Royal Society of London. Series B: Biological Sciences 265:1129.

Koslow, J. 1992. Fecundity and the stock-recruitment relationship. Canadian Journal of Fisheries and Aquatic Sciences 49:210–217.

Mace, P. 1994. Relationships between common biological reference points used as thresholds and targets of fisheries management strategies. Canadian Journal of Fisheries and Aquatic Sciences 51:110–122.

Mantua, N. J., and S. R. Hare. 2002. The Pacific decadal oscillation. Journal of Oceanography 58:35–44.

Mason, J. 1976. Response of underyearling coho salmon to supplemental feeding in a natural stream. Journal of Wildlife Management 40:775–788.

Maunder, M., and R. Deriso. 2011. A state-space multistage life cycle model to evaluate population impacts in the presence of density dependence: illustrated with application to delta smelt (*Hyposmesus transpacificus*). Canadian Journal of Fisheries and Aquatic Sciences 68:1285–1306.

McClatchie, S., R. Goericke, G. Auad, and K. Hill. 2010. Re-assessment of the stock-recruit and temperature-recruit relationships for Pacific sardine (*Sardinops sagax*). Canadian Journal of Fisheries and Aquatic Sciences 67:1782–1790.

Mduma, S., A. Sinclair, and R. Hilborn. 1999. Food regulates the Serengeti wildebeest: a 40 year record. Journal of Animal Ecology 68:1101–1122.

Morris, W., and D. Doak. 2002. Quantitative conservation biology: theory and practice of population viability analysis. 1st ed. Sinauer Associates Sunderland, Massachusetts, USA.

Mueter, F., R. Peterman, and B. Pyper. 2002. Opposite effects of ocean temperature on survival rates of 120 stocks of Pacific salmon (*Oncorhynchus* spp.) in northern and southern areas. Canadian Journal of Fisheries and Aquatic Sciences 59:456–463.

Myers, R. 1998. When do environment-recruitment correlations work? Reviews in Fish Biology and Fisheries 8:285–305.

———. 2001. Stock and recruitment: generalizations about maximum reproductive rate, density dependence, and variability using meta-analytic approaches. ICES Journal of Marine Science 58:937–951.

Newton, I. 1998. Population limitation in birds. 1st ed. Academic Pr, San Diego, CA.

Olsen, E. M., G. Ottersen, M. Llope, K. Chan, G. Beaugrand, and N. C. Stenseth. 2011. Spawning stock and recruitment in North Sea cod shaped by food and climate. Proceedings of the Royal Society B: Biological Sciences 278:504–510.

Pinheiro, J., and D. Bates. 2000. Mixed-effects models in S and S-PLUS. Statistics and Computing Series, 1st ed. Springer Verlag, New York, NY.

Pinheiro, J., D. Bates, D. Saikat, S. D, and R. D. C. team. 2011. nlme: Linear and Nonlinear Mixed Effects Models, r package version 3.1-98 ed.

Quinn, T., and R. Deriso. 1999. Quantitative fish dynamics. 1st ed. Oxford University Press, New York.

Reid, K., and J. Croxall. 2001. Environmental response of upper trophic-level predators reveals a system change in an Antarctic marine ecosystem. Proceedings of the Royal Society of London. Series B: Biological Sciences 268:377.

Schmitt, R., and S. Holbrook. 1984. Gape-limitation, foraging tactics and prey size selectivity of two microcarnivorous species of fish. Oecologia 63:6–12.

———. 1985. Patch selection by juvenile black surfperch (Embiotocidae) under variable risk: Interactive influence of food quality and structural complexity. Journal of Experimental Marine Biology and Ecology 85:269–285.

———. 1986. Seasonally fluctuating resources and temporal variability of interspecific competition. Oecologia 69:1–11.

———. 1990. Population responses of surfperch released from competition. Ecology 71:1653–1665.

———. 2007. Predicting the magnitude of temporal variation in young-of-the-year class strength of surfperch (Teleostei: Embiotocidae). Raffles Bulletin of Zoology S14:161–166.

Schultz, E. 2008. A sex difference in seasonal timing of birth in a livebearing fish. Journal Information 2008.

Shaffer, M. 1981. Minimum population sizes for species conservation. Bioscience 31:131–134.

Shelbourne, J. 1957. The feeding and condition of plaice larvae in good and bad plankton patches. Journal of the Marine Biological Association of the United Kingdom 36:539–552.

Wootton, R. 1998. Ecology of teleost fishes, vol. 24. 1st ed. Springer, New York.

Zuur, A., E. Ieno, N. Walker, A. Saveliev, and G. Smith. 2009. Mixed effects models and extensions in ecology with R. Statistics for Biology and Health, 1st ed. Springer Verlag, New York.

Tables

Table 1.1: Fit of YOY production models with columns indicating the Stock-Recruit model functional form, food variables included [food available to adults year (t) at site i ($F_{t,i}$) and/or to YOY the next year ($F_{t+1,i}$), number of estimated parameters (k), corrected Akaike Information Criterion (AICc), increase in AICc over the best model, and variance explained in YOY produced per adult by the model.

stock-recruit function	food variables included		df	AICc	ΔAICc	R^2
Cushing	$F_{t,i}$	$F_{t+1,i}$	6	447.0	0.0	0.41
Beverton-Holt	$F_{t,i}$	$F_{t+1,i}$	6	454.7	7.7	0.40
Cushing	$F_{t,i}$	—	5	462.2	15.2	0.31
Ricker	$F_{t,i}$	$F_{t+1,i}$	6	468.6	21.6	0.27
Beverton-Holt	$F_{t,i}$	—	5	471.3	24.3	0.30
Cushing	—	$F_{t+1,i}$	5	473.7	26.7	0.23
Ricker	$F_{t,i}$	—	5	478.9	31.9	0.18
Beverton-Holt	—	$F_{t+1,i}$	5	482.0	35.0	0.16
Ricker	—	$F_{t+1,i}$	5	482.5	35.5	0.16
Cushing	—	—	4	494.6	47.5	0.04
Linear	—	—	3	495.2	48.2	0.01
Beverton-Holt	—	—	4	497.1	50.1	0.01
Ricker	—	—	4	497.1	50.1	0.01

Table 1.2: Fit of YOY survival models with columns indicating the functional form of survival, the food variables included [food available at the ith site to YOY and in year (t) at site i ($F_{t,i}$) and/or to subadults the next year ($F_{t+1,i}$), number of estimated parameters (k), corrected Akaike Information Criterion (AICc), increase in AICc over the best model, and variance explained in survival by the model.

survival function	food variables included		df	AICc	ΔAICc	R^2
accelerating to linear	$F_{t,i}$	$F_{t+1,i}$	7	197.8	0.0	0.72
accelerating to linear	$F_{t,i}$	—	6	200.8	3.1	0.67
accelerating to linear	—	$F_{t+1,i}$	6	218.0	20.3	0.62
accelerating to linear	—	—	5	221.9	24.1	0.57
linear	—	—	4	240.7	42.9	0.26
linear	—	$F_{t+1,i}$	5	262.7	64.9	0.16
linear	$F_{t,i}$	—	5	263.0	65.3	0.21
linear	$F_{t,i}$	$F_{t+1,i}$	6	264.5	66.7	0.19

Figures

a) Cushing

b) Beverton–Holt

c) Ricker

YOY

adults (A) adults (A) adults (A)

d) accelerating to linear

subadults (S)

YOY

YOY production (a–c)
$$f(A) = A^{\beta} \qquad \text{[Cushing]}$$
$$f(A) = A/(A + \beta) \qquad \text{[Beverton–Holt]}$$
$$f(A) = A\,e^{(-\beta A)} \qquad \text{[Ricker]}$$

YOY survival (d)
$$f(YOY) = (YOY + 1)^{(YOY+1)/(YOY+\beta)}$$
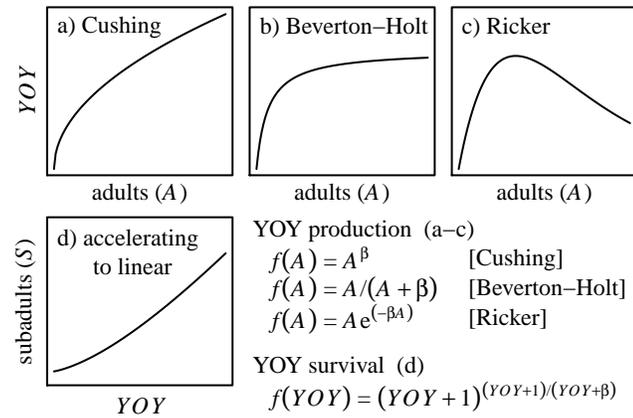
Figure 1.1: Nonlinear functional forms used in (a-c) YOY production models and (d) YOY survival models.
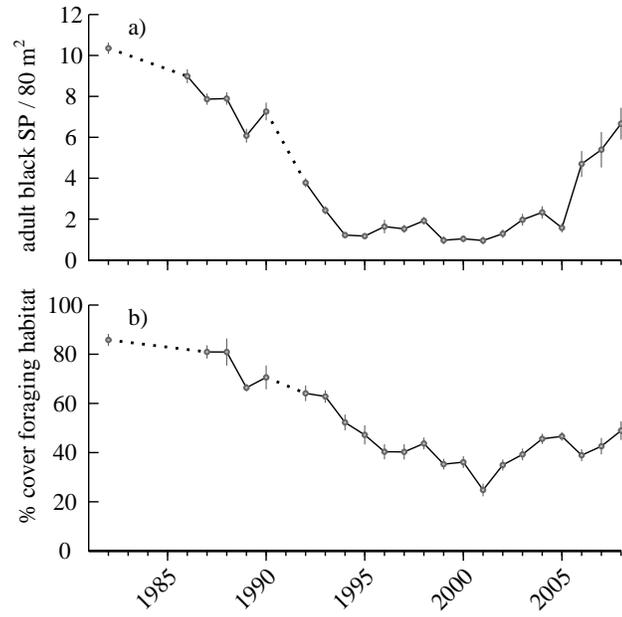
Figure 1.2: Temporal patterns of (a) adult black surfperch densities (mean SE) and (b) percent cover of foraging habitat . Foraging habitat is defined as foliose understory and turfing algae in which black surfperch feed.
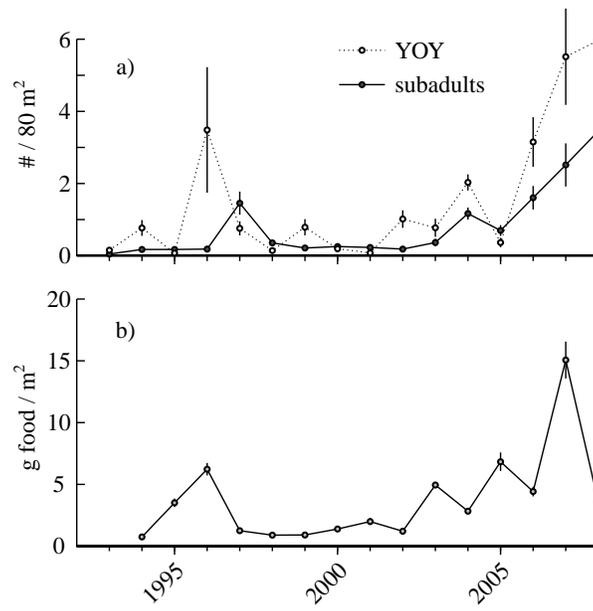
Figure 1.3: Temporal patterns (mean SE) of (a) YOY and subadult black surfperch densities and (b) index of food available to black surfperch.
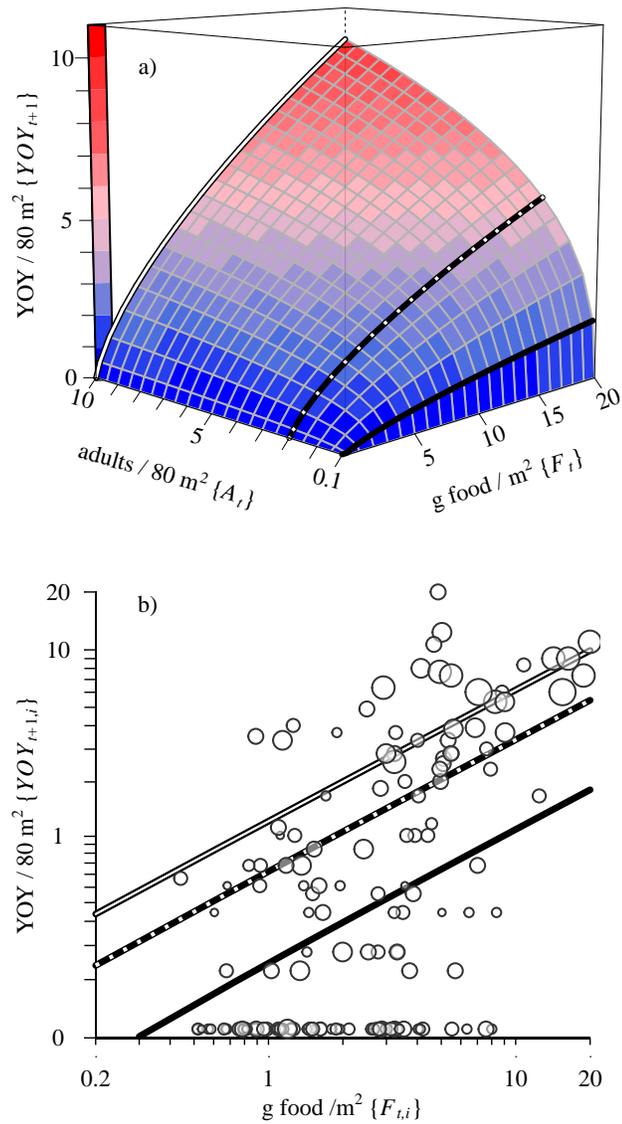
Figure 1.4: (a) Cushing YOY production model predictions, made with food available to YOY in year (t) fixed at its mean value of 0.35 g per 0.1 m^2. Lines are selected predictions along this surface that correspond to those in (b). The vertical axis represents densities of YOY in year (t+1) that were produced by adults in year (t) on the right axis. The left axis represents food available to adults in year (t). (b) Log-scale density of YOY in year (t+1) vs. log-scale food in year (t). Larger points indicate more adults in year (t) at that site-year combination. Lines correspond with those in (a).

34
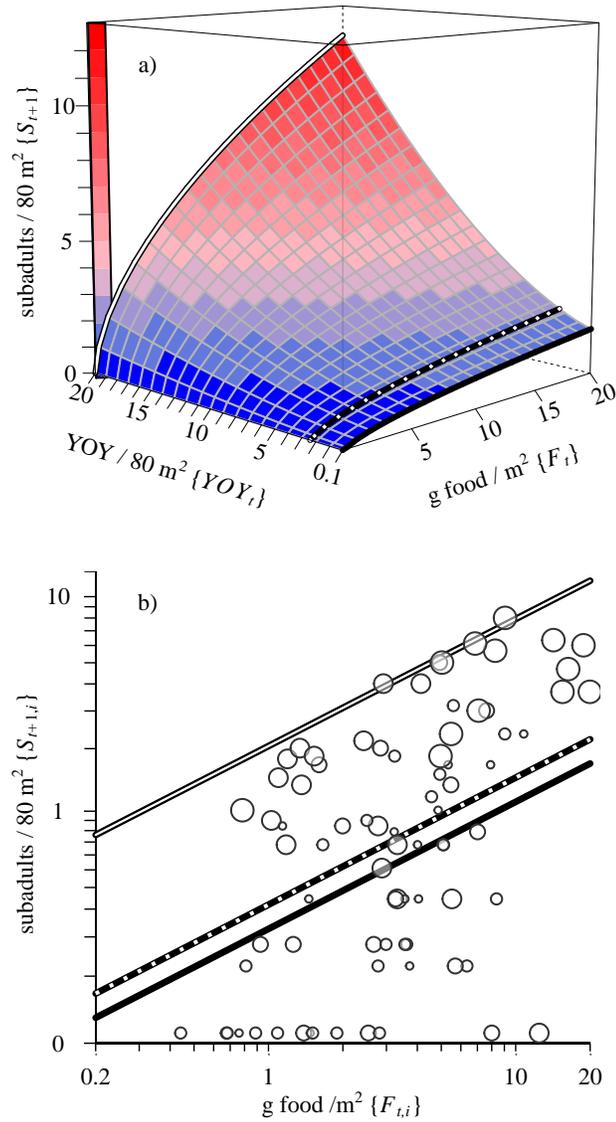
Figure 1.5: (a) YOY survival model predictions visualized with food in year (t) fixed at its mean value of 0.35 g per 0.1 m^2. Lines are selected predictions along this surface that correspond to those in (b) and represent predictions for different YOY densities (the maximum, mean and minimum). The vertical axis represents density of subadults in year (t+1) that survived from YOY in year (t) shown on the left axis. The right axis represents g of food in year (t). (b) Log-scale density of subadults in year (t) vs. log-scale food in year (t). Larger points indicate more YOY in year (t) at that site-year combination. Lines correspond to those in (a).
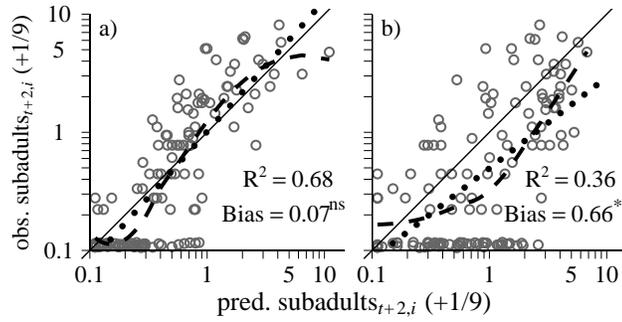
Figure 1.6: Observed versus predicted values for the combined models using: (a) the best fit models with food variables and (b) the Cushing model and linear YOY survival without food variables. Solid lines represent the 1:1 lines, dotted lines represent a fitted linear regression, and dashed lines represent a fitted Loess smoother; unbiased model predictions will yield no difference between the 1:1 line and the others. R^2 values are for variance in subadults explained by each model; bias values are the average difference between the predicted and the observed values; *P < 0.001, ns = not significant.
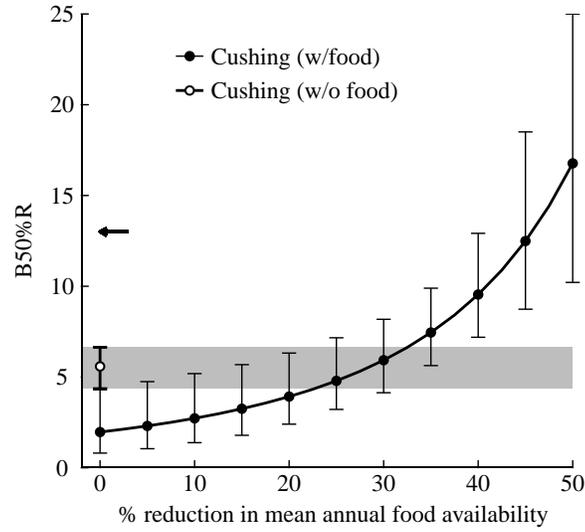
Figure 1.7: Number of adults required to produce 50% of maximum mean YOY recruitment (i.e., the Biological Reference Point B50%R) as estimated under the Cushing model with food (solid points) and without (open point) with the arrow indicating the historical mean maximum adult density. Error bars represent 95% confidence intervals; the grey band represents the 95% CI for the no-food Cushing model projected the across x-axis values.

Appendix A: Electronic Supplement S1-S5

The electronic supplement including electric supplementary sections S1-S5 for can be downloaded for free at `http://rspb.royalsocietypublishing.org/content/suppl/` `2012/09/20/rspb.2012.1862.DC1/rspb20121862supp1.pdf`

Chapter 2

Food supply and density dependence interact to drive annual survival in adult fish

Abstract

A traditional view of fish populations is that recruitment and not variable adult survival primarily controls population fluctuations. I challenged the assumption that adult survival is effectively independent of food availability or density by exploring a stage-structured, multi-decadal time series dataset for black surfperch (Embiotoca jacksoni). Using a Bayesian, state-space modeling approach, I found strong evidence from these time series that both food supply and population density regulate adult survival. Analysis of time series data and model simulation illustrate that food-mediated density dependence can dramatically alter the expected behavior of populations with respect to the mean and variance of adult density. The impact of such temporal variation in adult survival on population variance and equilibrium density rivaled the influence of recruitment variation; moreover density dependent adult survival dampened the impact of variability arising from stochastic recruitment. Results suggest that variability in food supply may contribute significantly to population fluctuations by regulating both recruitment and compensatory adult survival simultaneously.

Introduction

In moderate to long-lived vertebrates, population fluctuations have been argued to result in large part from variation in recruitment rather than in adult survival. This stems from the observation that variability in recruitment (driven by fecundity, juvenile survival rates, and/or variable delivery of new colonists) greatly exceeds that of adult survival (Charnov 1986, Gaillard et al. 2000, 1998, Gaillard and Yoccoz 2003). As a result, an assumption of constant adult survival rates is often deemed adequate or even to be a necessary simplifying assumption for modeling population dynamics (Brodziak et al. 2011, Quinn and Deriso 1999). However, several key findings of models suggest the potentially critical importance of considering the nature of variation in adult survival rates. First, population growth rates commonly exhibit higher elasticity to adult survival than recruitment processes (Gaillard and Yoccoz 2003, Heppell et al. 2000). Second, adult survival rates that covary with recruitment can either amplify or dampen population variance depending upon the sign of covariance (Shelton and Mangel 2011). Finally density dependent vital rates can lead to instability and hydra effects (Abrams 2009).

In marine species, several mechanisms that result in substantial changes in adult survival have been identified outside of direct fishing mortality, including variable predation (e.g. Hollowed et al. 2000) and environmental perturbations that lead to mass mortality (e.g. Lafferty and Kuris 1993). By contrast, the interactive influence of food

supply and adult density is more poorly understood. Food limitation in competitive systems can arise via changes in food supply, changes in adult density or both; such changes can potentially lead to reductions in fecundity, as well as survivorship of juveniles and adults (Clutton-Brock et al. 1997, Eberhardt 2002, Elliott and Hurley 1998, Fryxell 1987, Mduma et al. 1999). While examples of density-dependent population regulation are widespread for many vertebrates (Knape and de Valpine 2012), strong empirical evidence for food regulated density dependent adult survival, and the resultant implications for population dynamics, remains scarce (but see Clutton-Brock et al. 1997, Mduma et al. 1999). If adult mortality rates depend directly upon food supply and/or adult density, then the theoretical and practical understanding of a population's dynamics may contrast sharply to scenarios where adult survival rates are assumed to be constant.

Among marine reef fishes, there is considerable evidence of density-dependent mortality, primarily of juveniles, for species that shelter from predators (Holbrook and Schmitt 2002, Osenberg et al. 2002, Schmitt et al. 1999). That notwithstanding, marine fish are prime examples of systems in which population models commonly assume constant adult survival; a parameter that in many cases is poorly estimated or simply chosen (Quinn and Deriso 1999). Despite this convention, the pitfalls of using erroneous estimates of adult survival are well established and include inaccurate assessments of productivity, temporal trends in abundance or resilience to anthropogenic perturbation (Clark 1999, Lapointe et al. 1992). Moreover, survival rates can be shown to vary through time

when sufficient data to test for non-stationarity exist (Jiao et al. 2012). Thus, given the widespread evidence that adults of fish (as well as many other vertebrate taxa) occasionally experience nutritional stress and competition for food, variability in food supply has the potential to influence population dynamics via adult survival as well as via recruitment processes for some taxa.

Several biological mechanisms provide substantial challenges to understanding the population-level implications of food limitation in adults. Adults of a variety of vertebrates can buffer against food limitation by adjusting fecundity (Tyler and Dunn 1976) or skipping reproduction altogether (Rideout and Tomkiewicz 2011). However, sacrificing fecundity first under nutritional stress is neither expected nor observed to be a universal trait among fish (Jørgensenn et al. 2006) and adults doing so are likely to experience decreases in survival once reproductive energy stores are expended. In addition to individual plasticity, the effects of food supply are likely to differ at different densities (Eberhardt 2002). At lower densities, food supply may have little impact and recruitment dynamics may dominate population trends over time. In contrast, at high adult densities food supply may buffer against variation in recruitment. Thus, while recruitment variation is generally thought to control population variability (Shelton and Mangel 2011) to my knowledge no studies have estimated the individual and combined effects of food and density mediated adult survival on fish population dynamics. I used a Bayesian state-space modeling approach to evaluate whether conspecific density and food supply simultaneously affect adult survival rates in the black surfperch (*Embiotoca*

jacksoni), and whether incorporating any such effects alters expectations of population size and variance. Black surfperch provide a tractable system for studying this issue because they exhibit strong competition for foraging habitat (benthic turf and macroalgae) and the crustacean prey therein (Hixon 1981, Holbrook and Schmitt 1984, 1986, Schmitt and Holbrook 1984, 1986). Moreover, recruitment dynamics in this species are correlated with variation in food supply (Okamoto et al. 2012). I used multi-generational time series data for black surfperch from Santa Cruz Island, California to evaluate the evidence for, and expected implications of, resource-mediated compensatory adult survival. First I tested whether estimated survival varied through time. I then estimated and tested support for models that related survival to conspecific density, food supply and habitat availability. Using the estimated models of survival, I calculated effect size measures in terms of expected equilibrium densities and temporal variation in population density. Finally, I analyze a simple, generalized version of this population model to illustrate the general consequences of compensatory adult survival on population variance in the face of stochastic recruitment dynamics.

Methods

Field surveys

Data on stage-specific abundance of black surfperch, the amount of foraging habitat and the availability of their food were collected at 11 sites on the north shore of Santa

Cruz Island, CA in autumn intermittently from 1982 - 1992 and annually from 1993 - 2008. At each site, three fixed 40 m transects at 3, 6, and 9 m depth contours (the typical depth range of black surfperch) were surveyed for black surfperch (in a 40 x 2 m swath) and their foraging habitat by divers using SCUBA, and samples were collected to estimate their principal crustacean food items. Counts of fish distinguished among young-of-year (YOY), juveniles (1 year old subadults) and mature adults ($\geq$ 2 years old). Habitat and food density

Foraging habitat for each site in a given year was defined as the average percent cover of all low lying turf and foliose algae averaged across all transects within each location in each year, as these are the substrates from which surfperch harvest their crustacean prey (Holbrook and Schmitt 1984, Laur and Ebeling 1983, Schmitt and Holbrook 1984). Food density was defined as the biomass density of prey (g wet mass m^{-2}), which included jaeropsid isopods, idoteid isopods, gammarid amphipods, caprellid amphipods and crabs within the gape limitation of adult black surfperch (Schmitt and Holbrook 1984). Estimates of food density for each site were calculated as described in Okamoto et al. (2012) and include the density of prey sampled from replicate 0.1 m^2 patches of foraging habitat in each year from which individual prey were counted and sized. Food biomass was not normalized by the habitat percent cover on transects (as was done in Okamoto et al. (2012)) so habitat and density of food biomass could be evaluated independently. Annual means of the biomass density of food averaged over all sites for each year of the time series were used as values for food availability in all analyses.

Though predator densities may also influence survival of surfperch, in this system regional predator abundance (primarily harbor seals and California sea lions) remained relatively consistent over the period covered in our study (Carretta et al. 2011).

Modeling framework & model selection

I used stage-structured, state-space models formulated in a hierarchical Bayesian framework to estimate the strength of the relationships between survival rates and conspecific density and food availability. The basic stage structured model considers survival as a function of adult density in year (y) at the ith site $(A_{y,i})$, adults in the following year at that location $(A_{y+1,i})$ and one-year-old (juvenile) density in year (y) at the ith site $(J_{y,i})$. However, A and J were estimated from visual surveys and not truly known. Thus I used a hierarchical state-space model formulated as follows:

$$A_{y+1,i} = [A_{y,i}s_{y,i} + J_{y,i}s_{y,i}g]e^{\epsilon_{y,i}} \tag{2.1}$$

$$\hat{A}_{y,i} = A_{y,i} + \epsilon_{A,y,i} \tag{2.2}$$

$$J_{y,i} = \hat{J}_{y,i} + \epsilon_{J,y,i} \tag{2.3}$$

where $s_{y,i}$ is adult survival from year (y) to $(y+1)$ at site i and g is the maturation rate of juveniles in year (y) to adulthood in year $(y+1)$ (juveniles either graduate or die), and $\hat{A}_{y,i}$ and $\hat{J}_{y,i}$ are the observed densities from all surveys at that site in that year. $\epsilon_{A,y,i}$ and $\epsilon_{J,y,i}$ are the errors associated with each variable and $e^{\epsilon_{y,i}}$ is the multiplicative

process error. Eq. (2.2) facilitates probabilistic estimates of the actual but unobserved adult abundance, and eqn. (2.3) facilitates integrating inference over the error associated with juvenile abundance. To estimate error functions for eqns. (2.2) and (2.3) I used an independent training dataset in which fish surveys were replicated repeatedly over the late summer and fall season within each of several years (see Appendix B, Figure B.1 for details).

Using the survey data and estimates of survey error, I first evaluated evidence that survival varies by year using the product space method (Carlin and Chib 1995, Lodewyckx et al. 2011) and compared model support using Bayes factors. Bayes factors (Gelman et al. 2013, Kass and Raftery 1995) provide a metric of data-driven evidence in favor of a hypothesis after accounting for its prior probability, and 2 ln(Bayes factor) (hereafter referred to as 2lnB) transforms it to an interpretable scale. Values of 2lnB >10 are very strong evidence against the null (requiring greater than 99% support), which I used as a conservative threshold, while negative values support the null. I then estimated models that consider annual survival as a function of food availability in the previous year (y) and current year $(y + 1)$, foraging habitat in year (y) and $(y + 1)$, and conspecific density (adults and juveniles independently) with two model forms: the Logistic and the Shepherd. The Logistic Model (eq. 2.4) relates survival to density, food

and foraging habitat availability using a logistic function:

$$s_{y,i} = \frac{1}{1 + exp\left[(\beta_{0_i} + \beta_1 A_{y,i} + \beta_2 x_{2_{y,i}} + ... + \beta_6 x_{6_{y,i}})t\right]} \tag{2.4}$$

<div align="right">Logistic Model</div>

where β_0 is a scale parameter (intercept that controls the density independent survival rate), $A_{y,i}$ and $x_2 - x_6$ represent covariates (adult density, juvenile density, habitat and food supply) with $\beta_1 - \beta_6$ their associated coefficients, s represents the survival rate in year y at the ith location, and t is the exact fraction of the year elapsed since the previous time period.

The Shepherd Model (Shepherd 1982) provides additional flexibility and ease of biological interpretation (derived in Quinn and Deriso (1999)):

$$s_{y,i} = \frac{e^{-z_i t}}{1 + (1 - e^{-z_i t}) K (A_{y,i})^{\gamma}} \tag{2.5a}$$

<div align="right">Shepherd Model</div>

where e^{-z} is the density independent survival rate at the ith site, γ controls the intensity (shape) of density dependence, and K controls the strength of density dependence. If one considers K to be a function of environmental covariates, then the Shepherd Model can be represented as a linear combination of log scale predictors and coefficients as

shown in eq. (2.5b).

$$s_{y,i} = \frac{e^{-z_i t}}{1 + (1 - e^{-z_i t}) \exp(\beta_{0_i} + \gamma \ln A_{y,i} + \beta_2 \ln x_{2_{y,i}} + ... + \beta_6 \ln x_{6_{y,i}})} \qquad (2.5b)$$

The Shepherd Model provides unique flexibility in the parameterization because it can range from density independent ($\gamma = 0$), to a decelerating but non-saturating density dependent form ($0 < \gamma < 1$), to a saturating form ($\gamma = 1$), and finally to an overcompensatory form (when $\gamma > 1$) in which survivors (eventually) approach zero as abundance increases indefinitely. However, this model also requires an additional parameter because it separates the density independent survival rate (e^{-z}) from the scale parameter β_0, which now becomes a nuisance parameter. Thus I used the Logistic Model (eq. 2.4) for statistical simplicity and the Shepherd Model (eq. 2.5b) for biological flexibility. I compared the emergent properties of the two model forms to evaluate their qualitative agreement.

I applied stochastic search variable selection (SSVS, George and McCulloch (1993)) to the Logistic and Shepherd Models using Gibbs sampling to evaluate which combination of variables exhibited strong correlations with adult survival rates. SSVS searches across the multitude of unique covariate combinations and returns the probability that unique combinations should be included. Following SSVS model selection I re-estimated the best Shepherd and Logistic Model for analysis including only covariates supported by 2lnB >10 in the SSVS procedure. In performing model selection I included an AR(1) model on the error terms to account for potential bias due to serial autocorrelation in the

dataset. In all models I used vague or uninformative priors. Posterior predictive checks (Gelman et al. 2013), a table of prior specification and prior vs. posterior comparisons are provided in Appendix B. Posteriors were sampled using JAGS (Plummer 2013) called from R (R Core Team 2014). Comparative effect size of food supply on equilibrium abundance

The estimation of effect size is critical in generating inference (Osenberg et al. 2002). Thus I sought to determine the magnitude by which food supply and density dependence impact population dynamics in terms of equilibrium abundance and population variability using the modified Shepherd Model (eq. 2.5b) posterior. To quantify individual and combined effects of each significant covariate in the models, I combined correlative stock-recruit models (see Okamoto et al. 2012) with the modified Shepherd Model (eq. 2.5b) and numerically solved for the equilibrium density under steady food conditions. I did this for food supply ranging from low to high as it impacts both recruitment and adult survival, which allowed us to compare effect sizes of constant food supply on expected equilibria via adult survival and via recruitment. While these solutions provided information about mean effect sizes, I recognized that the environment is not constant and I expanded the analysis to evaluate expected population variability in response to simulated environmental variability.

Comparative effect size of nonlinearity and food supply on population vari-

ance

To assess how density dependent adult survival, recruitment variability, and food supply for adults comparatively impact population variability, I simulated temporal variability in food supply and projected the population size through time (using the parameterized model from the previous section) under 4 different alternative scenarios: (1) recruitment is unchanged by food supply, (2) adult survival is compensatory but unchanged by food supply, (3) adult survival is constant [fixed at the mean of (2)] with no compensatory response, and (4) both recruitment and adult survival respond to food supply, with compensatory adult survival. I simulated variability in food supply that is temporally correlated in time using a truncated multivariate normal distribution, with the truncation set to the maximum and minimum observed values with the correlation between food supply for adults and food supply for recruitment set to the observed value ($r = 0.88$). To simulate a relatively strong autocorrelated food supply, I generated values using Markov chain Monte Carlo, and tuned each simulation to provide a partial autocorrelation at lag 1 of $\phi = 0.65$. Simulations with no autocorrelation in the food supply provide qualitatively similar results.

Generalized buffering effect of density-dependent adult mortality against

recruitment variation

Both the degree of adult density dependence and the average ratio of juveniles to adults are likely to dictate the sensitivity of adult fluctuations to recruitment variability. Moreover, a variety of mechanisms (beyond food supply) may impose density dependent survival such as variability in shelter habitat. To generalize beyond this surfperch system, I explored the sensitivity of adult fluctuations to recruitment variability in hypothetical populations under a range of adult density dependence and recruitment productivity scenarios in a simplified, more general population model. To generalize the model, I combined the basic Shepherd Model of adult survival (eq. 2.5a) with a standard Cushing stock-recruitment function to provide a flexible model of adult survival and recruitment. A_{y+1} = surviving adults (Shepherd Model) + recruitment (Cushing SR function)

$$A_{y+1} = \frac{A_y e^{-zt}}{1 + (1 - e^{-zt}) K (A_y)^\gamma} + \alpha (A_{y-2})^\beta \tag{2.6}$$

where α is the density independent per-capita productivity parameter, and β controls density dependence in recruitment. Using this generalized model, I simulated how adult population variability responded to a gradient of temporal variability in α (CV = 0.1 to 1) across a factorial gradient of mean recruitment productivity values ($\bar{\alpha}$) and strength of adult density dependence (γ). I ranged γ from 0 (no density dependence) to 1 (saturating survival) up to 4 (strong overcompensation); ranged from = 0.25 to 1.50 (mean adult to

recruit ratios thus ranged from 0.1 to 0.5). For each set of simulations within a given level of variability in α, I tuned the density independent adult mortality (z) such that across the gradient of γ the time averaged adult survival rate was constant. Here I report results of simulations where α exhibited serial correlation at lag 1 of $\phi = 0.65$. Simulations with no autocorrelation in the food supply provide qualitatively similar results. Because CV in adults tended to increase linearly with CV in α, I measured sensitivity of population fluctuations to recruitment variability as the slope of this relationship, given by eq. (2.7).

$$\frac{\Delta CV_{adults}}{\Delta CV_{\alpha}}$$

(2.7)

Sensitivity of adult fluctuations

Results

These analyses indicated that adult survival rates varied among years; there was strong evidence against a single, static survival rate (2lnB = 19.4), despite large uncertainty in survival estimates within each year. The SSVS procedure with both the Logistic and Shepherd Models revealed strong correlations between estimated changes in survival and both food supply (positive) and adult conspecific density (negative) (Table 3.4; Figure 2.1). The posterior suggests that adult survival rates declined as density increased or as food became scarce (Figure 2.2). Moreover, the impact of food supply diminishes as adult density decreases, as indicated by the similar survivorship across the range of food supply for low-density circumstances (Figure 2.2). Despite the

strength and weight of evidence in favor of interactions observed, there was also sub-stantial uncertainty in the estimated effects of adults and food supply. The Shepherd Model indicates competition exists, with parameter estimates in the 95% credible set ranging from very weak to strong overcompensatory dynamics (Figure 2.2). Likewise, food impacts are strong but are highly uncertain where increased food supply and adult density occur together, illustrated by highly variable predictions of survivorship (Figure 2.2). Qualitatively similar results were obtained for the Logistic Model (see Appendix B, Figure B.3). Effect size of food supply on equilibrium population size

Model results indicate that the magnitude of the estimated effect on equilibrium densities from variation in adult survival due to food is nearly identical to that of the expected effects of recruitment variation due to food across the range of observed values. Unsurprisingly, these effects also combine to increase equilibrium densities. The impacts of food via recruitment and via adult survival, in this case, were estimated to be of near equal and additive importance (assuming temporally constant environmental conditions) (Figure 2.3). Comparative effect size of nonlinearity and food supply on population variability

These results revealed three key findings with respect to the response of population variability to food supply. First, the importance of recruitment variation on simulated fluctuations in adult numbers was diminished by compensatory survival. Second, simu-lated population variability was impacted similarly by variation in both recruitment and adult survival due to variability in food supply. Third, simulated variability in adult

numbers responded stronger to combined effects of recruitment variation and variation in adult survival due to food than individual effects alone. Variability in simulated adult density increased steeply with variability in food when variation in recruitment was driven by food supply and adult survival (Figure 2.4). However, by incorporating adult density dependent survival this variability in adult population size was minimized because not all recruitment variation is incorporated into adults (Figure 2.4. The separate impacts of food variability via recruitment and density dependent adult survival are similar in magnitude and when combined, result in markedly increased variability.

Generalized effects of density-dependent adult mortality on population variance

The final aspect of this study explored a general model of effects of fluctuations in adults regardless of the underlying mechanism. Increasing the strength of adult compensatory survival buffers against stochastic recruitment variability across a range of $\bar{\alpha}$ (density-independent per-capita reproductive rates) (Figure 2.5). This effect is independent of the mean adult survival rate because that rate is controlled for directly in the simulation. The dampening effect is strongest with overcompensatory adult survival and increases as $\bar{\alpha}$ increases. This change with increasing $\bar{\alpha}$ occurs because the overall contribution of new individuals to the adult stage (ratio of juveniles to adults) increases as $\bar{\alpha}$ increases; thus larger $\bar{\alpha}$ values make the contribution of recruitment overwhelm any adult density-related feedback.

Discussion

When populations are subject to dramatic decreases in food supply, it is reasonable in some cases to expect corresponding decreases in adult survival, especially when densities of competing adults are high. Whether populations actually experience a decrease will depend upon the magnitude of temporal variability in food availability and the extent to which reductions in fecundity, energy reserves or somatic growth can buffer survival against nutritional stress in adults (Charnov 1986, Gaillard and Yoccoz 2003). Here I demonstrated strong evidence that variation in adult density and food abundance impact survival rates of adult fish. These correlations run counter to the common assumption in many population models that adult survival is constant and density independent. I show that the estimated relationships provide very different expectations of population equilibria and temporal variance compared to the case where survival is assumed to be constant (Figure 2.4). In the case of black surfperch, the estimated effect size of food-driven adult survival on population size rivaled that of food-driven recruitment both in terms of estimated equilibrium density (Figure 2.3) and variance (Figure 2.4). Moreover, density dependent survival dampened the impact of recruitment variation on population variability (Figure 2.4). While parameter estimates of these models include uncertainty (Figure 2.2), the general conclusions from these analyses apply across a spectrum of parameter values and to systems where competition for resources varies through time (Figure 2.5).

Several questions remain unanswered regarding why black surfperch appear to exhibit resource-mediated density dependent survival of adults. Specifically, how the density-survival interactions are manifested mechanistically remains uncertain because I cannot parse the density related feedback into the components that drive survival. These data contain no sex specific information, nor any direct estimates of the demographics of adult mortality. In addition, extrinsic factors such as predation or habitat availability may be a mediator of these estimated food-density impacts. Predation, for example, may provide the ultimate source of mortality simply because weak fish are eaten (Cushing 1975), so while densities of their main predators remained steady at the site over the duration of the study (Carretta et al. 2011), predation rates may still increase as surfperch food becomes scarce and surfperch are either weaker or required to spend more time foraging (Holbrook and Schmitt 1988). In a similar fashion, low availability of foraging habitat may increase susceptibility of individuals to fluctuations in food density within those habitats. Black surfperch depend strongly upon their foraging habitat (Hixon 1981, Holbrook and Schmitt 1984, 1986, 1988, Schmitt and Holbrook 1986) and prior to the period covered by this study, a marked decrease in habitat availability corresponded with a decline in overall black surfperch abundance (Okamoto et al. 2012). Since then, habitat availability in the system exhibited little variability in comparison to within-habitat food density, which varied by an order of magnitude. The black surfperch population may therefore require higher food density currently than it did when habitat availability was greater. These other potential interactions point to the fact that the strength of

any density-resource interactions are likely to change over time via a complex set of interacting mechanisms. Thus, while there is a rich history of incorporating predator, food and ratio dependence into behavioral responses (Abrams and Ginzburg 2000), for most time series studies of population dynamics, the present included, the ability to capture the "true" functional responses rather than just general correlations is an elusive challenge.

This study highlights the general problem of low confidence in relationships between food, density and other factors driving demographic rates for most species. For many species, even estimating a mean survival rate over time provides a substantial challenge and there remains debate about whether it is possible without direct, empirical measurement (Francis 2012, Lee et al. 2011). Such assessments of annual vital rates through time often require ongoing mark recapture or other methods, and these approaches typically involve substantial logistic challenges and costs. So what alternatives remain given the potentially high likelihood of mischaracterizing dynamics by assuming stationary survival? Several powerful alternatives to standard stock-assessment type models exist that relax simplifying assumptions about complex systems. These include state-space reconstruction (SSR) techniques with little to no underlying model structure that have the potential to outperform explicit models in short term forecasting (Perretti et al. 2013). However, if the system population is strongly influenced by resources such as food availability, these methods still require experiments and ecosystem based studies to identify and provide time-series that can benefit predictive power (Dixon et al. 1999).

These findings provide important insight into the dynamics and stability of stage and age structured populations. In populations where adult survival and recruitment (via fecundity or juvenile survival) are sensitive to variation in food supply, there is a potential two-fold impact. Positive covariance between adult survival and recruitment can magnify the impact of the other (Jongejans et al. 2010). In this case, food supply directly lowers the number of reproductive adults but also reduces the number of recruits per adult. Yet environmental variability can be buffered or amplified by both density dependence as well as cohort effects (Lindström and Kokko 2002); thus the inertia of perturbations in affecting variability can be complicated and perhaps unpredictable. Recent studies using standard models suggest decreases in overall survival via fishing may increase population fluctuations (Anderson et al. 2008, Rouyer et al. 2012, Shelton and Mangel 2011). Here I show an important mechanism that can drive such variability: density dependent adult survivorship buffers against fluctuations driven by recruitment variability. As a result, a change in the density independent survival rate via exploitation will reduce this feeback and make populations much more sensitive to environmentally driven recruitment. As a result, fishing mortality (or any other surplus mortality) can decrease the stability of these systems by tampering with negative feedbacks in the adult stage. Given the challenges these concepts impose, standard metrics of population resilience and stability may be dangerously erroneous if density-dependent feedbacks and environmental variation individually or interactively drive survival of mature individuals. As a result, thorough, process-based studies are desperately needed to continually

evaluate whether the common assumptions of stationarity and linearity are valid and/or acceptable.

Acknowledgements

References

Abrams, P. A. 2009. When does greater mortality increase population size? The long history and diverse mechanisms underlying the hydra effect. Ecology Letters 12:462–474.

Abrams, P. A., and L. R. Ginzburg. 2000. The nature of predation: prey dependent, ratio dependent or neither? Trends in Ecology & Evolution 15:337–341.

Anderson, C. N., C.-h. Hsieh, S. A. Sandin, R. Hewitt, A. Hollowed, J. Beddington, R. M. May, and G. Sugihara. 2008. Why fishing magnifies fluctuations in fish abundance. Nature 452:835–839.

Brodziak, j., J. Ianelli, K. Lorenzen, and R. D. Methot. 2011. Estimating natural mortality in stock assessment applications. U.S. Dep. Commer., NOAA Tech. Memo. NMFS-F/SPO-119.

Carlin, B. P., and S. Chib. 1995. Bayesian model choice via Markov chain Monte Carlo methods. Journal of the Royal Statistical Society: Series B (Statistical Methodology) 57:473–484.

Carretta, J. V., K. A. Forney, E. Oleson, K. Martien, M. M. Muto, M. S. Lowry, J. Barlow, J. Baker, B. Hanson, D. Lynch, L. Carswell, R. L. B. Jr., J. Robbins, D. K. Mattila, K. Ralls, P. Opay, B. Norberg, J. Laake, D. Lawson, J. Cordaro, E. Petras,

D. Sweetnam, and C. Yates. 2011. U.S. Pacific Marine Mammal Stock Assessments. U.S. Dep. Commer., NOAA Tech. Memo. NMFS-SWFSC-488.

Charnov, E. L. 1986. Life history evolution in a" recruitment population": why are adult mortality rates constant? Oikos 46:129–134.

Clark, W. 1999. Effects of an erroneous natural mortality rate on a simple age-structured stock assessment. Canadian Journal of Fisheries and Aquatic Sciences 56:1721–1731.

Clutton-Brock, T., A. Illius, K. Wilson, B. Grenfell, A. MacColl, and S. Albon. 1997. Stability and instability in ungulate populations: an empirical analysis. American Naturalist 149:195–219.

Cushing, D. 1975. The natural mortality of the plaice. Journal du Conseil 36:150–157.

Dixon, P. A., M. J. Milicich, and G. Sugihara. 1999. Episodic fluctuations in larval supply. Science 283:1528–1530.

Eberhardt, L. 2002. A paradigm for population analysis of long-lived vertebrates. Ecology 83:2841–2854.

Elliott, J., and M. Hurley. 1998. Population regulation in adult, but not juvenile, resident trout (*Salmo trutta*) in a Lake District stream. Journal of Animal Ecology 67:280–286.

Francis, R. 2012. The reliability of estimates of natural mortality from stock assessment models. Fisheries Research 119:133–134.

Fryxell, J. 1987. Food limitation and demography of a migratory antelope, the white-eared kob. Oecologia 72:83–91.

Gaillard, J.-M., M. Festa-Bianchet, N. Yoccoz, A. Loison, and C. Toigo. 2000. Temporal variation in fitness components and population dynamics of large herbivores. Annual Review of Ecology and Systematics 31:367–393.

Gaillard, J.-M., M. Festa-Bianchet, and N. G. Yoccoz. 1998. Population dynamics of large herbivores: variable recruitment with constant adult survival. Trends in Ecology & Evolution 13:58–63.

Gaillard, J.-M., and N. G. Yoccoz. 2003. Temporal variation in survival of mammals: a case of environmental canalization? Ecology 84:3294–3306.

Gelman, A., J. Carlin, H. Stern, D. Dunson, A. Vehtari, and D. Rubin. 2013. Bayesian Data Analysis. 3rd ed. Chapman & Hall, London.

George, E. I., and R. E. McCulloch. 1993. Variable selection via Gibbs sampling. Journal of the American Statistical Association 88:881–889.

Heppell, S. S., H. Caswell, and L. B. Crowder. 2000. Life histories and elasticity patterns: perturbation analysis for species with minimal demographic data. Ecology 81:654–665.

Hixon, M. 1981. An experimental analysis of territoriality in the California reef fish *Embiotoca jacksoni* (Embiotocidae). Copeia 3:653–665.

Holbrook, S. J., and R. J. Schmitt. 1984. Experimental analyses of patch selection by foraging black surfperch (*Embiotoca jacksoni* Agazzi). Journal of Experimental Marine Biology and Ecology 79:39–64.

———. 1986. Food acquisition by competing surfperch on a patchy environmental gradient. Environmental Biology of Fishes 16:135–146.

———. 1988. Effects of predation risk on foraging behavior: mechanisms altering patch choice. Journal of experimental marine biology and ecology 121:151–163.

———. 2002. Competition for shelter space causes density-dependent predation mortality in damselfishes. Ecology 83:2855–2868.

Hollowed, A. B., J. N. Ianelli, and P. A. Livingston. 2000. Including predation mortality in stock assessments: a case study for Gulf of Alaska walleye pollock. ICES Journal of Marine Science 57:279–293.

Jiao, Y., E. P. Smith, R. O'Reilly, and D. J. Orth. 2012. Modelling non-stationary natural mortality in catch-at-age models. ICES Journal of Marine Science 69:105–118.

Jongejans, E., H. De Kroon, S. Tuljapurkar, and K. Shea. 2010. Plant populations track rather than buffer climate fluctuations. Ecology letters 13:736–743.

Jørgensenn, C., B. Ernande, Ø. Fiksen, and U. Dieckmann. 2006. The logic of skipped spawning in fish. Canadian Journal of Fisheries and Aquatic Sciences 63:200–211.

Kass, R. E., and A. E. Raftery. 1995. Bayes factors. Journal of the American Statistical Association 90:773–795.

Knape, J., and P. de Valpine. 2012. Are patterns of density dependence in the Global Population Dynamics Database driven by uncertainty about population abundance? Ecology Letters 15:17–23.

Lafferty, K. D., and A. M. Kuris. 1993. Mass mortality of abalone *Haliotis cracherodii* on the California Channel Islands: tests of epidemiological hypotheses. Marine Ecology Progress Series 96:239–239.

Lapointe, M., R. Peterman, and B. Rothschild. 1992. Variable natural mortality rates inflate variance of recruitments estimated from virtual population analysis (VPA). Canadian Journal of Fisheries and Aquatic Sciences 49:2020–2027.

Laur, D. R., and A. W. Ebeling. 1983. Predator-prey relationships in surfperches. Environmental Biology of Fishes 8:217–229.

Lee, H.-H., M. N. Maunder, K. R. Piner, and R. D. Methot. 2011. Estimating natural mortality within a fisheries stock assessment model: an evaluation using simulation analysis based on twelve stock assessments. Fisheries Research 109:89–94.

Lindström, J., and H. Kokko. 2002. Cohort effects and population dynamics. Ecology Letters 5:338–344.

Lodewyckx, T., W. Kim, M. D. Lee, F. Tuerlinckx, P. Kuppens, and E.-J. Wagenmakers. 2011. A tutorial on Bayes factor estimation with the product space method. Journal of Mathematical Psychology 55:331–347.

Mduma, S. A., A. Sinclair, and R. Hilborn. 1999. Food regulates the Serengeti wildebeest: A 40 year record. Journal of Animal Ecology 68:1101–1122.

Okamoto, D., R. Schmitt, S. Holbrook, and D. Reed. 2012. Fluctuations in food supply drive recruitment variation in a marine fish. Proceedings of the Royal Society B: Biological Sciences 279:4542–4550.

Osenberg, C. W., C. M. St Mary, R. J. Schmitt, S. J. Holbrook, P. Chesson, and B. Byrne. 2002. Rethinking ecological inference: density dependence in reef fishes. Ecology Letters 5:715–721.

Perretti, C. T., S. B. Munch, and G. Sugihara. 2013. Model-free forecasting outperforms the correct mechanistic model for simulated and experimental data. Proceedings of the National Academy of Sciences 110:5253–5257.

Plummer, M. 2013. Just Another Gibbs Sampler (JAGS) Software, Version 3.4.0. http://mcmc-jags.sourceforge.net/, 3rd ed.

Quinn, T., and R. Deriso. 1999. Quantitative fish dynamics. 1st ed. Oxford University Press, New York.

R Core Team. 2014. R: A language and environment for statistical computing. R Foundation for Statistical Computing, Vienna, Austria. URL http://www.R-project.org/.

Rideout, R. M., and J. Tomkiewicz. 2011. Skipped spawning in fishes: More common than you might think. Marine and Coastal Fisheries 3:176–189.

Rouyer, T., A. Sadykov, J. Ohlberger, and N. C. Stenseth. 2012. Does increasing mortality change the response of fish populations to environmental fluctuations? Ecology letters 15:658–665.

Schmitt, R. J., S. Holbrook, and C. Osenberg. 1999. Quantifying the effects of multiple processes on local abundance: a cohort approach for open populations. Ecology Letters 2:294–303.

Schmitt, R. J., and S. J. Holbrook. 1984. Gape-limitation, foraging tactics and prey size selectivity of two microcarnivorous species of fish. Oecologia 63:6–12.

———. 1986. Seasonally fluctuating resources and temporal variability of interspecific competition. Oecologia 69:1–11.

Shelton, A. O., and M. Mangel. 2011. Fluctuations of fish populations and the magnifying effects of fishing. Proceedings of the National Academy of Sciences 108:7075–7080.

Shepherd, J. 1982. A versatile new stock-recruitment relationship for fisheries, and the construction of sustainable yield curves. Journal du Conseil 40:67–75.

Tyler, A., and R. Dunn. 1976. Ration, growth, and measures of somatic and organ condition in relation to meal frequency in winter flounder, *Pseudopleuronectes americanus*, with hypotheses regarding population homeostasis. Journal of the Fisheries Research Board of Canada 33:63–75.

Tables

Table 2.1: Table of log-scale Bayes factors for variables influencing annual adult survival. Values greater than +10 are very strong evidence in favor of inclusion (shown in bold, requiring > 99% support given even prior odds); negative values indicate the null has more support than the alternative hypothesis. The values are calculated as 2lnB measuring strength of inference from the data in favor of the alternative hypothesis against the null. See Methods for model descriptions.

Variable	Shepherd Model	Logistic Model
Adult Density (y)	**12.3**	**14.9**
Prey Density (y)	**12.0**	**15.8**
Juvenile Density (y)	-4.9	-8.9
Prey Density ($y+1$)	-2.4	-7.3
Habitat Availability (y)	-4.9	-6.7
Habitat Availability ($y+1$)	-4.8	-6.7

Figures
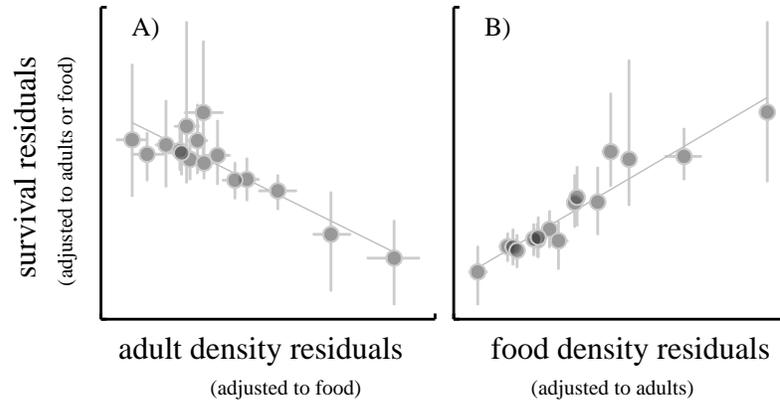
Figure 2.1: Added variable plots from the Logistic Model showing isolated relationships between logit-scale survival and A) adult density and B) food density in year (y) from the posterior samples with error bars showing the 10th and 90th posterior quantiles. Variables are adjusted by regressing both survival and the shown covariate against other covariates. The line represents the slope of the mean estimated relationship in the Logistic Model where this visualization technique can be applied; because the nonlinear survival function of food and adult density in the Shepherd Model is not linear under direct transformation, similar plots are not shown for this model. Non-dimensional axes are shown for simplicity because the data are residuals and are not directly interpretable.
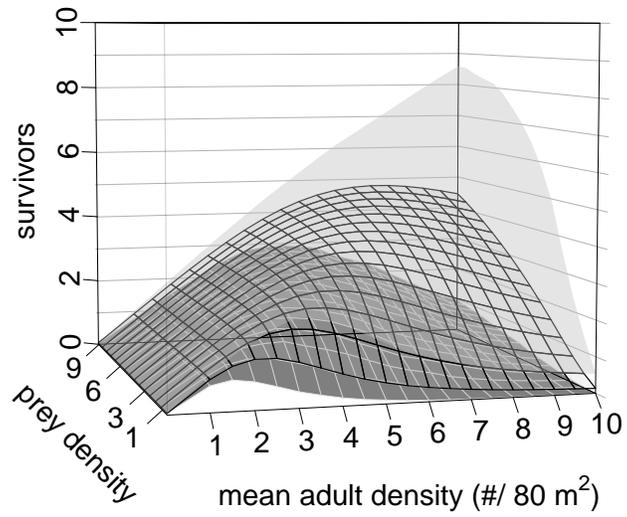
Figure 2.2: Survivorship as a function of both adult surfperch density and density of food based on posterior samples from the modified Shepherd Model (eq. 2.5b). The gridded surface represents the posterior mean expectation, while the grey surfaces represent the 95% posterior credible set for survival (z-axis) in each x-y combination. For a similar plot from the Logistic Model see Appendix B.
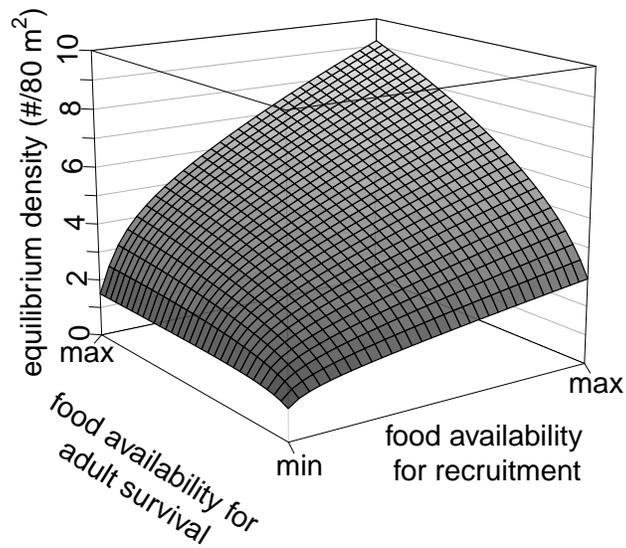
Figure 2.3: Estimated mean effect size of food availability on equilibrium density via recruitment and via adult survival from the correlative survival and recruitment models. The surface represents the prediction from the posterior mean from the Shepherd Model and the previously estimated recruitment models (Okamoto et al. 2012). The equilibrium density was solved numerically for each intersecting line, assuming a constant environment therein.
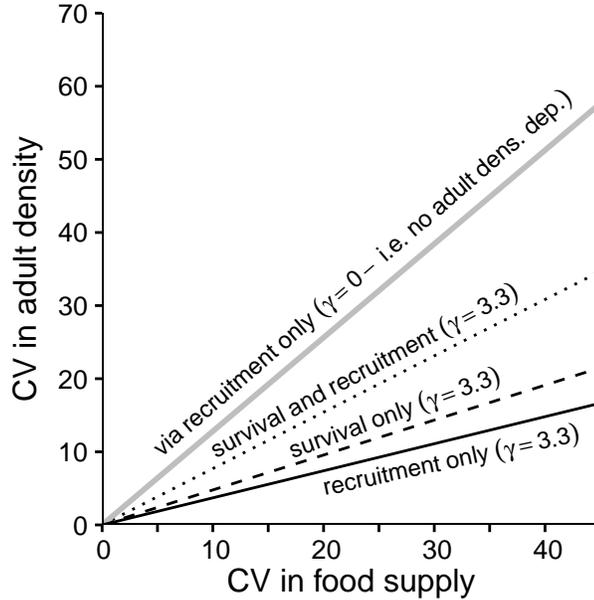
Figure 2.4: Effect of food variability on fluctuations in adult density under different model assumptions shown as the coefficient of variation (CV) in adult density versus CV in food supply. **Top (grey) line**: food variability only impacts the stock-recruit function, survival is density-independent and unaffected by food; **bottom (black) line**: food only impacts the stock-recruit function, survival is density dependent but unaffected by food; **dashed line**: food variability impacts only adult survival (with density dependence) and the stock recruit function is constant; **dotted line**: food variability impacts both recruitment and density dependent adult survival. **Top (grey) line vs bottom (black) line**: Reduction in slope due to density dependent adult survival alone. **Top (grey) line vs dashed line**: Isolated effects of food via adult survival vs recruitment. The first order autocorrelation in food supply for was set to $\phi = 0.65$; simulation sample size = 1000; parameter estimates were the posterior mean from the modified Shepherd Model and fitted values from the stock-recruit dynamics from Okamoto et al. (2012). Results from simulations with no autocorrelation are shown in Appendix B.
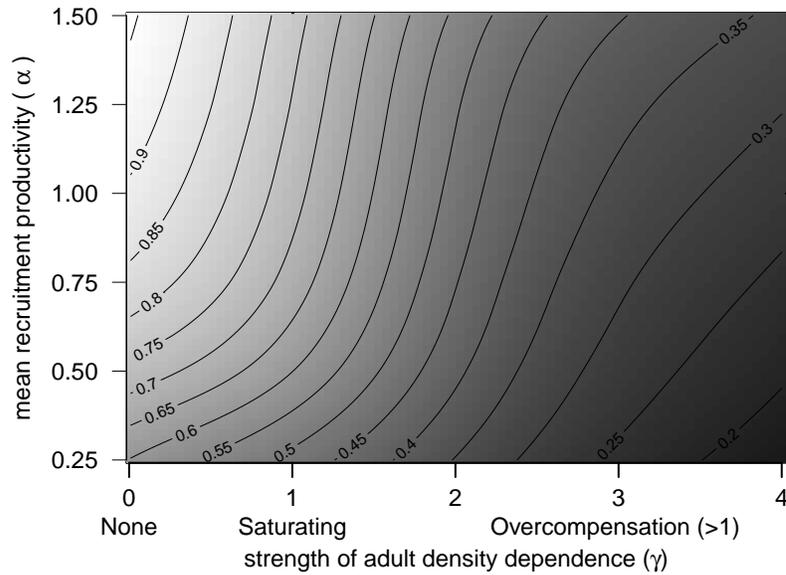
Figure 2.5: Contour plot of sensitivity of adult population fluctuations to stochastic recruitment variability as a function of adult density dependence (γ) and density-independent, per capita reproductive rate (mean recruitment productivity, $\bar{\alpha}$) in a simple, generalized population model (6). Stochasticity influences only α (i.e. no stochastic variability in γ) and for each level of $\bar{\alpha}$ density independent adult mortality is adjusted in the analysis such that the mean adult survival rate is constant for all values of γ. Sensitivity of adult fluctuations is the slope of the relationship between CV in adult density and CV in α (analogous to the slope of lines in Figure 2.4) and are indicated by the contour lines. Simulations for each $\bar{\alpha} - \gamma$ combination included simulating a unique 10,000 year time series for $CV(\alpha) \in 0.1, 0.2, , \dots, 1.0$.

Appendix B Supplemental tables and figures for "Effects of food limitation, density dependence and annual adult survival in a marine fish"
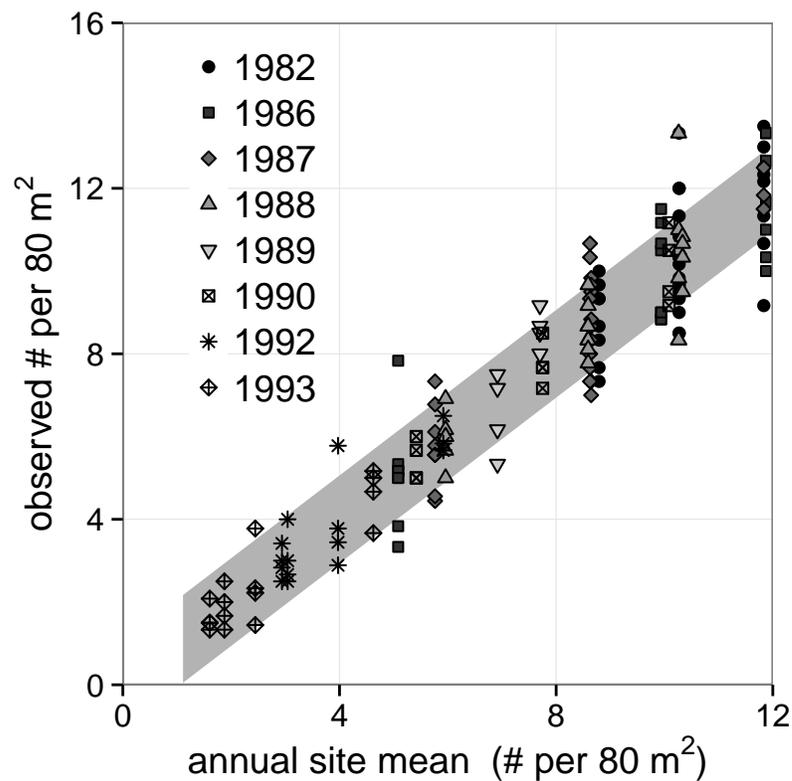
Figure B.1: Training dataset illustrating observed site densities versus the empirical mean for that site within that year. The grey bar represents the estimated standard error of 1.06 about the 1:1 line. The standard error was estimated using generalized least squares. There was no evidence that during this period within site error variance increased as a function of the mean, among years or among sites. These data represent sites that were visited by divers during late summer and early fall 4-16 times per year for replicate observation.

Table B.1: Parameter description for the Shepherd model under the SSVS procedure along with prior specification. The logistic model uses the same specification with the exception that there is no scale coefficient.

Parameter	Description	Prior
$\text{logit}\,(e^{-z_i})$	logit-scale density-independent annual survival rate for the ith site	$\text{N}\,(\mu[\text{logit}\,(e^{-z})], \sigma[\text{logit}\,(e^{-z})])$
$\mu[\text{logit}\,(e^{-z})]$	mean of $\text{logit}\,(e^{-z_i})$	$\text{N}\,(0, 1.5)$
$\sigma[\text{logit}\,(e^{-z})]$	among site variance in $\text{logit}\,(e^{-z_i})$	$\text{Uniform}\,(0, 1.5)$
β_{0i}	scale coefficient for the ith site	$\text{N}\,(\mu[\beta_0], \sigma[\beta_0])$
$\mu[\beta_0]$	mean scale coefficient	$\text{Uniform}\,(-5, 5)$
$\sigma[\beta_0]$	among site variance in scale coefficient	$\text{Uniform}\,(0, 5)$
γ	density dependent shape coefficient	$(1 - \psi_\gamma)\,\text{N}\,(0, 0.05) + \psi_\gamma N\,(0, 5)$
$\beta_2, \ldots, \beta_6$	other variable coefficients	$(1 - \psi_i)\,\text{N}\,(0, 0.05) + \psi_i N\,(0, 5)$
g	annual juvenile maturation rate	$\text{Uniform}\,(0, 1)$
ϕ	first-order autoregressive coefficient	$\text{Uniform}\,(0.9, 0.9)$
σ_{ϵ_i}	process error for the ith site	$\text{Uniform}\,(0, 100)$
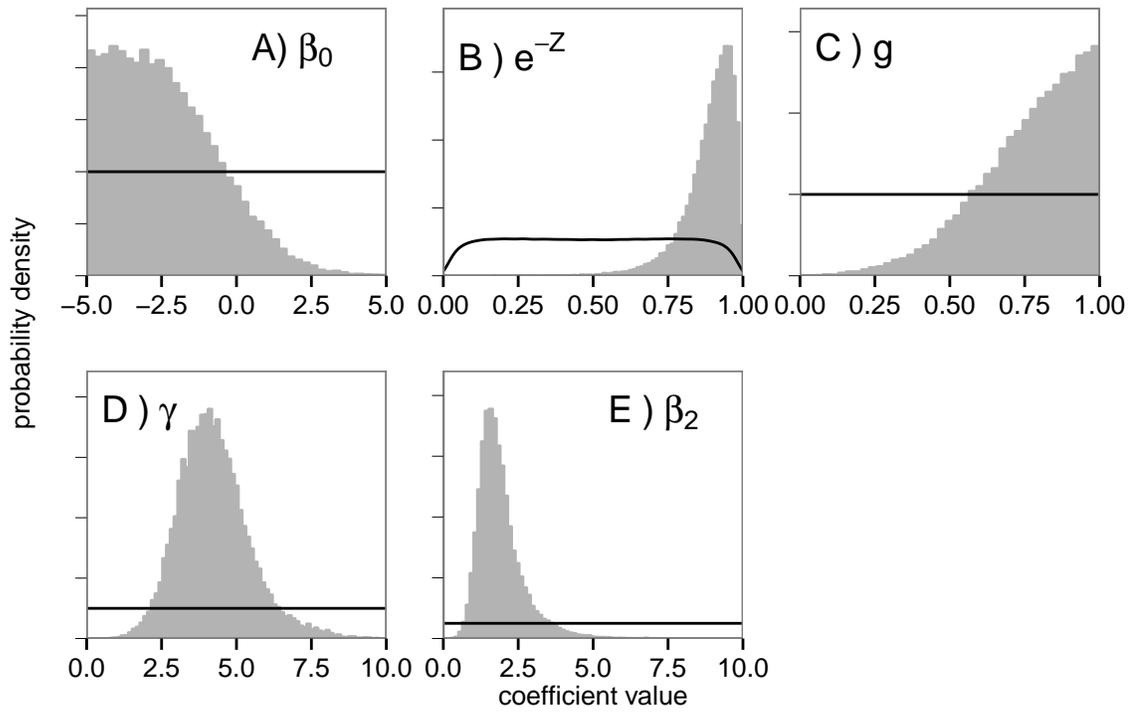
Figure B.2: Posterior (grey histograms) and prior (black line) densities for primary parameters in the Shepherd Model. Prior probabilities and parameter descriptions are shown in Table 3.4
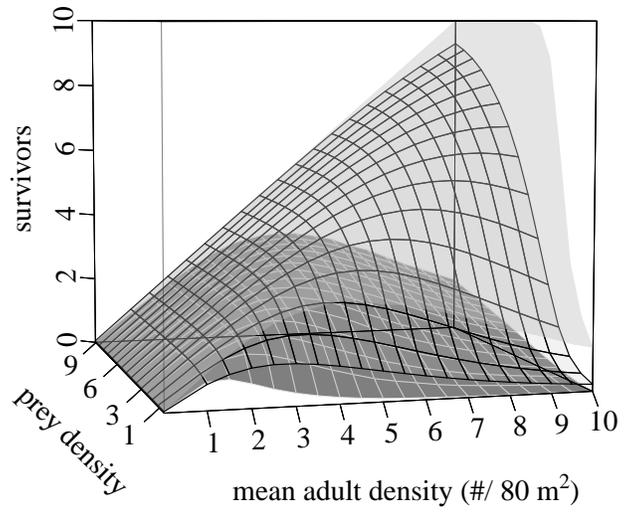
Figure B.3: Survivorship as predicted for given adult density and the observed range of prey density using posterior samples from the Logistic Model (eq 2.4). The gridded surface represents the posterior mean expectation, while the grey surfaces represent the 95% posterior credible set for survival (z-axis) in each x-y combination.
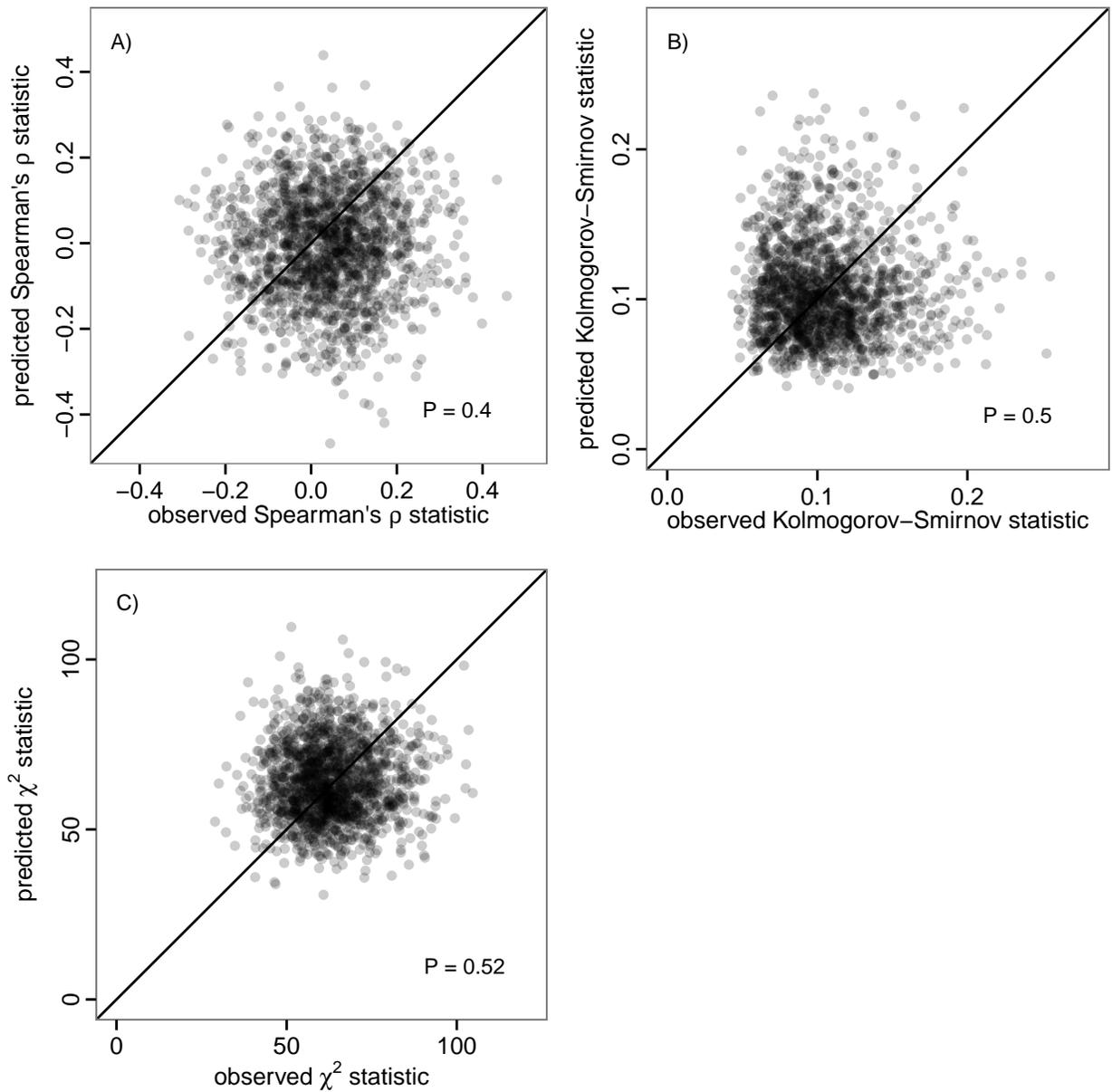
Figure B.4: Posterior predictive checks. Y-axes represent the predicted value, while x-axes represent realized statistics. P-values represent the number of values above the 1:1 line, where P-values approaching 0 or 1 represent a deviation from model assumptions. A) Spearman rank-order correlation statistics testing for correlation between error and the response values. B) Kolmogorov-Smirnov test statistics comparing adequacy of the lognormal likelihood function. C) Chi-squared goodness of fit-test statistics.

Chapter 3

Density-dependent sperm-egg interactions alter dynamics of fertilization and polyspermy in external fertilizers

Abstract

Current theory for species that have external fertilization suggests that the rates of fertilization and polyspermy (sperm toxicity) are dictated primarily by sperm concentrations. Although this suggests that individual zygote production and thus fitness increases monotonically with egg release rates, it ignores potentially important mechanisms such as competition for sperm among eggs and the potential for attraction of sperm to eggs, crowding effects or other density-dependent rates of sperm-egg interaction. Density-dependent interaction rates (such as attraction or crowding effects) may allow egg concentrations to affect the probability of viable fertilization. I experimentally test whether such egg effects occur using the urchin *Strongylocentrotus purpuratus* and expanded existing models to account for non-random interactions. The experiments revealed that at low sperm concentrations, eggs compete for sperm while at high sperm concentrations, high egg concentrations reduce the incidence of polyspermy. These observations are inconsistent with the random collision models but highly consistent with density-dependent sperm-egg interactions. As a result, there is a fitness trade-off of egg release: as sperm range from scarce to superabundant, interactions among eggs transition from highly competitive to facilitative in terms of viable fertilization rates.

Introduction

Fertilization of eggs tends to follow a fitness "Goldilocks" principle. Too few sperm results in low probability of fertilization while too many leads to polyspermy (multiple sperm entering one egg) and egg death (Franke et al. 2002, Levitan and Ferrell 2006, Levitan et al. 2007, Sewell et al. 2013). Because egg production is generally costly to females, achieving a middle ground for fertilization confers a substantial fitness advantage (Levitan 2004). Empirical and theoretical work on fertilization in broadcast spawners and has focused mostly on the role of sperm concentrations in shaping fertilization. In contrast, how egg concentrations affect fertilization dynamics remains surprisingly unexplored (but see Levitan et al. 1991 and Vogel et al. 1982). Egg concentrations have the potential to impact fertilization maxima in two primary ways. First, egg concentrations can alter the sperm-egg ratio and as eggs concentrations increase more sperm are needed to maximize fertilization because eggs deplete the sperm population. Second, the rate of per-capita sperm-egg interactions (also called "collision rates") may depend on egg concentrations with the result that faster or slower collision rates may shift the optimal range of sperm concentrations. If fertilization rates are dependent on the concentration of eggs then fitness of females may depend not only on sperm concentrations, but also on the rate of egg release during spawning.

Under existing models of broadcast spawning with purely random sperm-egg collisions, egg concentrations have little to no impact on fertilization rates (Bode and Mar-

shall 2007, Lauzon-Guay and Scheibling 2007, Levitan et al. 1991, Vogel et al. 1982). These models assume collision rates are unaffected by attraction of sperm to eggs, non-random search patterns or egg crowding effects. Yet sperm can exhibit attraction (Evans et al. 2012, Kaupp et al. 2006, Zimmer and Riffell 2011), structured search patterns (Farley 2002) and chemical cues from eggs can induce behavioral changes in swimming direction (Guerrero et al. 2010) and swimming speed (Wood et al. 2007) These properties provide strong potential for density-dependent collision rates, where per capita collision rates (no. per sperm, per egg, per second) decrease as egg concentrations increase.

Empirically demonstrating the presence of interaction parameters that vary with density presents a serious challenge for many biological processes, including disease transmission (McCallum et al. 2001) and predator-prey interactions (Cosner et al. 1999) in part because directly observing the interactions remains difficult. Instead interaction rates are estimated from the product of interactions integrated over space and time (i.e. total number of people infected, prey consumed or fertilized zygotes produced), yet this product often results from a complicated, unknown and highly variable series of processes. Because of its mathematical simplicity density-independence in interaction rates is commonly assumed. Whether or not this assumption is valid can have significant theoretical and practical consequences

Despite arguments in favor of the random sperm-egg collision model (also described as "mass action"; Millar and Anderson 2003, Styan 1998, Vogel et al. 1982), sperm and eggs from free-spawning species have the potential to exhibit per capita collision rates

that vary with egg concentration. For example, sperm that are attracted to eggs may move towards eggs when flow dynamics allow such autonomous behavior (Riffell and Zimmer 2007, Zimmer and Riffell 2011). To illustrate how this behavior leads to density dependent per capita rates of interaction, consider the following two circumstances: A) eggs are abundant and densely concentrated or B) eggs are rare and sparsely concentrated. Sperm concentrations are initially identical between the two. Sperm that are attracted to eggs will aggregate in higher density around individual eggs in case (B) than case (A). This greater density leads to higher overall interaction rates per sperm, per egg in (A) than (B). Thus, as egg concentrations vary from dense to sparse, the per capita collision rate increases and is likely to saturate at some maximum (restricted perhaps by limitations to attraction and motility). This is sensible given that chemoattractants can increase the "target size" of eggs (Jantzen et al. 2001), which is directly related to the collision rate. In contrast, purely random interactions (assumed by most models) yield identical per capita interaction rates between cases (A) and (B). Other mechanisms beyond attraction may yield similar density-dependent collision functional responses, such as crowding (where increasing concentrations of eggs can inhibit search patterns of sperm, for example).

If autonomous movement such as attraction is responsible for density-dependent per capita collision rates, then patterns in nature are likely to only exhibit such dynamics contextually. Specifically, water velocity and shear stress can alter the effectiveness of attractive behavior because the capacity form sperm autonomous motion of sperm

diminishes (Riffell and Zimmer 2007, Zimmer and Riffell 2011). In this case, laboratory systems are unlikely to relate well to nature and direct comparisons across taxa from lab experiments may not be possible. Bias may result from using or comparing conditional subsets of highly variable parameter space. Thus, from both a theoretical and practical standpoint it is important to understand whether the extend to which fertilization is governed by density-dependent interaction rates.

In this study I evaluate whether egg concentrations impact fertilization maxima, and explicitly test for random versus density-dependent sperm-egg collision rates. To achieve these goals I developed a new dynamic model, expanding upon existing fertilization dynamics models and then conducted an extensive laboratory fertilization experiment using purple sea urchin (*Strongylocentrotus purpuratus*) eggs and sperm. Finally I paramerterized and compared the performance of models that included random or density-dependent collision parameters by utilizing several different basic model forms and my empirical observations of fertilization and polyspermy.

Methods

In order to evaluate whether the trade off in sperm concentration is affected by egg concentrations I conducted multiple trials of a laboratory experiment that vary concentrations of eggs and sperm. I used two analytic approaches to test hypotheses. First I used a classical statistical approach by estimating generalized linear mixed effects models and tested for effects of sperm and egg concentrations on fertilization

and polyspermy. This method is valuable for empirically determining the effects of interaction rates on fertilization and polyspermy. Second I generated a set of new dynamic model and within this new model and within existing models compare constant vs density-dependent sperm-egg collision rates using a Bayesian hierarchical framework. This method is useful for comparing hypothetical dynamic processes rather than just emergent properties of the system.

Expanded dynamic and modified fertilization models

Existing models

Existing fertilization kinetics models, and interpretations thereof, assume purely random interactions between sperm and eggs. This means the instantaneous per capita rate of sperm-egg interactions (number of interactions per sperm, per egg) are independent of sperm and egg concentrations. Specifically, the model of Vogel et al. (1982) and extensions to include effects of polyspermy by Styan (1998) and Millar and Anderson (2003) are based upon a system of equations that describe the loss of viable sperm (S) and the reduction in unfertilized eggs (E_U) over time. These models assume: (1) sperm (S) attack a fixed population of eggs (fertilized or unfertilized, E_T) at a constant, per capita rate β, (2) a fixed proportion of sperm attacks result in fertilization (ϕ), and (3)

a sperm collision with an egg (successful or unsuccessful) renders that sperm inert. Such dynamics are given by eqns (3.1a) & (3.1b):

$$\frac{dS}{dt} = -\beta S(t) E_T \tag{3.1a}$$

$$\frac{dE_U}{dt} = -\phi \beta S(t) E_U \tag{3.1b}$$

This system of differential equations has solution given by eqns. (3.2a) & (3.2b):

$$S(t) = S_0 \exp\left(-t\beta E_T\right) \tag{3.2a}$$

$$E_U(t) = E_0 \exp\left(-\phi \frac{S_0}{E_T} \left(1 - \exp\left(-t\beta E_T\right)\right)\right) \tag{3.2b}$$

Styan (1998) and subsequently Millar and Anderson (2003) used this solution to generate an equation for the number of eggs that are fertilized and viable (E_M, monospermic zygotes); hereafter their models are referred to as the Styan and MA models (see Appendix C for the explicit model forms). These models explicitly describe the hypothetical process by which eggs mount defensive polyspermy block following the first successful sperm to penetrate the jelly layer. They consider the block to be a step function in that some time period after the first invader eggs are no longer penetrable, but are fully susceptible in the interim to a second fertilizer.

There are two drawbacks to using these methods as a null model against which to test for density-dependent interactions. First, there is no explicit term for sperm degradation over time. Instead Vogel et al. (1982) suggest substituting a sperm "half-life" (τ) for the duration of sperm-egg "contact time" t if the $t > \tau$. This assumes that the asymptotic dynamics are equivalent to a step function where there is no degradation until contact time reaches τ, and thereafter τ 100% of the sperm are not viable. A dynamic process of sperm viability decay is preferable to this method. Moreover, the Vogel et al. (1982) method of estimating τ is biased towards higher values as sperm concentrations increase (see Appendix C). Second, the models are also not generalizable to other applications because the dynamical system does not explicitly incorporate additional compartments; additional compartments which in this case include a) fertilized eggs vulnerable to polyspermy, b) polyspermic eggs, and c) monospermic zygotes invulnerable to a second sperm.

New dynamic model

In addition to using the Styan and MA models, I also generated an expanded model based upon a fully compartmentalized system of differential equations and I subsequently introduced non-random interactions to each of the three model forms. In the case of the new dynamic model, sperm (S) decay (per capita) at a natural rate r after release and, like eq. (3.1a), sperm collide with eggs (ET) at a constant rate β (density-depdendent interactions are accounted for later). The overall loss rate of sperm is given by eq. (3.3a):

$$\frac{dS}{dt} = -\beta S(t) E_T(t) - rS(t) \tag{3.3a}$$

Unfertilized eggs (E_U) are fertilized at a rate given by eq. (3.3b):

$$\frac{dE_U}{dt} = -\phi \beta S(t) E_U(t) \tag{3.3b}$$

but newly fertilized eggs (E_V) are still vulnerable to a second fertilizer. If these eggs induce a polyspermy block at rate θ and are fertilized by a second sperm at the same rate as unfertilized eggs, then the rate of change of vulnerable eggs is given by eq. (3.3c):

$$\frac{dE_V}{dt} = \phi \beta S(t) E_U(t) - \theta E_V(t) - \phi \beta S(t) E_V(t) \tag{3.3c}$$

Clearly this is a simplistic representation of polyspermy block dynamics, but I use this representation for simplicity. Eggs that successfully induce a polyspermy block without being fertilized by a second sperm (E_M) accumulate at the rate given by eq. (3.3d):

$$\frac{dE_M}{dt} = \theta E_V(t) \tag{3.3d}$$

while eggs that become fertilized by a second sperm (E_P) accumulate at the rate given by eq. (3.3e):

$$\frac{dE_P}{dt} = \phi \beta S(t) E_V(t) \tag{3.3e}$$

The value of such a system of equations is that the equations can be expanded to a system of partial differential equations (for time and space), to include advection of sperm and eggs, to incorporate any sperm degradation function, or to include introduction of fresh sperm and eggs as additional individuals spawn in space and time. The system above can easily be applied to laboratory settings for testing of hypotheses concerning fertilization dynamics.

Application to closed laboratory environments

If the system is closed (i.e. no advection) and fresh, virgin sperm and eggs are introduced all at once to the system at time $t = 0$, then the system which includes equations (3.3a), (3.3b), and (3.3c) can be integrated analytically with respect to t (and does not depend on equations (3.3d) or (3.3e)). In this case, $E_T(\text{t})$ becomes the constant E_T (initial number of eggs), all eggs at time $t \approx 0$ are unfertilized (i.e. $E_U(t = 0) = E_T$

and let $S(t = 0) = S_0$. The solutions in such a circumstance are given by eq. (3.4a)-(3.4c):

$$S(t) = S_0 \exp\left(t\left(-\beta_0 E_T - r\right)\right) \tag{3.4a}$$

$$E_U(t) = E_T \exp\left(-\frac{\beta_0 S_0 \phi}{\beta_0 E_T + r} - \frac{\beta_0 S_0 \phi e^{-t(\beta_0 E_T + r)}}{-\beta_0 E_T - r}\right) \tag{3.4b}$$

$$E_V(t) = \frac{\beta E_T S_0 \phi \left(e^{t(\beta E_T - \theta + r)} - 1\right)}{\exp\left(t(\beta E_T - \theta + r) + \frac{\beta S_0 \phi e^{t(-(\beta E_T + r))}}{-\beta E_T - r} + \frac{\beta S_0 \phi}{\beta E_T + r} + \theta t\right)(\beta E_T - \theta + r)} \tag{3.4c}$$

The number of eggs successfully fertilized by a single sperm that are invulnerable to a second sperm (the integral of eq. (3.3d)) cannot be generated analytically. However, because eq. (3.3d) is solely a function of θ and $E_V(t)$, its solution can be expressed as given by eq. (3.4d):

$$E_M(t) = \theta \int_0^t E_V(t)dt \tag{3.4d}$$

where $E_V(t)$ is given by eq. (3.4c). This is now a single differential equation and the integral can quickly and accurately be approximated numerically using simple numerical integration methods (see *Parameter estimation for the dynamic model and other fertilization models*).

Addition of density-dependent sperm-egg interactions to kinetics models

Incorporation of non-random sperm-egg interactions, specifically attraction, can be incorporated into models of fertilization in a variety of ways (including the above systems as well as the model of Styan (1998) or Millar and Anderson (2003)). The simplest manner of incorporating such dynamics is by allowing therate at which sperm attack eggs (β) to vary with egg concentration. The justification for such an approach is the fact that the chomoattractant act to increase the "target siz" of eggs. I incorporate varying collision rates by simply allowing unique collision rates (β_i) for each egg concentration treatment (E_{Ti}) which is valuable given there is no known functional relationship that drives non-random sperm egg interactions. One could easily employ a Type II functional response (Cosner et al. 1999, Holling 1959) on the per-capita collision parameter, but without experimentation there is no way to evaluate what shape is biologically appropriate.

Laboratory experiments

I conducted eight laboratory trials of an experiment the purple sea urchin *Strongylocentrotus purpuratus* between February 23 and March 8, 2014 during their spawning season. Each trial included a factorially crossed gradient of four egg concentrations with six sperm concentrations, using gametes from one male and one female. The experiment took place in a climate-controlled room at 13 C, and each experimental unit consisted of a 20 ml vial with 10 ml seawater. For each trial I first added 8 ml seawater to the 24 experimental vials, followed by 1ml appropriate egg solution and finally providing

each vial with 1ml freshly diluted sperm solution. Vials were gently agitated and left for 120 minutes to allow fertilization and first cleavage to occur. Following the 120 minute incubation period,vials were agitated and emptied into shallow petri dishes for examination under an inverted compound microscope where 100 random, undamaged eggs were scored for fertilization, cleavage and polyspermy. Fertilization criteria included the presence of a raised vitelline membrane or cell division; cleavage criteria included only cells that divided normally (radial division) at least once; positive recognition of polyspermy required tetrahedral or further abnormal division of the cell.

Urchins were collected with the help of the Santa Barbara Coastal Long Term Ecological Research (SBC LTER) program at a depth of approximately 7 m below mean low water at the Mohawk Reef near Santa Barbara, California in late February, 2014. I maintained urchins in flow through seawater tables until needed (generally 3-5 days). To obtain eggs, females were induced to spawn by injecting 1 ml 0.55M KCl adjacent to the Aristotle's lantern, gently agitated, and placed upright into a small container with seawater. Once a female began profusely extruding eggs, 1 ml of concentrated egg material was extracted in 200 μl batches directly from the gonopores and placed into 50 ml seawater. This solution was then diluted and added to each vial such that vials had final concentrations of approximately 1, 0.25, 0.0625, or 0.0124 eggs μl^{-1}. To obtain sperm, I injected males with KCl in the same manner as females but extracted 100 μl "dry" sperm directly from the gonopore without submerging the animal. Sperm were immediately diluted 100x in seawater, directly followed by six serial 10x dilutions. Sperm solutions

were then added in 1ml aliquots to the vials prepared with eggs (final concentrations $\approx 10^{-3}, 10^{-4}, 10^{-5}, 10^{-6}, 10^{-7}$ & 10^{-8} μl^{-1}). Actual sperm concentrations in vials varied slightly because of small variability in sperm counts (see Figure 3.1 for range).

To estimate sperm concentrations used in each trial, I preserved the 10^{-3} μl^{-1} sperm solution with 2% buffered formalin and conducted five replicate sperm cell counts on a hemocytometer. I estimated egg concentrations for each trial by counting the number of eggs in five replicate 100 μl subsamples (agitated and homogeneous) using an inverted microscope.

Classic statistical analysis

I first analyzed data using generalized linear mixed effects models (GLMMs) with a binomial likelihood to evaluate whether egg concentrations influence rates of fertilization and polyspermy. I conducted separate analyses on the proportion of eggs that were fertilized and the proportion of eggs with polyspermy. In each model, trial (an individual-male female combination) was treated a random effect. Covariates for fertilization included a third order polynomial of the log of sperm concentration, log of egg concentration and their interaction as the full model. For polyspermy I used the log of sperm concentration and log of egg concentration as the full model. I tested hypotheses of individual effects of eggs and sperm on fertilization using likelihood ratio tests. I estimated GLMMs using the R library lme4 (Bates et al. 2014). These statistical mod-

els were employed to evaluate whether fertilization rates responded to sperm and egg concentrations.

Parameter estimation for the dynamic model and other fertilization models

In contrast to the statistical models described above, I employed the mechanistic models to test whether collision rates exhibit random or density dependent behavior. I estimated all models within a Bayesian hierarchical framework via the no-U-turn sampler variant of Hamiltonian Monte Carlo (HMC) (Hoffman and Gelman 2014) in Stan (Stan Development Team 2014a,b) using R (R Core Team 2014). The hierarchical framework is essential to account for potential among-pair variability in dynamics while also estimating overall means for those parameters. For all model formulations (the dynamic model, and the Styan and MA models), I included hierarchical effects for sperm collision rates (β) and egg selectivity (ϕ) to account for potential variability in rates among pairs. I assume no among-pair variability in other parameters. I assumed the response variable (fraction of 100 assessed eggs that were fertilized and viable = fraction fertilized - fraction with polyspermy) conformed to a binomial likelihood for all models.

For each model form (the Styan and MA models and the dynamic model) all parameters were given uniform priors over the boundaries of their realistic range. A constant sperm half-life was used for the Styan and MA models (though results are qualitatively insensitive to whether a constant value or a sperm concentration-dependent equation

95

provided by Levitan (1993) is used (see Appendix C for estimation of the sperm decay rate for the dynamic model, as well as for estimation and justification for using a constant sperm "half-life" for the Styan and MA models).

All parameters are described, along with their priors, in Table 3.1. For each parent model form I estimated models that consider the sperm collision rate (β) fixed (random collision model) or a function of each mean egg concentration. Sampling included 3200 total iterations from four chains, each of which included a 200 iteration burn in period. Because (3.4d) does not have an explicit form, each iteration in the MCMC chain of the dynamic model included generating the numerical solutions (expected fertilization given the parameter values) using Gauss-Legendre quadrature rules for each observation given parameter values.

I compared models using WAIC (widely applicable information criterion, Watanabe 2010), a Bayesian analog to the Akaike Information Criterion (AIC) with full theoretical support (Watanabe 2010).

Results

There was a clear trade-off between maximizing total fertilization and minimizing polyspermy in terms of both egg and sperm concentration. Egg concentration negatively affected the rate of fertilization, requiring more sperm to achieve similar fertilization rates with higher egg concentrations (Figure 3.1A, Table 3.2). The densest egg concentrations (1 μl^{-1}) required an order of magnitude more sperm than sparsest egg

concentrations ($\frac{1}{64}\mu l^{-1}$) to achieve the same fertilization rate (Figure 3.1A) with intermediate egg concentrations showing intermediate sperm requirements. In contrast rates of polyspermy decreased with egg concentration, where low concentrations of eggs resulted in much higher rates of polyspermy (Figure 3.1B, Table 3.2). Sparse egg concentrations increased rates of polyspermy by 25% at the highest sperm concentrations compared to the most concentrated egg samples.

Fertilization models

In all model forms, there was strong support for density-dependent interaction rates (Table 3.3). When allowed to vary, collision rates declined substantially as egg concentration increased. Compared to the lowest egg concentration ($\frac{1}{64}$ eggs μl^{-1}), the sperm collision rate declined by an estimated 45%, 108% and 138% at $\frac{1}{16}$, $\frac{1}{4}$, and 1 eggs μl^{-1} (Figure 3.2), respectively in the dynamic model (given as a proportion of the collision rate at $\frac{1}{64}$ eggs μl^{-1} in Table 3.4). None of the 95% credible sets for the decreases in collision rates overlap except those at 1 and $\frac{1}{4}$ eggs μl^{-1}. A similar decrease in collision rate was found for all three model forms. Predictions from the density-dependent collision model forms were consistent with the results of the experiment, reproducing the observed separation in fertilization curves between egg treatments (Figure 3.3)

In terms of model expectations, the largest difference between the random and density-dependent forms was between rates of polyspermy. The random collision models, where collision rates are constant, exhibit no separation among egg treatments at

high sperm concentration. In contrast, inclusion of collision rates that varied by egg concentration were consistent with the results of the experiment and had strong support over the null models (Table 3.3, Figure 3.4 C,D) for all three model forms. In other words, the effects of egg concentrations on polyspermy cannot be explained with the basic model outlined in eqns. (3.3a)-(3.3e) or the models of Styan (1998) or Millar and Anderson (2003).

The variability in total fertilization among egg concentrations (Figure 3.1A) can only partially be explained by the null model, while the density-dependent models explain the patterns well (Figure 3.4 A,B). This is because when sperm are rare, egg concentrations can affect fertilization by two independent processes The reduction in fertilization rates in the null model due to egg concentrations is solely a result of exploitative competition for sperm (i.e. more eggs use up more sperm, leaving fewer sperm attacks per individual egg). In contrast, both interference and exploitative competition explain the phenomenon in the density-dependent model. In this case, more eggs exist to attract sperm reducing the effective concentration around each egg (interference) *and* more eggs use up more sperm.

The observed pattern in Figure3.1A can plausibly be explained by exploitation of sperm by eggs alone, while the observed divergence in Figure 3.1B requires density-dependent collision rates in addition to depletion of sperm by eggs to yield the combined curve shown in Figure 3.3. The best supported models and the data illustrate that

increasing egg concentrations effectively shift the fertilization curve, thereby shifting the region of optimal sperm concentrations, previously expected to be static.

In all models there was considerable uncertainty in the parameter estimate for egg selectivity (ϕ, Table 3.4). This means that parameter estimates are averaged over the realistic range for this parameter. While the uncertainty in parameter estimates is substantial, this uncertainty does not undermine the support of the more complex models over the null given that WAIC directly accounts for parameter uncertainty. Thus, despite the lack of information about ϕ, there is sufficient information to support the density-dependent model over the null.

Results are robust to the sperm "half-life" that is used in the Styan (1998) or Millar and Anderson (2003) models. This occurs because using a longer or shorter half-life simply results in an inversely proportional change in the baseline collision rate because in all cases for these two models the two are multiplied together. Thus, while exact estimates of the collision rates differ, the WAIC, as well as estimates of all other parameters do not change.

In all cases, the Styan and MA models had far less support than the new dynamic model (Table 3.3).

Discussion

A rich body of evolutionary and ecological work is based upon the dynamics of sperm limitation in fertilization across a host of taxa (Bode and Marshall 2007, Levitan

99

1993, 1998, 2010, Parker and Lehtonen 2014, Podolsky and Strathmann 1996, Yund 2000). Yet current models of external fertilization assume random collision rates between sperm and eggs; moreover most work ignores the impact of egg concentrations (but see Levitan et al. 1991). If per-capita sperm-egg collisions are instead dependent upon egg concentrations this complicates the basic dynamics governing fertilization success and may provide additional targets of selective pressure. Here I show that 1) controlled laboratory experiments produced observations consistent with density-dependent sperm-egg collision rates, and 2) models that explicitly include such dynamics are required to capture the observed behavior at high sperm concentrations. These findings illustrate that changes in egg concentrations can cause considerable shifts in the range of sperm concentrations required for maximizing rates of fertilization.

The observed shifts in fertilization due to egg concentration are not trivial given the importance of successful fertilization in maximizing lifetime fitness, especially for external fertilizers. Evidence for such fitness effects include both selective pressure on gamete traits related to fertilization and plasticity in those traits. For example frequency of alleles associated with egg selectivity may have changed in association with average population density in the red urchin *Strongylocentrotus franciscanus* (Levitan 2012). Moreover, gamete traits appear to be directly controlled by both males and females depending upon the density of spawning adults in the tunicate *Styela plicata* (Crean and Marshall 2008).

In this study, the effect of egg concentration on fertilization presents a potential additional source of selective pressure. Releasing too many eggs under conditions of low sperm concentrations can further reduce the already probability of fertilization. In contrast releasing fewer eggs at high sperm concentrations heightens the risk of polyspermy by increasing the rate of sperm attacks per egg. The density-dependent sperm-egg interactions may provide another behavioral source of selection in terms of egg release rate if these interactions also exist in nature. Under this model, females locally exposed to high concentrations of sperm during a spawning event may benefit from releasing many eggs rapidly to minimize polyspermy. In contrast, females surrounded by low sperm concentrations may benefit from releasing fewer eggs over longer durations or over multiple spawning events to maximize fertilization probability. Yet how predictions play out in nature remains speculative because the mechanism behind the density-dependence are at present unknown.

Accumulation of sperm near eggs is a likely mechanism for the observed density-dependent interactions. This can arise directly from attraction. In their original work Vogel et al. (1982) discounted the possibility of attraction of sperm by eggs. Others, however, have subsequenty demonstrated to occurrence of sperm chemotaxis in broadcast spawners (Kaupp 2012, Riffell et al. 2004). To my knowledge there are not any studies that provide an explicit demonstration of attraction via directional chemotaxis in *S. purpuratus* in the laboratory. Yet observations of sperm aggregating around individual eggs in *S. purpuratus* date back more than a century (Elder 1912) and a primary

commercial chemoattractant (speract) derived from *S. purpuratus* eggs (Hansbrough and Garbers 1981) is capable of altering the behavior and swimming speed of *S. purpuratus* sperm (Wood et al. 2007). Moreover, directional chemoattraction is not needed to yield accumulation of sperm around eggs (Jaiswal et al. 1999). In addition to attraction, other mechanisms may explain the density-dependent collision rates. For example, egg crowding effects that interfere with sperm search patterns may also explain the pattern consistent with density-dependent interactions. Regardless of the mechanism that leads to density-dependent collision rates, my results illustrate that the assumptions of random collisions and minimal impact of egg concentrations on fertilization are, in this case, invalid.

Models include simplifying assumptions for tractable purposes, yet inferences gleamed from simplistic models parameterized with laboratory data remain constrained by the unique context of the study. Historical use of simple fertilization kinetics models includes comparison of parameters across taxa, across experimental treatments and extrapolation of parameters to the field. In such cases, experimental analysis should carefully examine sensitivity of results to relaxation of those assumptions. In controlled laboratory studies, water motion is generally minimal and sperm and eggs are introduced simultaneously. In nature, spawning events can occur in a dynamic fluid environment where sperm and eggs meet in turbulent circumstances. Flow and shear stress can inhibit the ability of sperm to directionally seek eggs and alter fertilization rates (Riffell and Zimmer 2007, Zimmer and Riffell 2011) and turbulence may overwhelm such mechanisms (Denny and

Shibata 1989). Thus, if accumulation of sperm around eggs is the process that results in density-dependent collision rates, then such density-dependence will likely be relaxed if sperm behavior is altered by physical conditions. Moreover, sperm often exhibit circular or patterned search behavior (Farley 2002) that can induce complex vortexes and the hydrodynamic conditions controlling such behavior likely differ in the ocean. Such differences include the dispersal of chemoattractive gradients, shear stress that impedes swimming speed and direction, or heterogeneity in sperm concentrations where wisps of sperm rather than broad clouds mix with pockets of eggs in suspension. In addition to the challenges in extrapolating from the laboratory to the field, comparisons across taxa, even among congeners can be dangerous. For example fertilization dynamics in *Strongylocentrotus franciscanus*, the congener of *S. purpuratus*, showed no sensitivity to egg concentration in the laboratory (Levitan et al. 1991) in stark contrast to results shown here. Despite these concerns, my findings clearly indicate that egg concentrations can, in some taxa, play an important role in controlling fertilization rates.

The capacity for egg concentrations to alter fertilization dynamics may empower females with an additional behavioral control over fertilization. Varying in egg release rates may provide a buffering effect against both under-fertilization (because of too few sperm) and polyspermy (too many sperm). Fewer eggs released when sperm are sparse increases collision rates and decreases the number of sperm depleted, thereby increasing fertilization probabilities. More eggs released when sperm are abundant decreases collision rates and buffers against polyspermy. As a result fertilization rates and thus

reproductive efficiency may be controlled not only by the timing of egg release (Levitan 2005) but by varying the rate of egg release as well. As sperm concentrations increase, the effect of eggs on one another transitions from passive competition for sperm to cooperation.

Acknowledgements

References

Bates, D., M. Maechler, B. Bolker, and S. Walker. 2014. lme4: Linear mixed-effects models using Eigen and S4. http://CRAN.R-project.org/package=lme4.

Bode, M., and D. J. Marshall. 2007. The quick and the dead? Sperm competition and sexual conflict in sea. Evolution 61:2693–2700.

Cosner, C., D. L. DeAngelis, J. S. Ault, and D. B. Olson. 1999. Effects of spatial grouping on the functional response of predators. Theoretical Population Biology 56:65–75.

Crean, A. J., and D. J. Marshall. 2008. Gamete plasticity in a broadcast spawning marine invertebrate. Proceedings of the National Academy of Sciences 105:13508–13513.

Denny, M. W., and M. F. Shibata. 1989. Consequences of surf-zone turbulence for settlement and external fertilization. American Naturalist 134:859–889.

Elder, J. C. 1912. The relation of the Zona pellucida to the formation of the fertilization membrane in the egg of the sea-urchin (*Strongylocentrotus purpuratus*). Development Genes and Evolution 35:145–164.

Evans, J. P., F. Garcia-Gonzalez, M. Almbro, O. Robinson, and J. L. Fitzpatrick. 2012. Assessing the potential for egg chemoattractants to mediate sexual selection in a broadcast spawning marine invertebrate. Proceedings of the Royal Society B: Biological Sciences 279:2855–2861.

Farley, G. S. 2002. Helical nature of sperm swimming affects the fit of fertilization-kinetics models to empirical data. The Biological Bulletin 203:51–57.

Franke, E., R. Babcock, and C. Styan. 2002. Sexual conflict and polyspermy under spermlimited conditions: in situ evidence from field simulations with the freespawning marine echinoid *Evechinus chloroticus*. The American Naturalist 160:485–496.

Guerrero, A., T. Nishigaki, J. Carneiro, Y. Tatsu, C. D. Wood, and A. Darszon. 2010. Tuning sperm chemotaxis by calcium burst timing. Developmental biology 344:52–65.

Hansbrough, J., and D. Garbers. 1981. Speract. Purification and characterization of a peptide associated with eggs that activates spermatozoa. Journal of Biological Chemistry 256:1447–1452.

Hoffman, M. D., and A. Gelman. 2014. The No-U-Turn Sampler: adaptively setting path lengths in Hamiltonian Monte Carlo. Journal of Machine Learning Research 15:1593–1623.

Holling, C. S. 1959. Some characteristics of simple types of predation and parasitism. The Canadian Entomologist 91:385–398.

Jaiswal, B. S., I. Tur-Kaspa, J. Dor, S. Mashiach, and M. Eisenbach. 1999. Human sperm chemotaxis: is progesterone a chemoattractant? Biology of Reproduction 60:1314–1319.

Jantzen, T., R. De Nys, and J. Havenhand. 2001. Fertilization success and the effects of sperm chemoattractants on effective egg size in marine invertebrates. Marine Biology 138:1153–1161.

Kaupp, U. 2012. 100 years of sperm chemotaxis. The Journal of General Physiology 140:583–586.

Kaupp, U., E. Hildebrand, and I. Weyand. 2006. Sperm chemotaxis in marine invertebrates—molecules and mechanisms. Journal of cellular physiology 208:487–494.

Lauzon-Guay, J.-S., and R. E. Scheibling. 2007. Importance of spatial population characteristics on the fertilization rates of sea urchins. The Biological Bulletin 212:195–205.

Levitan, D. 1993. The importance of sperm limitation to the evolution of egg size in marine invertebrates. American Naturalist 141:517–536.

———. 1998. Sperm limitation, gamete competition, and sexual selection in external fertilizers. Pages 173–215 *in* T. Birkhead and A. Møller, eds. Sperm competition and sexual selection. Academic Press, New York.

———. 2004. Density dependent sexual selection in external fertilizers: Variances in male and female fertilization success along the continuum from sperm limitation to sexual conflict in the sea urchin *Strongylocentrotus franciscanus*. The American Naturalist 164:298–309.

———. 2005. Sex-specific spawning behavior and Its consequences in an external fertilizer. The American Naturalist 165:682–694.

———. 2010. Sexual selection in external fertilizers. Pages 365–378 *in* D. Westneat and C. Fox, eds. Evolutionary Behavioral Ecology. Oxford University Press.

———. 2012. Contemporary evolution of sea urchin gamete-recognition proteins: experimental evidence of density-dependent gamete performance predicts shifts in allele frequencies over time. Evolution 66:1722–1736.

Levitan, D., and D. Ferrell. 2006. Selection on gamete recognition proteins depends on sex, density, and genotype frequency. Science 312:267–269.

Levitan, D., M. Sewell, and F. Chia. 1991. Kinetics of fertilization in the sea urchin *Strongylocentrotus franciscanus*: interaction of gamete dilution, age, and contact time. The Biological Bulletin 181:371–378.

Levitan, D., C. TerHorst, and N. Fogarty. 2007. The risk of polyspermy in three congeneric sea urchins and its implications for gametic incompatibility and reproductive isolation. Evolution 61.

McCallum, H., N. Barlow, and J. Hone. 2001. How should pathogen transmission be modelled? Trends in Ecology & Evolution 16:295–300.

Millar, R. B., and M. J. Anderson. 2003. The kinetics of monospermic and polyspermic fertilization in free-spawning marine invertebrates. Journal of Theoretical Biology 224:79–85.

Parker, G. A., and J. Lehtonen. 2014. Gamete evolution and sperm numbers: sperm competition versus sperm limitation. Proceedings of the Royal Society B: Biological Sciences 281:20140836.

Podolsky, R., and R. Strathmann. 1996. Evolution of egg size in free-spawners: consequences of the fertilization-fecundity trade-off. American Naturalist 148:160–173.

R Core Team. 2014. R: A language and environment for statistical computing. R Foundation for Statistical Computing, Vienna, Austria. URL http://www.R-project.org/.

Riffell, J. A., P. J. Krug, and R. K. Zimmer. 2004. The ecological and evolutionary consequences of sperm chemoattraction. Proceedings of the National Academy of Sciences of the United States of America 101:4501–4506.

Riffell, J. A., and R. K. Zimmer. 2007. Sex and flow: the consequences of fluid shear for sperm–egg interactions. The Journal of experimental biology 210:3644–3660.

Sewell, M. A., R. B. Millar, P. C. Yu, L. Kapsenberg, and G. E. Hofmann. 2013. Ocean acidification and fertilization in the Antarctic sea urchin *Sterechinus neumayeri*: the importance of polyspermy. Environmental Science & Technology 48:713–722.

Stan Development Team. 2014*a*. RStan: the R interface to Stan, Version 2.4. http://mc-stan.org/rstan.html.

———. 2014*b*. San: A C++ Library for Probability and Sampling, Version 2.4. http://mc-stan.org.

Styan, C. A. 1998. Polyspermy, egg size, and the fertilization kinetics of free-spawning marine invertebrates. The American Naturalist 152:290–297.

Vogel, H., G. Czihak, P. Chang, and W. Wolf. 1982. Fertilization kinetics of sea urchin eggs. Mathematical Biosciences 58:189–216.

Watanabe, S. 2010. Asymptotic equivalence of Bayes cross validation and widely applicable information criterion in singular learning theory. The Journal of Machine Learning Research 11:3571–3594.

Wood, C. D., T. Nishigaki, Y. Tatsu, N. Yumoto, S. A. Baba, M. Whitaker, and A. Darszon. 2007. Altering the speract-induced ion permeability changes that generate flagellar Ca2+spikes regulates their kinetics and sea urchin sperm motility. Developmental biology 306:525–537.

Yund, P. O. 2000. How severe is sperm limitation in natural populations of marine free-spawners? Trends in Ecology & Evolution 15:10–13.

Zimmer, R. K., and J. A. Riffell. 2011. Sperm chemotaxis, fluid shear, and the evolution of sexual reproduction. Proceedings of the National Academy of Sciences 108:13200–13205.

Tables

Table 3.1: Description of parameter values and state-variables in the system of differential equations described by eqns. (3.3a)-(3.3e).

Parameter	Description
β	sperm collision rate
ϕ	egg selectivity
θ	per capita polyspermy block rate
r	viable sperm decay rate
S_0	initial sperm concentration
E_T	total number of eggs in the system
State Variable	**Description**
E_U	unfertilized eggs in the system
E_V	fertilized eggs vulnerable to polyspermy
E_M	monozygotic eggs invulnerable to polyspermy
E_P	eggs fertilized by multiple sperm (polyspermy)
S	viable sperm in the system

Table 3.2: Parameter estimates, confidence intervals and likelihood ratio tests for generalized linear mixed effects models represented in Figure 3.1-3.3. Biological model results are shown in Table 3.4. All models include a random effect of trial pair (i.e. intercepts vary by individual male-female pairs), the standard deviations among pairs is listed as σ_{pair}. Predictor variables (sperm and egg concentration) were log-transformed in the analyses.

Response	Parameter	Estimate	95% CI	χ^2	df	P-value
	log(Eggs)	-0.56	-0.56 : -0.61	501.74	1	< 0.0001
Total	log(Sperm) [1 polynomial]	48.2	46.3 : 51.3	14850	3	< 0.0001
Fertilization	[2 polynomial]	0.40	-1.29 : 2.44			
(Fig 1A)	[3 polynomial]	-4.33	-5.59 : -2.57			
	intercept	0.40	0.01 : 0.85			
	σ_{pair}:intercept	0.55	0.25 : 0.79			
	log(Eggs)	-0.72	-0.84 : -0.58	124.45	1	< 0.0001
Polyspermy	log(Sperm)	1.55	1.42 : 1.67	1455.5	1	< 0.0001
(Fig 1B)	intercept	-7.56	-6.99 : 8.11			
	σ_{pair}:intercept	0.52	0.22 : 0.76			

Table 3.3: WAIC of individual models within each base model and assumption thereof. The model with the lowest WAIC is favored.

Base Model	Interaction form	WAIC	pWAIC	ΔWAIC
dynamic model (eqns 3.4c-3.4d)	**density-dependent**	**2346.7**	**164.0**	**0.00**
Styan (1998)	density-dependent	2368.5	162.6	21.8
Millar &Anderson (2004)	density-dependent	2377.2	162.7	30.5
dynamic model (eqns 3.4c-3.4d)	random	2494.0	183.2	147.3
Styan (1998)	random	2549.0	163.1	202.4
Millar &Anderson (2004)	random	2564.2	167.6	217.5

Table 3.4: Table of parameters, description, estimated posterior mean, 95% credible set from the MCMC posterior, and the range provided in the uniform prior for the dynamic model with unique collision rates (the model with the lowest WAIC)

Param.	Description	Mean	95% Cred. Set	Uniform Prior
$\beta_{\frac{1}{64}}$	mean collision rate $(\frac{1}{64})$	1.43×10^{-3}	$(0.18 - 2.46) \times 10^{-3}$	$0.00 - 0.10$
$\beta_{\frac{1}{16}}/\beta_{\frac{1}{64}}$	collision rate ratio	0.70	0.62 - 0.78	$0.00 - 2.00$
$\beta_{\frac{1}{4}}/\beta_{\frac{1}{64}}$	collision rate ratio	0.49	0.42 - 0.56	$0.00 - 2.00$
$\beta_1/\beta_{\frac{1}{64}}$	collision rate ratio	0.42	0.36 - 0.50	$0.00 - 2.00$
ϕ	mean egg selectively	0.089	0.005 - 0.148	$0.000 - 0.150$
θ	polypsermy block rate	0.91	0.81 - 1.01	$0.20 - 20.00$

Figures
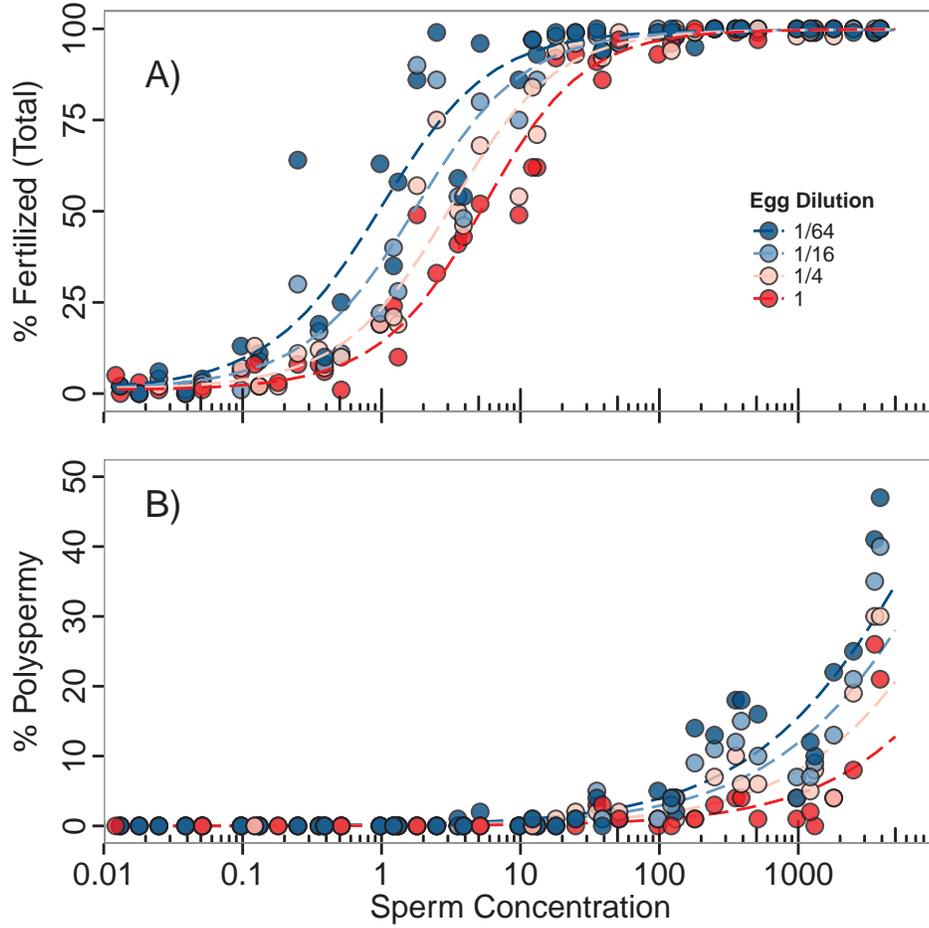
Figure 3.1: Percent total egg fertilization (A) and percent polyspermy (B) in experimental treatments. Broken lines represent GLMM model fixed effects (see Table 2); deviation from the fixed effect consists of both error within and among individual pairs. Egg dilution represents the mean concentration (μl^{-1}) of eggs. Colors indicate different egg concentrations, with blue representing lower concentrations.

116
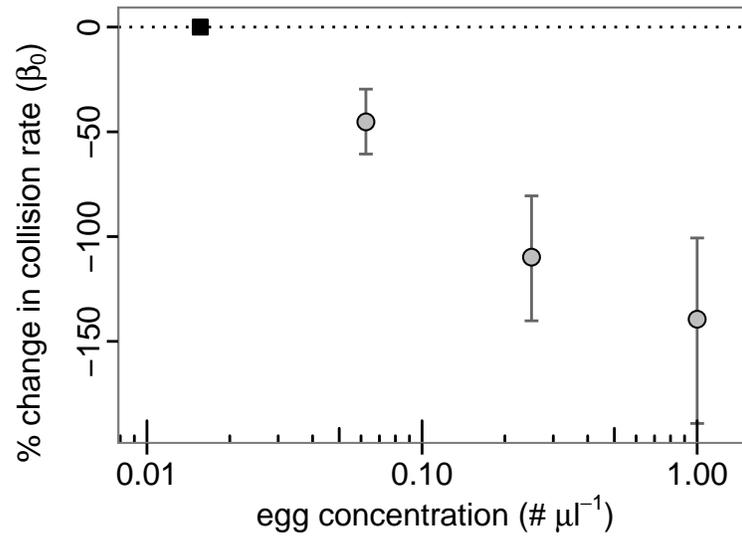
Figure 3.2: Estimated % change in collision rate (β) at each mean egg concentration (egg concentration among pairs varied slightly) from the collision rate at $1/64$ eggs μl^{-1}. Each unique collision rate is estimated as the collision rate at $1/64$ eggs μl^{-1} times the value shown. Egg dilution represents the mean concentration (μl^{-1}).
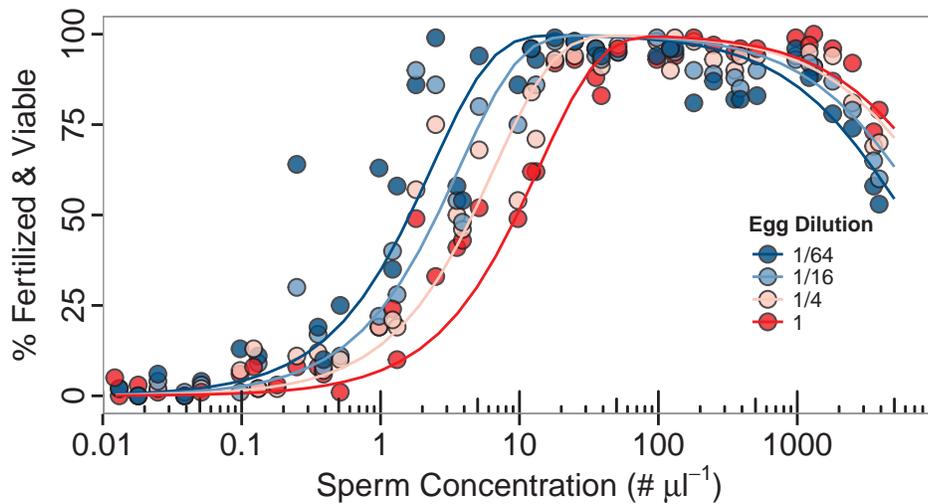
Figure 3.3: Viable fertilization rate (percent total fertilization minus polyspermy) in experimental treatments. Lines represent the hierarcichal mean from the dynamic model with density-dependent sperm-egg interactions (different collision rates by egg dilution). Egg dilution represents the mean concentration (μl^{-1}). Models with purely random sperm-egg interactions do not capture the separation by egg dilution in rates of polyspermy at high sperm concentrations. Colors indicate different egg concentrations, with blue representing lower concentrations.
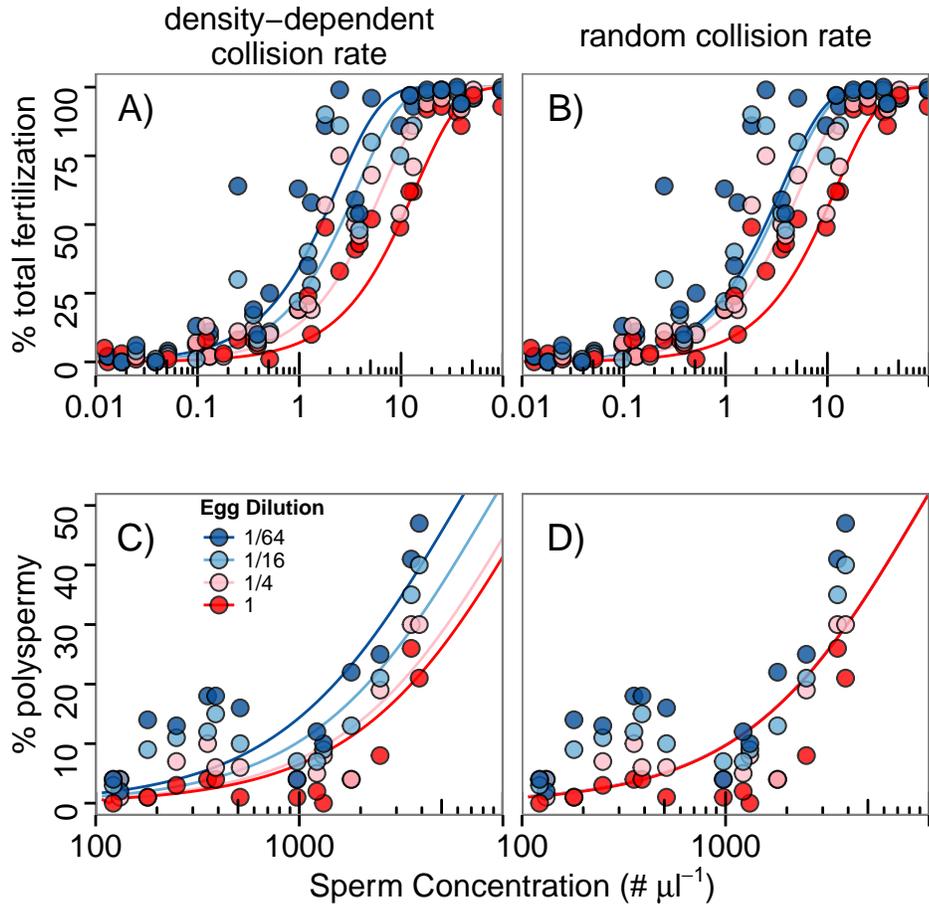
Figure 3.4: Model predictions under density-dependent collision rates (A & C) or random collision rates (B & D) for %total fertilization (A & B) and polyspermy (C & D). Lines represent the hierarcichal mean from the dynamic model. Panels A & C represent the same predictions as Figure 3.3 parsed into total fertilization and polyspermy. Colors indicate different egg concentrations, with blue representing lower concentrations.

Appendix C: "half-life" and decay rates

The sperm "half-life" is described by Vogel et al. (1982) as the time after which total fertilization capacity of sperm in solution is reduced to 50% of the capacity at release. However, the degradation of sperm does not linearly scale with the fertilization capacity of that population of sperm. Let the definition of Vogel et al. (1982) be called "fertilization half-life" and the half-life of sperm be called "sperm half-life". It can easily be shown that a sperm half-life can be independent of sperm concentration but fertilization half-life is not, as observed by Levitan (1993) and Levitan et al. (1991). The exact bias of the Vogel et al. (1982) method will differ depending upon the sperm loss function. Consider a constant decay rate as in eq. (3.3a). In this case percent fertilization at a given time is $1 - E_U(t)/E_U(t = 0)$, where $E_U(t)$ is provided by eq. (3.4b). The sperm half life is given by $\log(0.5)/r$. If we use parameter estimates from the model estimated here (with constant egg concentrations) the sperm-half life is constant but the fertilization half-life is biased and increases with sperm concentration
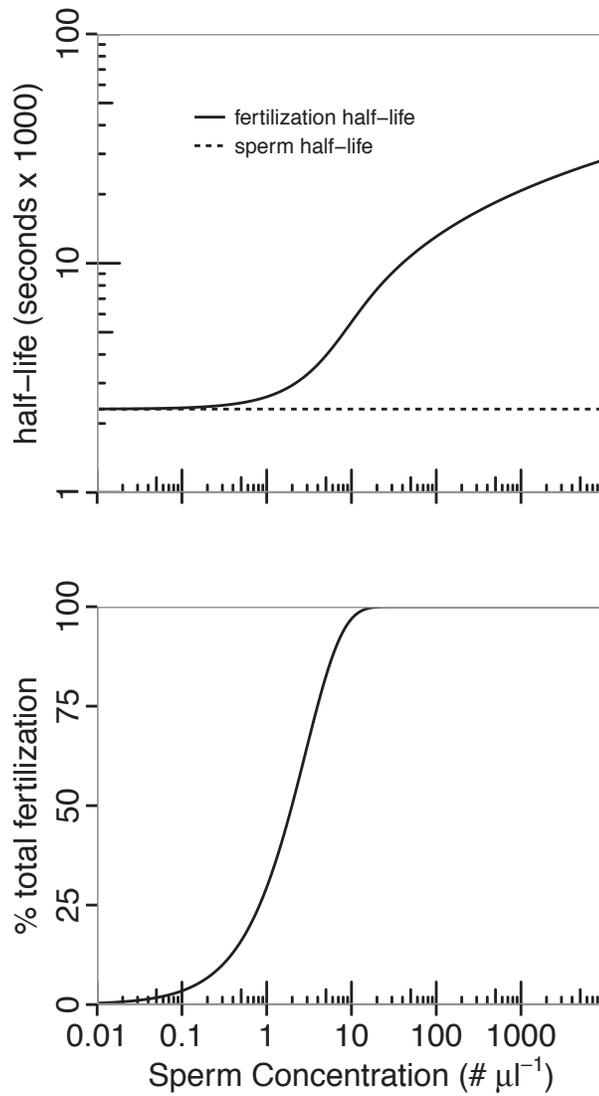
Figure C.1: A) Half-life values produced under a constant sperm decay rate. The sperm half-life (dotted) is constant while the fertilization half-life (solid line) of Vogel et al. (1982) is biased towards higher values, increasing as sperm concentrations and fertilization rates (B) increase.

Thus using the definition of Vogel et al. (1982) will naturally produce biased estimates if the decay function is independent of sperm concentration. To produce unbiased estimates, one must 1) estimate the empirical relationship between sperm concentrations and fertilization rates for virgin sperm at age ≈ 0. 2) conduct a factorial age-concentration experiment, 3) use only sperm concentrations that produce less than 100% fertilization at age ≈ 0, 4) for each result calculate the number of sperm required to achieve such fertilization 5) estimate the loss of sperm at each age within each concentration and 6) estimate the age at which 50% of initial sperm concentrations are lost.

A better solution is to directly estimate the decay rate and use a model that explicitly includes decay rate, such as eqns. (3.3a)-(3.3e).

Experimental estimation of "half-life" τ and decay rate r

In order to estimate the sperm decay rate (r) and half-life, I conducted an experiment identical to that described above, but used only one egg concentration (assuming egg concentration does not affect the intrinsic decay rate), adding sperm to vials containing eggs at $t \in 0, 600, 1200, 2700, 3600$ and 7200 seconds after initial sperm release and dilution for each of four sperm dilutions ($10^{-4}, 10^{-5}, 10^{-6}, \& 10^{-7} \mu l^{-1}$). I excluded sperm concentration treatments that started with 100% fertilization for age 0 sperm. For each I used the fertilization fraction and the empirical fertilization-sperm concentration relationship (see figure 3.1) to calculate the expected initial sperm concentration. From these curves I then calculated both the expected decay rate and the "half-life". In addition

122

to a constant decay rate, I also estimated other decay functions including: Gompertz, logistic, log-logistic and decay rates that vary by sperm concentration. Each function was estimated using nonlinear least squares and compared using AICc (corrected Akaike Information Criterion).

Table C.1: Table of model comparison of nonlinear decay functions. Lower AICc values are favored and the model within 2 AICc units of the minimum is preferred.

Model	AICc	df	Δ AICc	AICc weight
constant decay	**29.9**	**2**	**0.1**	**0.36**
decay (varies by sperm concertration)	32.2	4	2.4	0.11
log-logistic	29.8	3	0.0	0.38
Gompertz	31.7	3	1.9	0.15
logistic	41.2	2	11.5	0.01

There is no support from these data for a decay rate that varies by sperm concentration. However, these data are not explicitly designed to test for such differences and thus may lack power for such inference.

From the constant decay function the decay rate is estimated to be $r = 2.7 \times 10^{-4}$ per second ($\pm 0.34 \times 10^{-4}$), from which the "half-life" is estimated to be 2310.5 seconds.

Chapter 4

Climatic regulation of planktonic recruitment in purple sea urchins (*Strongylocentrotus purpuratus*) in California

Abstract

Purple sea urchins *Strongylocentrotus purpuratus* serve as a model system to evaluate how oceanographic conditions interact with food supply for adults and larvae to influence patterns of planktonic settlement in benthic marine invertebrates. Using spatially replicated, 23-year time series of sea urchin settlement I show that multi-year fluctuations in the strength of settlement exhibit a strong, negative relationship with both sea surface temperature and the El Niño Southern Oscillation on the monthly and annual scale, but do not appear related to food supply for larvae, food supply for adults, or local offshore transport. Such correlations are consistent in southern California throughout the time series. Several potential mechanisms could explain these patterns, including temperature limitation to adult spawning or changes in ocean transport. Importantly, interannual patterns of regional settlement were correlated with subsequent densities of juvenile sea urchins, indicating that the mechanisms affecting the magnitude of larval settlement play a pivotal role in regional population dynamics.

Introduction

Settlement of larvae in species of benthic marine invertebrates often varies dramatically in time. Such variability has the potential to exert strong control on adult population dynamics (Shanks and Roegner 2007) and ecological communities (Gaines and Roughgarden 1985). Yet the underlying factors that drive variability in settlement remain poorly understood for many species, especially those with planktonic larvae. Major bottlenecks to settlement of larvae at a destination include 1) production and fertilization of gametes, 2) delivery of larvae from source to destination, 3) growth, development, and survival of larvae during transport, and 4) successful metamorphosis and settlement. Each of these includes potential for control by various exogenous environmental factors, many of which are interrelated in space and time. Understanding how patterns of settlement are related to global and local scale environmental dynamics can help identify testable hypotheses regarding what drives major temporal trends in settlement of larvae.

For decades research has focused on the role of adult stocks in driving recruitment patterns in space and time (Shepherd and Cushing 1980). Yet for many species the relationship between adults and recruitment is weak, perhaps because environmental filtering can mask any such relationships. These filtering effects can occur via impacts on reproduction or survival and delivery of larvae. In purple sea urchins *Strongylocentrotus purpuratus* for example, size-specific female fecundity can vary by orders of magnitude between urchins living in food rich vs. food poor habitats (see Appendix D), and their

food supply (primarily kelp) varies substantially from year to year in response to climate (Cavanaugh et al. 2011). Thus, production of larvae may be controlled not only by the number of adults but also their individual reproductive capacity. Moreover, settlement at a destination is also impacted by current patterns that can vary dramatically in time (Mitarai et al. 2009, Siegel et al. 2008).

Variability in ocean circulation is thought to drive temporal patterns in larval supply (Ebert and Russell 1988, Gaines and Roughgarden 1985, Parrish et al. 1981, Roughgarden et al. 1988). Strong wind-driven upwelling periods have been hypothesized to force larvae offshore to upwelling fronts, reducing their probability of settling on suitable habitat (Connolly et al. 2001, Roughgarden et al. 1991, Shkedy and Roughgarden 1997, Wing et al. 2003). However, behavioral responses, such as position in the water column, appear to be able to partially buffer against this effect (Morgan and Fisher 2010, Morgan et al. 2009a,b, Poulin et al. 2002, Shanks and Brink 2005). In addition to the simplistic offshore/onshore delivery dichotomy, complex processes of ocean circulation vary dynamically from year to year and season to season (Mitarai et al. 2009) causing significant variation in larval source/sink dynamics.

While upwelling is hypothesized to negatively affect the shoreward transport of larvae, it also generally corresponds to changes in primary productivity and sea surface temperature. For obligate planktotrophic larvae, the abundance of phytoplankton can affect growth, development and survival in planktotrophic larvae (Beddingfield and McClintock 1998, Bertram and Strathmann 1998, Byrne et al. 2009, Hoegh-Guldberg and

Pearse 1995, Meidel et al. 1999, Meyer et al. 2007, Miller and Emlet 1999, Miner 2007, Strathmann 1987, Vaïtilingon et al. 2001). Direct effects of temperature can also play a role in larval survival by influencing metabolic rates, growth, development or survival (Azad et al. 2012, Byrne et al. 2008, Chen and Chen 1992, Hoegh-Guldberg and Pearse 1995, Ling et al. 2008, McEdward 1985, Padilla-Gamiño et al. 2013, Vaïtilingon et al. 2001). For example, temperature tolerance of larvae is the hypothesized mechanism for poleward range expansion and rear edge contraction for two disparate species in of sea urchins in Tasmania (Ling et al. 2008).

Finally, these hypothetical drivers of larval settlement are all potentially affected by global oceanographic dynamics, such as El Niño or decadal scale regime fluctuations as indicated by the Pacific Decadal Oscillation (Mantua and Hare 2002). Multiannual fluctuations in global ocean conditions can have complex and cascading impacts on local sea surface temperature, primary productivity, current patterns, and many other biological and physical processes that may affect larvae individually or interactively.

I investigated how temporal settlement patterns of the purple urchin *S. purpuratus* in different regions along the California coast are related to 1) global indices of ocean conditions and 2) local environmental metrics that include temperature, upwelling, food supply for larvae, food supply for adults, and adult density. To do this I used a 23-year dataset of settlement at seven different sites in three major regions spanning California. I conducted analyses on both the annual scale and the monthly scale using a combination of linear mixed effects models, generalized additive mixed effects models, quantile

regression and partial wavelet coherence analysis. I used settlement data at four sites in conjunction with benthic monitoring data to investigate whether regional patterns in settlement translate to subsequent recruitment of juvenile urchins.

Methods

Study system

Populations of *S. purpuratus* occupy shallow subtidal and intertidal rocky substrata from roughly $23°N$ on the western coast of the Baja Peninsula to southern Alaska. *S. purpuratus* are broadcast spawners and the seasonality of spawning in California is generally thought to be driven by photoperiod (Cochran and Engelmann 1975, Gonor 1973, Pearse et al. 1986). Fertilized zygotes develop into planktonic echinoplutei and are obligate planktivores that consume phytoplankton. After spending anywhere from several weeks to 86 days in the plankton (Strathmann 1978), individuals begin final metamorphosis and sink to the benthos. Along the geographic range, there is clear evidence for annual variation in settlement of these newly metamorphosed larvae among many sites (Ebert 2010, Ebert et al. 1994).

Collection of newly settled urchins along the coast of California, USA (1991-2013)

Settlement of newly metamorphosed urchins was sampled at three major regions along the California coast from 1991 through 2013. Sampling regions (from south to north) included San Diego County (32.7°N, two sites [Scripps Pier and Ocean Beach]), the Santa Barbara Channel (34°N, four sites [Anacapa Island, Scripps Pier, Ellwood Pier and Gaviota Pier]) and Fort Bragg (39°N, one site) (Figure 4.1). San Diego County and the Santa Barbara Channel lie within the Southern California Bight and Fort Bragg is in northern California. At each site, urchins were collected using nylon-bristled scrub brushes (2.5 cm long bristles and a 6 x 9 cm wooden base) suspended 1 to 2 m from the benthos. The majority of deployments included eight replicate brushes collected weekly from 1991 to 2003, and biweekly thereafter through 2013. Upon collection brushes were transported to the laboratory in zip-loc plastic bags and rinsed through a 350 μm mesh sieve. *S. purpuratus* individuals were then sorted from other organisms, counted and preserved. Counts of newly settled purple sea urchins were converted to average number of settlers per brush, per day for each month during the 23-year study period.

Global covariate time series data

I used two major global indices of oceanographic climate. These include

- **The multivariate El Niño Southern Oscillation Index (MEI)** provides a metric of the intensity of El Niño/La Niña fluctuations and is derived from several metrics of sea surface temperature, surface winds, sea level pressure, and cloudiness of the sky (Wolter and Timlin 1993, 1998).

- **The Pacific Decadal Oscillation (PDO)** is the 1st principle component of sea surface temperature variability in the north Pacific (Mantua and Hare 2002).

Regional/local covariates

- **Bakun Index (monthly, 1991-2013)**

   The Bakun index provides an index of coastal upwelling and specifically describes the volume of water that is transported offshore from Ekman transport (Bakun 1973, available from `http://www.pfel.noaa.gov/`). Negative values indicate downwelling and surface waters that moved onshore, while positive values indicate upwelling and surface waters moving offshore. This index has been used in relation to delivery of larvae onshore and advection from shore in addition to its value as a metric of coastal productivity. For the Southern California Bight sites, I used data from the 33°N-119°W lat-long site, while in Northern California I used data from the 39°N-125°W lat-long site.

- **Sea surface chlorophyll (monthly, 1997-2013)**

Satellite imagery of sea surface chlorophyll provides a spatially and temporally well-resolved metric of ocean primary productivity that in situ sampling cannot provide. Thus, as a metric of planktonic food availability around each site I used merged OCTS, SeaWIFs and MODIS time series (Kahru et al. 2012) and used the biweekly time series available from `http://spg.ucsd.edu/Satellite_Data/California_Current/`.

Because sea surface chlorophyll concentration data are spatial grids of time series, I included averaged cells meeting particular geographic conditions for each site. For mainland sites, all cells had to lay within 5 km offshore of the mainland coastline that stretched 150 km in coastline length from the urchin settlement collection point or within 5 km of any island coastline of any island within a 150 km radius. For the site at Anacapa Island, I included any point within a 150 km radius and within 5 km of any coastline. I used 150 km because that is the Lagrangian estimate for dispersal distances for species with a 30-day planktonic larval duration (PLD). However, this is potentially an overestimate for a 30-day PLD as behavior and complex current patterns may reduce this distance substantially (Shanks 2009). Figure 4.1 depicts the chlorophyll boundary used for Fort Bragg, Stearns Wharf and Scripps Pier.

- **Sea surface temperature (monthly, 1991-2013)**

  I used sea surface temperature data derived from Pathfinder AVHRR (advanced very high resolution radiometer) that were optimally interpolated on 1 day and

0.25°latitude/longitude resolution (Reynolds et al. 2007, available from `http://www.ncdc.noaa.gov/thredds/oisst-catalog.html`);. To produce monthly scale time series, I ran data through a 30-day moving average filter with a rectangular, backwards looking window in order to capture general temporal trends in the data.

SST data are also a spatial grid of time series. The data are already interpolated and exist at lower resolution than chlorophyll data. Thus, I used the same boundary conditions, modified to points within 10 km of those coastline ranges. Figure 4.1 illustrates mean spatial trend in winter sea surface temperature for the entire study region.

- **Fall kelp canopy coverage (Santa Barbara Channel and San Diego County only, 1991-2010)**

    The regional biomass of giant kelp *Macrocystis pyrifera* can fluctuate dramatically from year to year (Cavanaugh et al. 2011). Giant kelp is a major constituent of *S. purpuratus* diets in southern California. Given that fecundity in *S. purpuratus* can vary by orders of magnitude as a result of food supply, these fluctuations in *M. pyrifera* may in part influence urchin reproduction. Thus, the aerial extent of *M. pyrifera* was derived from LANDSAT 5 Thematic Mapper satellite imagery (Cavanaugh et al. 2014). Data were aggregated over the Santa Barbara Channel including both islands and mainland (from Point Conception to Santa Monica Bay) or San Diego region (from the US-Mexico border to Los Angeles County). I used the 3-month running mean during the period leading into the spawning

season because marked declines in reproductive capacity require several months of consistently low food supply (see Appendix D).

- **Mean adult urchin density in the Channel Islands (Santa Barbara Channel only)**

As an index of regional adult densities in the Santa Barbara Channel, I used the weighed average of survey data from The Channel Islands Kelp Forest Monitoring Program (Kushner et al. 2013). Specifically I used *S. purpuratus* density data from 33 sites across the Channel Islands from 1991 through 2011. Because the data include size frequency information, I calculated the density of adults in each location by multiplying total *S. purpuratus* density by the fraction of urchins that were above 2.5 cm in test diameter (the approximate cutoff size for reproduction; Kenner and Lares 1991). For each year I used the weighted average among islands.

General model averaging framework

I used a model averaging approach in multiple regression models to evaluate the statistical significance of covariate relationships with urchin settlement. Model averaging weights parameter estimates and standard errors by applying information-theory across all candidate models rather than having to select a single best model, which can increase the chances of identifying spurious relationships (Burnham and Anderson 2002, Lukacs et al. 2010). Thus, for all multiple regression type models I used the following model averaging approach: 1) estimate models with every possible combination of environmental

covariates available using maximum likelihood; 2) for each model calculate the corrected Akaike Information Criterion (AICc) and the AICc weight for that model; and 3) use the full set of AICc weights to calculate model average coefficients, standard errors and statistical significance (see Lukacs et al. (2010) and Burnham and Anderson (2002) for details).

Dealing with covariates that only partially overlap in time

Because time series of covariates are not all equal in temporal and spatial coverage, analyses were repeated for each subset of overlapping covariates and examined for agreement in space and time. For example, there are two windows for analysis on the monthly scale: analyses with all covariates including sea surface chlorophyll (1997-2013) and analyses excluding sea surface chlorophyll (1991-2013).

Models incorporating only global indices of ocean conditions

To evaluate how settlement patterns were related to global indices of ocean climate I estimated linear mixed effects models of settlement and included the mean winter (December through April) MEI and the mean winter (December through April) PDO index as covariates in the model, allowing the relationships to vary between the Santa Barbara Channel and San Diego County. I used means from December through April because most settlement occurs in the winter and spring. Data limitations at Fort Bragg preclude its use in multiple regression and so I only present simple correlations for this

135

site. To evaluate statistical support and statistical significance of individual covariates in the models, I used the model averaging approach outlined above. I included site as a random effect and to account for potential problems associated with serial correlation within each site, I included first order autoregressive models [AR(1)] on the regression errors (for each analysis AR(1) models adequately addressed serial correlation in the full models and thus were included in all regression models). I estimated mixed-effects models using the R package nlme (Pinheiro et al. 2011).

Because correlations may arise from a few major anomalies or consistent paired fluctuations in time, I examined the coherence between settlement and significant variables using wavelet coherence analysis (Cazelles et al. 2008, Ng and Chan 2012). Wavelet coherence analysis calculates the coherence at different frequency domains (i.e., do time series fluctuate together at the monthly, annual, inter-annual or decadal scales). This method is also useful for evaluating whether correlations are persistent over time because unlike standard spectral analysis, wavelet coherence analysis allows relationships to vary through time. Because monthly scale data included here are also highly seasonal, I directly accounted for seasonality as an explicit covariate in the analysis.

Models incorporating regional/local covariates

Settlement for purple sea urchins generally begins in December, and thus the settlement year was considered December through September for all locations. I analyzed monthly data in a multiple regression framework using generalized additive mixed effects

models (GAMM, Wood 2011) for sites in the Southern California Bight. Data from Fort Bragg were too sparse for multiple regression. GAMM models are useful for 1) incorporating potential nonlinear relationships between the response and the covariates and 2) directly accounting for inherent seasonality in the system. For environmental covariates I imposed cubic regression splines with a maximum of 3 degrees of freedom (i.e., the shape can range from linear, hump shaped, curvilinear or S-shaped, but cannot extend beyond these). For the seasonal trend, I imposed cyclic cubic regression splines (which forces the trend at the beginning of December to match the value at the end of November) with a maximum of 6 degrees of freedom (allowing for a maximum of 2 modes). Model averaging of GAMM regressions provides a challenge because different models potentially include different smoother shapes for each covariate. Thus I report only the sign of the general relationship if there was strong support from cumulative AICc weights and relationship was consistently the same sign and significantly different than zero (e.g., a relationship was reported as negative if the models included either a curvilinear trend or a linear trend that was statistically significant, negative and collectively supported with AICc weights).

I used unique lags for each time series in the monthly analysis because echinoplutei spend substantial time in the plankton, and each variable may influence settlement at different lags. I examined cross correlations from 0 to 60 day lags and for each time series chose the lag with the maximum significant correlation coefficient. For final lags I used 60 days for offshore transport, 30 days for sea surface temperature and 15 days

137

for sea surface chlorophyll. Despite these choices, results are robust to choice of lags because of the moving average window.

As before I considered site a random effect and accounted for within site serial autocorrelation using an AR(1) model on the residuals. The errors also tended to increase with the mean and varied by site so I allowed the site-specific error variance to increase exponentially with the predicted response.

I supplemented the GAMM models with quantile regression because long-term patterns in settlement may be driven by the upper quantiles rather than the mean settlement. I only included covariates in the quantile regressions that were significant in the GAMM models in order to describe how the upper and lower range of settlement relates to those variables. I allowed for similar nonlinear trends by imposing a b-spline with 3 degrees of freedom (see above) to the selected covariates and 6 degrees of freedom to the seasonal trend. I estimated quantile regressions using the R package quantreg (Koenker 2013).

Finally, as in the global analysis, I conducted partial wavelet coherence analysis between settlement at Gaviota Pier and the individual significant monthly covariates in that region while controlling for seasonal trends in settlement.

Impact of settlement patterns on juvenile recruitment

I evaluated whether interannual variability in settlement patterns translate generally to variability in subsequent juvenile densities on reefs. I aggregated the annual mean

density of new juvenile recruits in benthic quadrats across the Channel Islands and compared it to the annual mean settlement patterns (from brushes) in the Santa Barbara Channel using Gamma regression.

Results

Monthly settlement patterns varied by orders of magnitude among years and among sites, though sites in southern California (including both the Santa Barbara Channel and San Diego County) generally showed some synchrony in interannual fluctuations (Figure 4.2). The seasonal pattern in southern California sites was pronounced, generally increasing from December, peaking around April or May and tapering off during summer months (Figure 4.3). Settlement in the Santa Barbara Channel generally exceeded that in San Diego County and at Fort Bragg (for periods when data were available).

Models incorporating only global indices of ocean conditions

Annual settlement data from sites in the Southern California Bight were negatively correlated with the multivariate El Niño Southern Oscillation index (MEI) while data from Fort Bragg were positively correlated with MEI (Figure 4.4). When including only global scale indices of ocean condition on the annual scale, mixed-effects model results for the Southern California Bight included a significant, negative relationship between settlement and the El Niño Southern Oscillation as measured by the MEI (Table 4.1) after accounting for serial correlation and random site level effects. There

MEI relationships with settlement did not differ significantly between San Diego County and the Santa Barbara Channel in this analysis. There was no significant relationship with the Pacific Decadal Oscillation (Table 4.1). Partial wavelet coherence analysis of monthly data at the Gaviota Pier in the Santa Barbara Channel indicates that settlement and the MEI time series exhibit coherence throughout the time series. The time series were coherent at the 36-60 month (3-5 year) period and after 2007 coherence shifted to the 18-24 month (1.5-2 year) period (Figure 4.5a). In contrast to southern California, settlement at Fort Bragg was positively correlated with MEI ($r = 0.65$, $t_{10} = 2.69$, P = 0.023, Figure 4.4) [insufficient data for multiple regression]) but not with the PDO ($r = 0.49$, $t_{10} = 1.76$, P = 0.11). There were insufficient continuous monthly data at Fort Bragg to conduct partial wavelet coherence analysis.

Models incorporating only regional/local covariates

Settlement data in the Santa Barbara Channel and San Diego County showed a significant, negative correlation with temperature (Figure 4.6). While data at Fort Bragg were limited, settlement exhibited a positive correlation with temperature (Figure 4.6). Annual scale models using data only from sites in the Santa Barbara Channel (the only region where adult density estimates were available) included a significant negative relationship with mean winter sea surface temperature and a significant positive relationship with adult density from the previous summer (Table 4.2). Mean winter sea surface chlorophyll concentrations (Dec-April), and mean winter offshore and onshore

transport (Dec-April) (Table 4.2). Fall kelp canopy coverage actually showed a significant negative relationship (Table 4.2) which contradicts my hypothesis concerning kelp availability amplifying settlement. When I included data from both the Santa Barbara Channel and San Diego County in the models (but excluded adult density), there was also a significant negative winter sea surface temperature relationship with no significant difference in slopes between the Santa Barbara Channel and San Diego County (Table 4.3). These results for southern California were robust to the different time domains that incorporated covariates with different time spans (Table 4.3). Urchin settlement at Fort Bragg, where water was generally colder than in the Southern California Bight, exhibited a positive correlation with sea surface temperature ($r = 0.69$, $t_{10} = 3.02$, P = 0.01), but not with net offshore transport ($r = -0.35$, $t_{10} = 1.2$, P = 0.26) or chlorophyll concentrations ($r = 0.49$, $t_{10} = 1.76$, P = 0.11).

Monthly settlement data in the Southern California Bight also showed significant, negative correlations with temperature. The GAMM models for these regions include consistent, negative sea surface temperature relationships after accounting for seasonality, random site effects, serial autocorrelation and heteroscedasticity in error variance (Table 4.4). There was not strong support for different relationships between the Santa Barbara Channel and San Diego County sites. As with the annual analyses, monthly sea surface chlorophyll and mean monthly offshore transport indices did not factor significantly into the GAMM models. These models include unimodal mean seasonal patterns of settlement in the Southern California Bight that were similar among the 6 Southern

141

California Bight sites (increase in AICc of 2.9 when allowing seasonality to vary by site versus using a constant seasonality among sites, Figure 4.3). These results are consistent regardless of the time domain used (i.e., when excluding sea surface chlorophyll that restricts analysis to 1997 and later).

Quantile regressions also showed significant negative sea surface temperature relationships in the Santa Barbara Channel (at and above the 0.20 quantile to the 0.80 quantile, the upper quantile examined) and San Diego County (above the 0.45 quantile to the 0.80 quantile). The SST relationship versus the 0.2 and 0.8 quantiles are shown as dashed lines in Figure 4.6. These results indicate the lower limit of settlement was similar among even the warmest (El Niño years) and coldest periods (La Niña years) but the median and upper limits, as well as the mean (as indicated by the GAMM regressions) were much higher during those cold periods. Correlations result primarily from out-of-phase coherent fluctuations that occur on multi-year time scales in the time series. Partial wavelet coherence analysis of data from the Gaviota Pier show there was significant coherence between monthly settlement and sea surface temperature at the 36-60 month (3-5 year) period after accounting for seasonality that persists throughout the time series (Figure 4.5b).

Relationship between settlement and subsequent juvenile densities

Mean settlement from the winter and spring across the Santa Barbara Channel sites were positively correlated with the mean density of juvenile sea urchins averaged across

the Channel Islands ($\chi^2 = 5.15, df = 1, P = 0.003$, deviance explained ($D^2$) $= 0.32$, adjusted $D^2 = 0.29$). In years when settlement was extremely low, mean juvenile density was less than 5 m^{-2}, while in years of high settlement the mean density of juveniles was consistently greater than 10 m^{-2} (Figure 4.7).

Discussion

Settlement patterns in *S. purpuratus* in the Southern California Bight showed negative correlations with sea surface temperature and El Niño Southern Oscillation . On the annual scale, this correlation represents a more than an order of magnitude reduction in recruitment from the coldest years (La Niña) to the warmest (El Niño). In contrast, settlement at Fort Bragg in Northern California shows the opposite trend. Such temporal changes have the potential to impact population dynamics given that settlement patterns are correlated with subsequent juvenile urchin densities in the Santa Barbara Channel.

Results from southern California are consistent with prior observations of sea urchin recruitment. Between 1969 and the early 1980's recruitment patterns of juvenile sea urchins were anomalously low in years with persistently warm sea surface temperatures (Ebert 1983, Tegner and Dayton 1991). Between 1969 and 1977, recruitment was lowest during the three El Niño years of 1970, 1973, and 1977 at False Point, California near San Diego (Ebert 1983). At nearby Point Loma, similar reductions in recruitment followed the 1982-83 El Niño event (Tegner and Dayton 1991). These patterns are consistent

with my results that show a persistent temperature/ENSO correlation with sea urchin settlement in southern California.

In contrast, sea urchin settlement at Fort Bragg exhibited a positive correlation with temperature and El Niño. Unfortunately the data are limited at Fort Bragg, making it difficult to evaluate whether offshore transport on the monthly scale influences settlement. The positive temperature correlation may be consistent with this hypothesis, and off the coast of northern California and Oregon, strong, persistent upwelling periods are thought to negatively impact settlement patterns (Connolly et al. 2001, Ebert and Russell 1988, Gaines and Roughgarden 1985, Parrish et al. 1981, Roughgarden et al. 1988, Shkedy and Roughgarden 1997, Wing et al. 2003). However, measurements of pelagic larvae have thus far not supported this hypothesis (Morgan and Fisher 2010, Morgan et al. 2009a,b, Shanks and Shearman 2009)

Potential mechanisms underlying correlations with settlement and SST/ENSO in southern California

The negative correlations between settlement and both ENSO and temperature in southern California may persist for several reasons. Warm, El Niño type events are also associated with different patterns of circulation in the Southern California Bight. Thus, these observations may arise from direct effects of temperature (i.e., direct survival impacts on larvae or impediments to reproduction) or patterns of circulation associated with ENSO fluctuations.

Along the California coast, interannual and seasonal variation in current patterns may have altered delivery of larvae from adequate source populations to suitable destinations (Mitarai et al. 2009, Shanks and Eckert 2005). For example, the strong El Niño event of 1998 included a major shift from net equatorial flow in the California Current to net poleward flow (Lynn and Bograd 2002). In this case, water masses that reached San Diego and the Santa Barbara Channel may have increased connectivity to regions near or beyond the southern boundary of *S. purpuratus*. Similarly, El Niño events may have limited thermal stratification which can inhibit onshore delivery. Finally, unfortunately we have no metric of pelagic larval supply and inference about total delivery and connectivity is challenging without such data (Pineda 2000, Pineda et al. 2007).

Direct effects of temperature may also have played a role in producing the observed trends. The exact temperature ranges that impact survival in nature for *S. purpuratus* are unknown. Azad et al. (2012) showed that larvae of *S. purpuratus* survived optimally in the laboratory between 11-14°C, with stark changes in survival at 17°C and Schroeder and Battaglia (1985) showed abnormal larval development occurred above 16°C. Temperature may also impact zygote formation in *S. purpuratus*, and several observations suggest that even healthy adults may not produce viable gametes above approximately 17°C (Basch and Tegner 2007, Cochran and Engelmann 1975) despite observations of urchins with large and healthy gonads when living above this value (Lester et al. 2007). These thresholds lie above the typical range experienced in the Southern California Bight by adults and larvae of *S. purpuratus*. However, if in certain years nearshore

water pushed larvae from the southern boundary on the Baja California Peninsula into the Southern California Bight, then direct temperature effects may have played a role in driving the observed patterns.

Lack of correlation with sea surface chlorophyll in Southern California

Surprisingly, settlement patterns show no direct correlation with sea surface chlorophyll. The lack of evidence for planktonic food limitation (or other potentially influential exogenous dynamics for that matter) does not imply it was not important for larvae. In general, capturing a relationship between food supply and nutrition of planktonic provides a substantial challenge because of limitations on the spatial resolution of food availability and the difficulty in determining exactly where larvae have fed. Particular geographic areas can retain productive water, producing a highly heterogeneous environment (Vander Woude et al. 2006). Thus, incorporating information only where larvae were likely to actually be present (i.e., along the paths from source to destination for a given time period) may provide a valuable avenue for examining food limitation hypotheses for planktonic larvae. However, in the Santa Barbara Channel chlorophyll concentrations were not linearly correlated with recent El Niño/ La Niña events (Otero and Siegel 2004) and thus are unlikely to explain the correlation with recent ENSO cycles.

Importance of regional adult density and larval production

Data from the Santa Barbara Channel revealed a positive correlation between density of *S. purpuratus* adults in the Channel Islands in the prior summer and subsequent settlement (Table 4.2). While the positive correlation is supported and statistically significant after model averaging, interpreting the real meaning of this correlation presents a challenge. Specifically the question of whether adults increase recruitment or recruitment increases adults is unanswered. There is a debate over the value of such stock-recruit type correlations because of a chicken or egg dilemma where one can often mistake a recruit-stock relationship for a stock-recruit relationship (Szuwalski et al. 2014). Thus, observed adult-settlement correlations should be interpreted with caution.

There is no evidence my results that regional kelp coverage positively impacts settlement patterns. However, there is no metric for total adult food supply. Tegner and Dayton (1991) hypothesized that decreases in *S. purpuratus* recruitment during the 1983-1984 El Niño occurred because of decreased reproductive capacity inferred from fisheries yields. Change in adult urchin food supply may still have impacted recruitment and is worth future exploration in red urchins (*S. franciscanus*) where fisheries yields might lend insight into changes in per capita reproductive capacity through time.

Importance of settlement on juvenile recruitment

Regardless of what drives settlement patterns, settlement patterns are related to subsequent recruitment of juvenile urchins (Figure 4.7). Specifically, the spatial means among the Channel Islands show a strong correlation between settlement and subsequent juvenile recruitment. Patterns of juvenile density at individual sites respond to local stressors (i.e., predation or habitat limitation (Rowley 1989)). However when larval settlement is driven by regional forces (as appears the case here) the average recruitment of juveniles throughout the Channel Islands appears to have responded.

Conclusions

Here I demonstrate that settlement dynamics of *S. purpuratus* in Southern California are negatively correlated with sea surface temperature and El Niño fluctuations. The patterns are consistent across sites in southern California, where settlement dynamics appear to fluctuate somewhat synchronously, indicating at least some of the major variability may result from factors influencing ocean conditions throughout the Southern California Bight. These negative correlations with El Niño and sea surface temperatures appear to extend beyond the present time series (1991-2013) back to the El Niño events in the 1970s and early 1980s. These unique time series provide a relatively unprecedented illustration of climate related impacts on settlement dynamics that are notoriously difficult to investigate. Given that patterns of settlement tend to translate

into recruitment of juveniles, mechanistic investigations focusing on what processes lead to these observations can lend insight into how climate change may influence regional population dynamics in this and other marine species.

Acknowledgements

References

Azad, A. K., C. M. Pearce, and R. S. McKinley. 2012. Influence of stocking density and temperature on early development and survival of the purple sea urchin, *Strongylocentrotus purpuratus* (Stimpson, 1857). Aquaculture Research 43:1577–1591.

Bakun, A. 1973. Coastal upwelling indices, west coast of North America, 1946-71. Report, US Department of Commerce, National Oceanic and Atmospheric Administration, National Marine Fisheries Service.

Basch, L. V., and M. J. Tegner. 2007. Reproductive responses of Purple sea urchin (*Strongylocentrotus purpuratus*) populations to environmental conditions across a coastal depth gradient. Bulletin of Marine Science 81:255–282.

Beddingfield, S. D., and J. B. McClintock. 1998. Differential survivorship, reproduction, growth and nutrient allocation in the regular echinoid *Lytechinus variegatus* (Lamarck) fed natural diets. Journal of Experimental Marine Biology and Ecology 226:195–215.

Bertram, D., and R. Strathmann. 1998. Effects of maternal and larval nutrition on growth and form of planktotrophic larvae. Ecology 79:315–327.

Burnham, K., and D. Anderson. 2002. Model selection and multimodel inference: a practical information-theoretic approach. 2nd ed. Springer Verlag, New York.

Byrne, M., M. Ho, P. Selvakumaraswamy, H. D. Nguyen, S. A. Dworjanyn, and A. R. Davis. 2009. Temperature, but not pH, compromises sea urchin fertilization and early development under near-future climate change scenarios. Proceedings of the Royal Society B: Biological Sciences 276:1883–1888.

Byrne, M., M. Sewell, and T. Prowse. 2008. Nutritional ecology of sea urchin larvae: influence of endogenous and exogenous nutrition on echinopluteal growth and pheno-typic plasticity in *Tripneustes gratilla*. Functional Ecology 22:643–648.

Cavanaugh, K., D. Siegel, D. Reed, and P. Dennison. 2011. Environmental controls of giant kelp biomass in the Santa Barbara Channel. Marine Ecology Progress Series 429:1–17.

Cavanaugh, K. C., D. Siegel, D. Reed, and T. Bell. 2014. SBC LTER: Time series of kelp biomass in the canopy from Landsat 5, 1984 -2011. Santa Barbara Coastal LTER. knb-lter-sbc.54.6 http://metacat.lternet.edu/knb/metacat/knb-lter-sbc.54.6/lter.

Cazelles, B., M. Chavez, D. Berteaux, F. Menard, J. Vik, S. Jenouvrier, and N. Stenseth. 2008. Wavelet analysis of ecological time series. Oecologia 156:287–304.

Chen, C.-P., and B.-Y. Chen. 1992. Effects of high temperature on larval development and metamorphosis of *Arachnoides placenta* (Echinodermata: Echinoidea). Marine Biology 112:445–449.

Cochran, R. C., and F. Engelmann. 1975. Environmental regulation of the annual reproductive season of *Strongylocentrotus purpuratus* (Stimpson). The Biological Bulletin 148:393–401.

Connolly, S. R., B. A. Menge, and J. Roughgarden. 2001. A latitudinal gradient in recruitment of intertidal invertebrates in the northeast Pacific Ocean. Ecology 82:1799–1813.

Ebert, T. 1983. Recruitment in echinoderms. Echinoderm Studies 1:169–203.

———. 2010. Demographic patterns of the purple sea urchin *Strongylocentrotus purpuratus* along a latitudinal gradient, 1985-1987. Marine Ecology Progress Series 406:105–120.

Ebert, T., S. Schroeter, J. Dixon, and P. Kalvass. 1994. Settlement patterns of red and purple sea urchins (*Strongylocentrotus franciscanus* and *S. purpuratus*) in California, USA. Marine Ecology Progress Series 111:41–52.

Ebert, T. A., and M. P. Russell. 1988. Latitudinal variation in size structure of the west coast purple sea urchin: a correlation with headlands. Limnology and Oceanography 33:286–294.

Gaines, S., and J. Roughgarden. 1985. Larval settlement rate: a leading determinant of structure in an ecological community of the marine intertidal zone. Proceedings of the National Academy of Sciences 82:3707–3711.

Gonor, J. 1973. Reproductive cycles in oregon populations of the echlnoid, *Strongylocentrotus purpuratus* (Stimpson). I. Annual gonad growth and ovarian gametogenic cycles. Journal of Experimental Marine Biology and Ecology 12:45–64.

Hoegh-Guldberg, O., and J. Pearse. 1995. Temperature, food availability, and the development of marine invertebrate larvae. American Zoologist 35:415–425.

Kahru, M., R. M. Kudela, M. Manzano-Sarabia, and B. Greg Mitchell. 2012. Trends in the surface chlorophyll of the California Current: Merging data from multiple ocean color satellites. Deep Sea Research Part II: Topical Studies in Oceanography 77:89–98.

Kenner, M., and M. Lares. 1991. Size at first reproduction of the sea urchin *Strongylocentrotus purpuratus* in a central California kelp forest. Marine Ecology Progress Series 76:303–306.

Koenker, R. 2013. quantreg: Quantile Regression. R package version 5.05.

Kushner, D. J., A. Rassweiler, J. P. McLaughlin, and K. D. Lafferty. 2013. A multidecade time series of kelp forest community structure at the California Channel Islands: Ecological Archives E094-245. Ecology 94:2655–2655.

Lester, S., S. Gaines, and B. Kinlan. 2007. Reproduction on the edge: large-scale patterns of individual performance in a marine invertebrate. Ecology 88:2229–2239.

Ling, S. D., C. Johnson, S. Frusher, and C. King. 2008. Reproductive potential of a marine ecosystem engineer at the edge of a newly expanded range. Global Change Biology 14:907–915.

Lukacs, P. M., K. P. Burnham, and D. R. Anderson. 2010. Model selection bias and Freedman's paradox. Annals of the Institute of Statistical Mathematics 62:117–125.

Lynn, R., and S. Bograd. 2002. Dynamic evolution of the 1997–1999 El Niño–La Niña cycle in the southern California Current system. Progress in Oceanography 54:59–75.

Mantua, N. J., and S. R. Hare. 2002. The Pacific decadal oscillation. Journal of Oceanography 58:35–44.

McEdward, L. R. 1985. Effects of temperature on the body form, growth, electron transport system activity, and development rate of an echinopluteus. Journal of Experimental Marine Biology and Ecology 93:169–181.

Meidel, S. K., R. E. Scheibling, and A. Metaxas. 1999. Relative importance of parental and larval nutrition on larval development and metamorphosis of the sea urchin *Strongylocentrotus droebachiensis*. Journal of Experimental Marine Biology and Ecology 240:161–178.

Meyer, E., A. Green, M. Moore, and D. Manahan. 2007. Food availability and physiological state of sea urchin larvae (*Strongylocentrotus purpuratus*). Marine Biology 152:179– 191.

Miller, B., and B. Emlet. 1999. Development of newly metamorphosed juvenile sea urchins (*Strongylocentrotus franciscanus* and *S. purpuratus*): morphology, the effects of temperature and larval food ration, and a method for determining age. Journal of Experimental Marine Biology and Ecology 235:67–90.

Miner, B. 2007. Larval feeding structure plasticity during pre-feeding stages of echinoids: not all species respond to the same cues. Journal of Experimental Marine Biology and Ecology 343:158–165.

Mitarai, S., D. A. Siegel, J. R. Watson, C. Dong, and J. C. McWilliams. 2009. Quantifying connectivity in the coastal ocean with application to the Southern California Bight. Journal of Geophysical Research: Oceans 114.

Morgan, S. G., and J. L. Fisher. 2010. Larval behavior regulates nearshore retention and offshore migration in an upwelling shadow and along the open coast. Marine Ecology Progress Series 404:109–126.

Morgan, S. G., J. L. Fisher, and A. J. Mace. 2009*a*. Larval recruitment in a region of strong, persistent upwelling and recruitment limitation. Marine Ecology Progress Series 394:79–99.

Morgan, S. G., J. L. Fisher, S. H. Miller, S. T. McAfee, and J. L. Largier. 2009*b*. Nearshore larval retention in a region of strong upwelling and recruitment limitation. Ecology 90:3489–3502.

Ng, E. K., and J. C. Chan. 2012. Geophysical applications of partial wavelet coherence and multiple wavelet coherence. Journal of Atmospheric and Oceanic Technology 29:1845–1853.

Otero, M. P., and D. Siegel. 2004. Spatial and temporal characteristics of sediment plumes and phytoplankton blooms in the Santa Barbara Channel. Deep Sea Research Part II: Topical Studies in Oceanography 51:1129–1149.

Padilla-Gamiño, J. L., M. W. Kelly, T. G. Evans, and G. E. Hofmann. 2013. Temperature and CO2 additively regulate physiology, morphology and genomic responses of larval sea urchins, *Strongylocentrotus purpuratus*. Proceedings of the Royal Society B: Biological Sciences 280:2536–2546.

Parrish, R. H., C. S. Nelson, and A. Bakun. 1981. Transport mechanisms and reproductive success of fishes in the California Current. Biological Oceanography 1:175–203.

Pearse, J., V. Pearse, and K. Davis. 1986. Photoperiodic regulation of gametogenesis and growth in the sea urchin *Strongylocentrotus purpuratus*. Journal of Experimental Zoology 237:107–118.

Pineda, J. 2000. Linking larval settlement to larval transport: assumptions, potentials, and pitfalls. Oceanography of the Eastern Pacific 1:84–105.

Pineda, J., J. Hare, and S. Sponaungle. 2007. Larval transport and dispersal in the coastal ocean and consequences for population connectivity. Oceanography 20.

Pinheiro, J., D. Bates, D. Saikat, S. D, and R. D. C. team. 2011. nlme: Linear and Nonlinear Mixed Effects Models.

Poulin, E., A. Palma, G. Leiva, D. Narvaez, R. Pacheco, S. Navarrete, and J. Castilla. 2002. Avoiding offshore transport of competent larvae during upwelling events: the case of the gastropod *Concholepas concholepas* in central Chile. Limnology and Oceanography 47:1248–1255.

Reynolds, R. W., T. M. Smith, C. Liu, D. B. Chelton, K. S. Casey, and M. G. Schlax. 2007. Daily high-resolution-blended analyses for sea surface temperature. Journal of Climate 20:5473–5496.

Roughgarden, J., S. Gaines, and H. Possingham. 1988. Recruitment dynamics in complex life cycles. Proceedings of the National Academy of Sciences 85:1460–1466.

Roughgarden, J., J. Pennington, D. Stoner, S. Alexander, and K. Miller. 1991. Collisions of upwelling fronts with the intertidal zone: the cause of recruitment pulses in barnacle populations of central California. Acta Oecologica 12:35–51.

Rowley, R. 1989. Settlement and recruitment of sea urchins (*Strongylocentrotus* spp.) in a sea-urchin barren ground and a kelp bed: are populations regulated by settlement or post-settlement processes? Marine Biology 100:485–494.

Schroeder, T., and D. Battaglia. 1985. "Spiral asters" and cytoplasmic rotation in sea urchin eggs: induction in *Strongylocentrotus purpuratus* eggs by elevated temperature. The Journal of cell biology 100:1056–1062.

Shanks, A. 2009. Pelagic larval duration and dispersal distance revisited. The Biological Bulletin 216:373–385.

Shanks, A., and G. Eckert. 2005. Population persistence of California Current fishes and benthic crustaceans: a marine drift paradox. Ecological Monographs 75:505–524.

Shanks, A., and R. Shearman. 2009. Paradigm lost? Cross-shelf distributions of intertidal invertebrate larvae are unaffected by upwelling or downwelling. Marine Ecology Progress Series 385:189–204.

Shanks, A. L., and L. Brink. 2005. Upwelling, downwelling, and cross-shelf transport of bivalve larvae: test of a hypothesis. Marine Ecology Progress Series 302:1–12.

Shanks, A. L., and G. C. Roegner. 2007. Recruitment limitation in Dungeness crab populations is driven by variation in atmospheric forcing. Ecology 88:1726–1737.

Shepherd, J., and D. Cushing. 1980. A mechanism for density-dependent survival of larval fish as the basis of a stock-recruitment relationship. Journal du Conseil 39:160–167.

Shkedy, Y., and J. Roughgarden. 1997. Barnacle recruitment and population dynamics predicted from coastal upwelling. Oikos pages 487–498.

Siegel, D., S. Mitarai, C. Costello, S. Gaines, B. Kendall, R. Warner, and K. Winters. 2008. The stochastic nature of larval connectivity among nearshore marine populations. Proceedings of the National Academy of Sciences 105:8974–8979.

Strathmann, M. 1987. Reproduction and development of marine invertebrates of the northern Pacific coast: data and methods for the study of eggs, embryos, and larvae. Univ. of Wash. Press, Seattle.

Strathmann, R. 1978. Length of pelagic period in echinoderms with feeding larvae from the northeast Pacific. Journal of Experimental Marine Biology and Ecology 34:23–27.

Szuwalski, C. S., K. A. VertPre, A. E. Punt, T. A. Branch, and R. Hilborn. 2014. Examining common assumptions about recruitment: a metaanalysis of recruitment dynamics for worldwide marine fisheries. Fish and Fisheries In Press.

Tegner, M., and P. Dayton. 1991. Sea urchins, El Ninos, and the long term stability of Southern California kelp forest communities. Marine Ecology Progress Series 77:49–63.

Vaïtilingon, D., R. Morgan, P. Grosjean, P. Gosselin, and M. Jangoux. 2001. Effects of delayed metamorphosis and food rations on the perimetamorphic events in the echinoid *Paracentrotus lividus* (Lamarck, 1816)(Echinodermata). Journal of Experimental Marine Biology and Ecology 262:41–60.

Vander Woude, A., J. Largier, and R. Kudela. 2006. Nearshore retention of upwelled waters north and south of Point Reyes (northern California)—Patterns of surface temperature and chlorophyll observed in CoOP WEST. Deep Sea Research Part II: Topical Studies in Oceanography 53:2985–2998.

Wing, S. R., L. W. Botsford, L. E. Morgan, J. M. Diehl, and C. J. Lundquist. 2003. Inter-annual variability in larval supply to populations of three invertebrate taxa in the northern California Current. Estuarine, Coastal and Shelf Science 57:859–872.

Wolter, K., and M. S. Timlin. 1993. Monitoring ENSO in COADS with a seasonally adjusted principal component index. Pages 52–7 *in* Proc. of the 17th Climate Diagnostics Workshop.

———. 1998. Measuring the strength of ENSO events: how does 1997/98 rank? Weather 53:315–324.

Wood, S. N. 2011. Fast stable restricted maximum likelihood and marginal likelihood estimation of semiparametric generalized linear models. Journal of the Royal Statistical Society: Series B (Statistical Methodology) 73:3–36.

Tables

Table 4.1: Table of coefficients, adjusted P-values, and cumulative AICc weight for the Multivariate El Niño Southern Oscillation Index (MEI), Pacific Decadal Oscillation (PDO) and regional interactions in the linear mixed effects models of annual settlement (December - September) at sites in the Santa Barbara Channel and San Diego. AICc was calculated for every possible combination of covariates (8 total models) and model averaged coefficient estimates and standard errors were calculated using AICc weights for each estimate to account for model uncertainty in estimates, standard errors and P-values. All models included an autoregressive model [AR(1)] on the errors to account for the observed significant first order serial autocorrelation.

variable	sign	P-value	ΣAICc weights
MEI (El Niño/La Niña)	**-**	**<0.001**	**>0.999**
PDO	NS	0.855	0.280
Int[MEI : SB channel vs. SD]	NS	0.164	0.796
Int[PDO : SB channel vs SD]	NS	0.954	0.052
Site Only			0.000

Table 4.2: Table of coefficient signs, adjusted P-values, and cumulative AICc weight for each variable in the linear mixed effects models of annual settlement (December - September) at sites in the Santa Barbara Channel. AICc was calculated for every possible combination of covariates (i.e.,64 models for data between 1997 and 2008) and model averaged coefficient estimates and standard errors were calculated using AICc weights for each estimate to account for model uncertainty in estimates, standard errors and P-values. The analyses are repeated in each overlapping time span due to inconsistent coverage of covariates. All models included an autoregressive model [AR(1)] on the errors to account for the observed significant first order serial autocorrelation.

	(1997-2008)			(1991-2008)			(1997-2012)		
variable	sign	P-value	Σ weights	sign	P-value	Σ weights	sign	P-value	Σ weights
SST	**-**	**<0.001**	**>0.999**	**-**	**<0.001**	**>0.999**	**-**	**<0.001**	**>0.999**
adult density	**+**	**<0.001**	**0.994**	**+**	**<0.001**	**0.999**	**+**	**<0.001**	**0.997**
kelp coverage	-	0.001	0.990	-	<0.001	0.998			
upwelling	+	0.876	0.057	-	0.898	0.137	-	0.455	0.481
downwelling	+	0.999	0.051	+	0.910	0.134	+	0.569	0.358
chlorophyll	-	0.247	0.663				-	0.816	0.200
site only			0.000			0.000			0.000
	[64 combinations: N= 28]			[32 combinations: N= 41]			[32 combinations: N= 48]		

	(1991-2012)			(1991-2013)			
variable	sign	P-value	Σ weights	sign	P-value	Σ weights	
SST	**-**	**<0.001**	**>0.999**	**-**	**<0.001**	**>0.999**	
adult density							
kelp coverage							
upwelling	-	0.396	0.556	-	0.396	0.556	
downwelling	-	0.959	0.232	-	0.959	0.232	
chlorophyll							
site only			0.000			0.000	
	[16 combinations: N= 68]			[8 combinations: N= 72]			

Table 4.3: Table of coefficient signs, adjusted P-values, and cumulative AICc weight for each variable in the linear mixed effects models of annual settlement (December - September) at sites in the Southern California Bight (including the Santa Barbara Channel and San Diego area sites). AICc was calculated for every possible combination of covariates and nested interactions (i.e.,113 models for data between 1997 and 2008) and model averaged coefficient estimates and standard errors were weighted by AICc weights for each estimate to account for model uncertainty in P-values. The analyses are repeated in each overlapping time span due to inconsistent coverage of covariates. All models included: (1) an autoregressive model [AR(1)] model on the errors to account for the observed significant first order serial autocorrelation, and (2) separate error variance by site to account for heteroscedasticity.

variable		(1997-2008)			(1991-2008)	
	sign	P-value	Σ weights	sign	P-value	Σ weights
SST	**-**	**<0.001**	**>0.999**	**-**	**<0.001**	**>0.999**
kelp coverage	-	0.640	0.289	-	0.708	0.301
chlorophyll	-	0.770	0.189			
upwelling	-	0.900	0.244	-	0.323	0.761
downwelling	+	0.927	0.152	+	0.786	0.268
Int[SST: SB vs SD]	+	0.919	0.018	+	0.882	0.070
Int[kelp coverage SB vs SD]	+	0.872	0.029	+	0.789	0.083
Int[chlorophyll: SB vs SD]	+	0.979	0.001			
Int[upwelling:SB vs SD]	-	0.833	0.080	-	0.636	0.331
Int[downwelling: SB vs SD]	-	0.993	0.000	-	0.825	0.060
site only			0.000			0.000
		[113 combinations: N= 49]			[43 combinations: N= 72]	

variable		(1997-2013)			(1991-2013)	
	sign	P-value	Σ weights	sign	P-value	Σ weights
SST	**-**	**<0.001**	**>0.999**	**-**	**<0.001**	**>0.999**
kelp coverage						
chlorophyll	-	0.001	0.991			
upwelling	-	0.474	0.556	-	0.603	0.671
downwelling	+	0.643	0.334	+	0.628	0.369
Int[SST: SB vs SD]	+	0.714	0.151	+	0.681	0.206
Int[kelp coverage SB vs SD]						
Int[chlorophyll: SB vs SD]	+	0.890	0.062			
Int[upwelling:SB vs SD]	+	0.884	0.258	-	0.590	0.423
Int[downwelling: SB vs SD]	-	0.963	0.017	-	0.933	0.036
site only			0.000			0.000
		[43 combinations: N= 96]			[17 combinations: N= 137]	

Table 4.4: Cumulative support for individual covariates from generalized additive model multiple regression in the Southern California Bight (Santa Barbara Channel and San Diego County). Sign represents the general direction of the smoother, and is only shown when significant under model uncertainty. Cumulative AICc weight represents cumulative AICc support from all possible covariate combinations. All models included (1) an autoregressive model [AR(1)] on the errors to account for the observed significant first order serial autocorrelation and (2) error variance that increased exponentially with the predicted response.

variable	(1996-2013)		(1991-2013)	
	smoother sign	ΣAICc weights	smoother sign	ΣAICc weights
SST	-	**>0.999**	-	**>0.999**
offshore transport	NS	0.953	NS	0.127
chlorophyll	NS	0.200		
site & seasonal trend only		0.000		0.000
	[8 combinations: N= 845]		[4 combinations: N= 1197]	

Figures
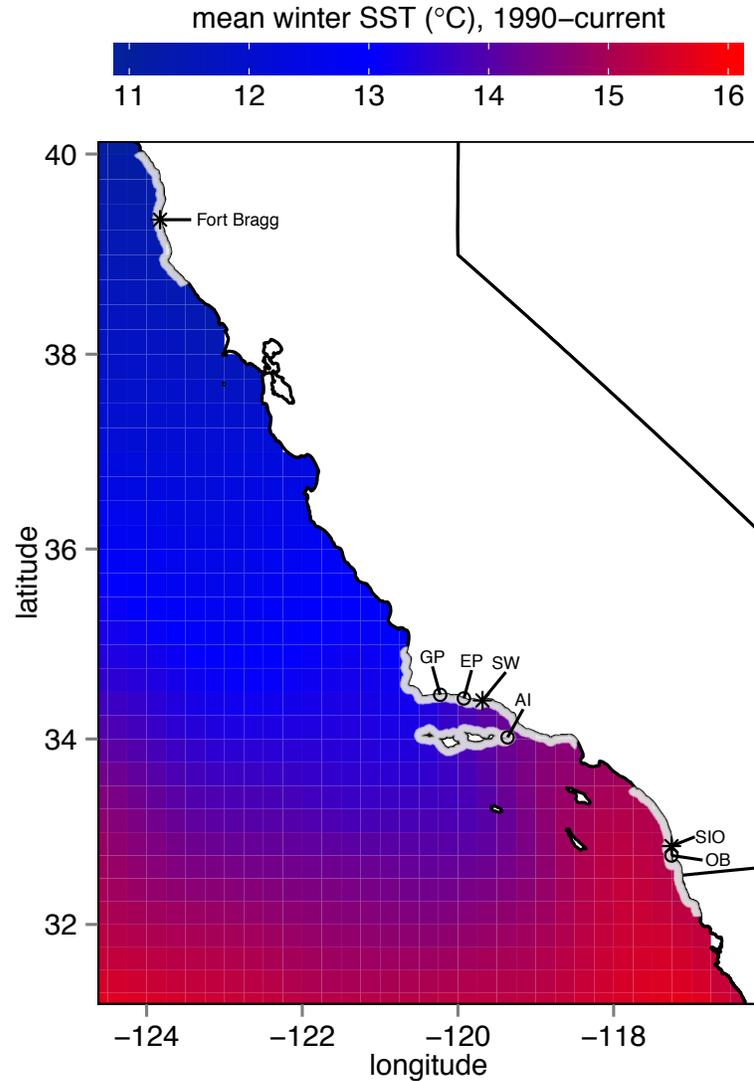
Figure 4.1: Map of collection sites in California superimposed on mean winter sea surface temperature (Dec 21-Mar 21) in each1/4 °Lat/Long cell from AVHRR satellite imagery. From North to South, sites are Fort Bragg, GP = Gaviota Pier, EP = Ellwood Pier, SW = Stearns Wharf, AI = Anacapa Island (on the North shore), SIO= Scripps Pier at Scripps Institute of Oceanography and OB = Ocean Beach Pier. The grey areas along the coastline represent the spatial buffers from which sea surface chlorophyll concentration data are included for around Fort Bragg, Stearns Wharf or Scripps Pier (see Methods for details).
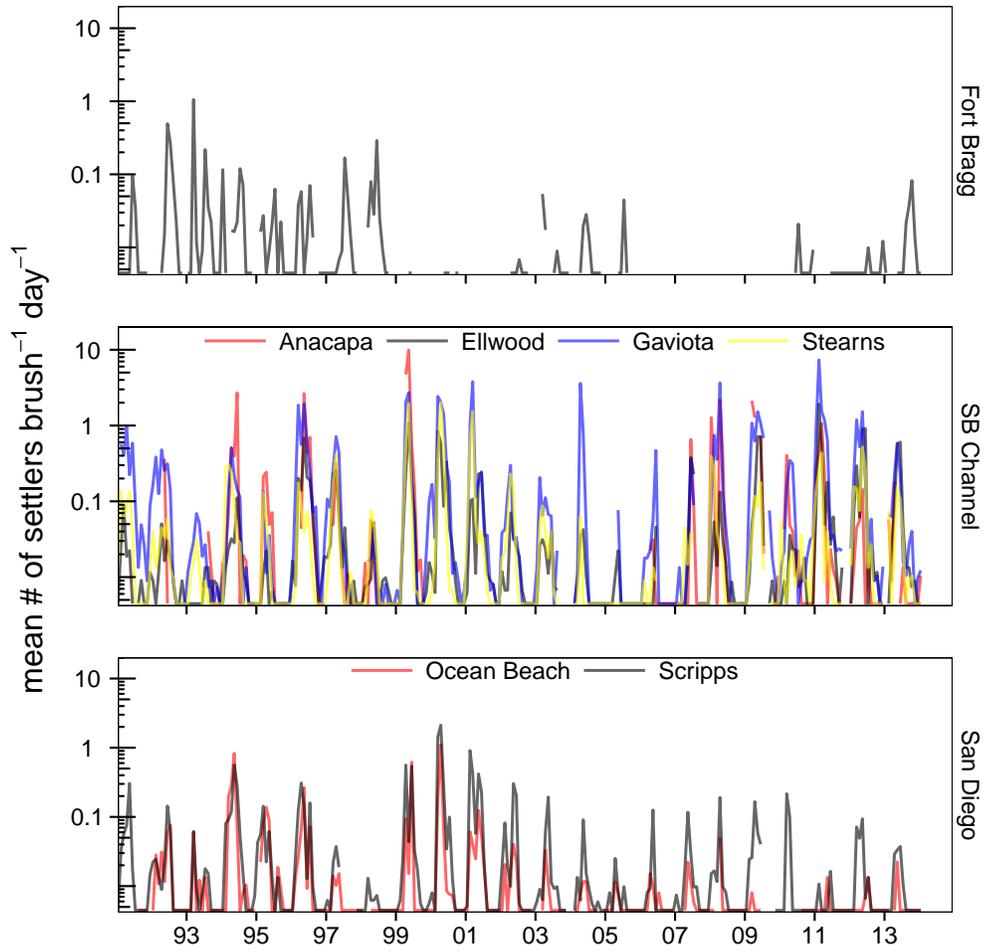
Figure 4.2: Monthly mean settlement density at each collection site, grouped by region.
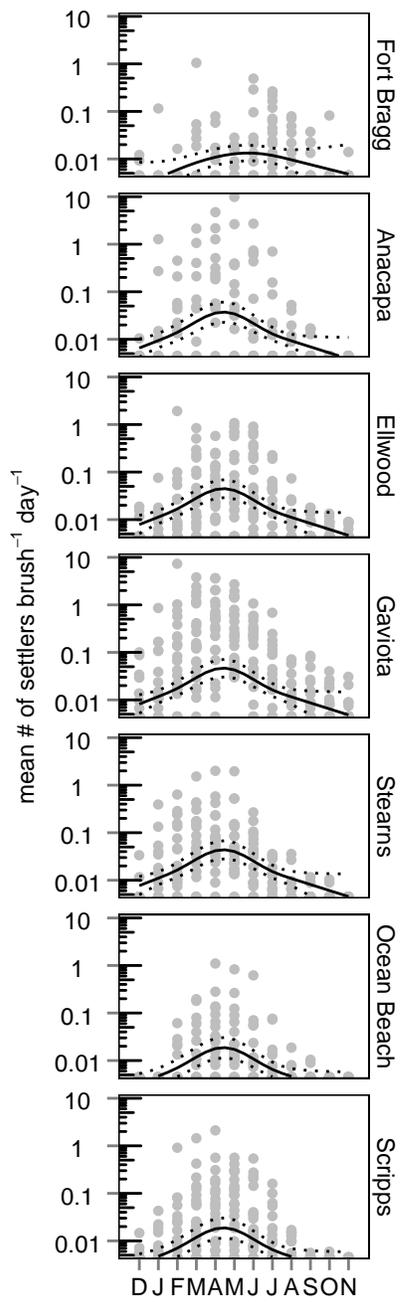
Figure 4.3: Monthly settlement by month at each site. Lines represent the GAMM smoother of the average seasonal trend with dotted lines indicating upper and lower 95% confidence intervals.
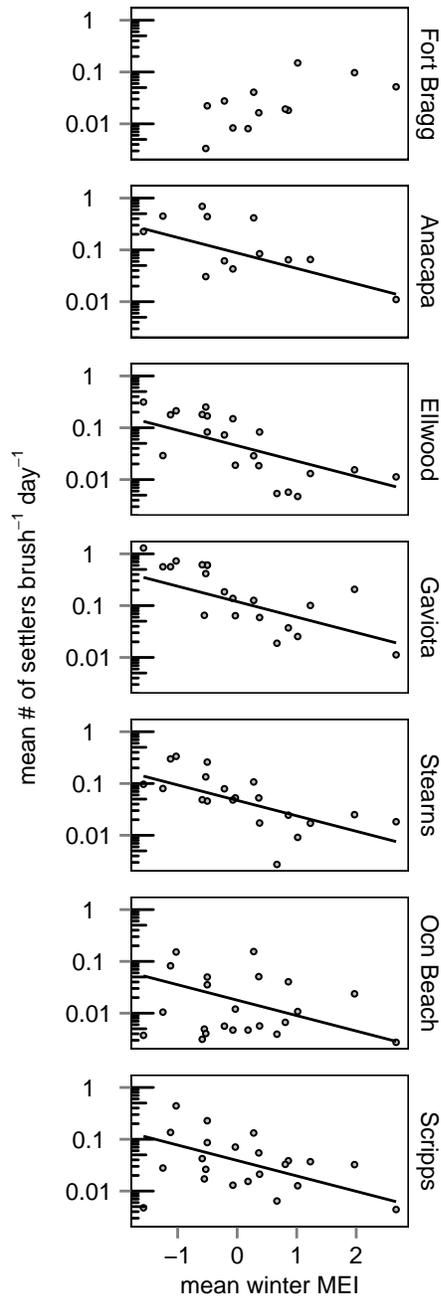
Figure 4.4: Annual mean settlement at each collection location versus the mean Multivariate El Niño Southern Oscillation Index (MEI) from January through April. Lines represent the predictions from the linear mixed effects model. The LME includes an AR(1) model of the errors with each site.
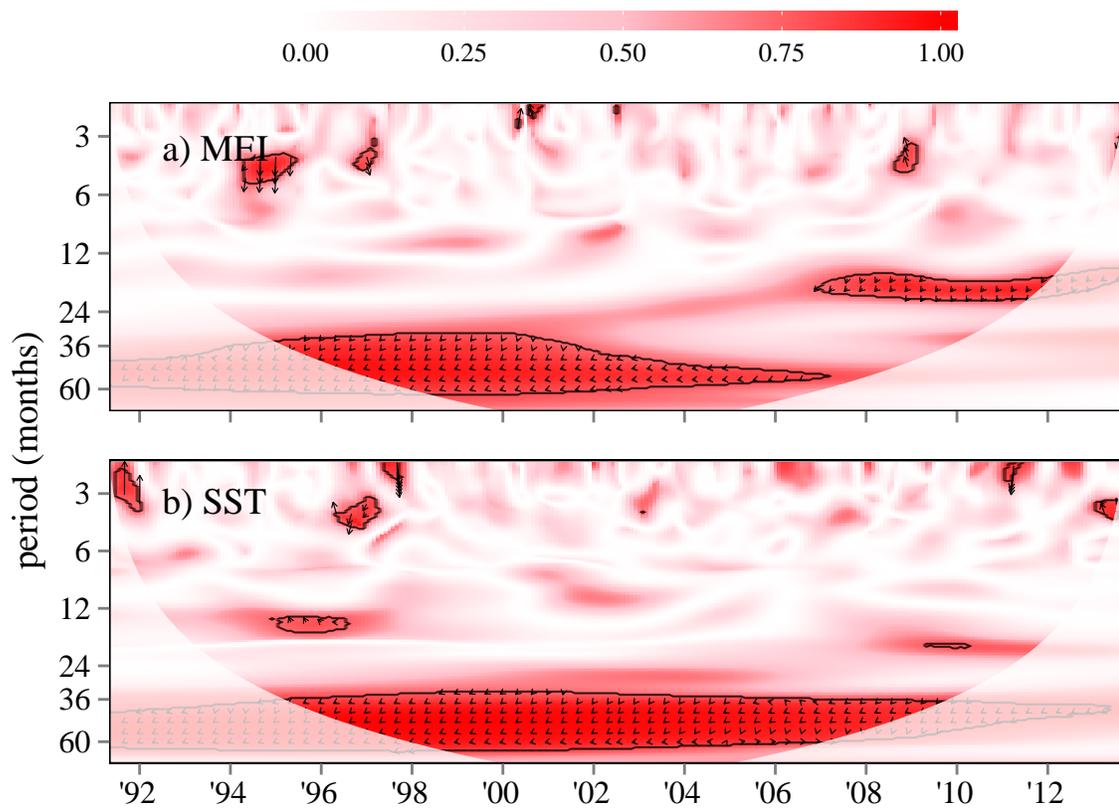
Figure 4.5: Partial wavelet coherence between fluctuations in settlement and temperature time series generated for the Gaviota Pier. The seasonal settlement cycle is accounted for directly in the analysis. Coherence between the time series is significant and persistent at the 3-5 year period (significant coherence denoted by black contour lines), indicating coherent fluctuations occur on the multi-year scale. Arrows indicate the phase relationship; those pointing to the left indicate time series are out of phase (i.e.,negatively correlated) while arrows pointing downward indicate MEI or SST leads settlement.
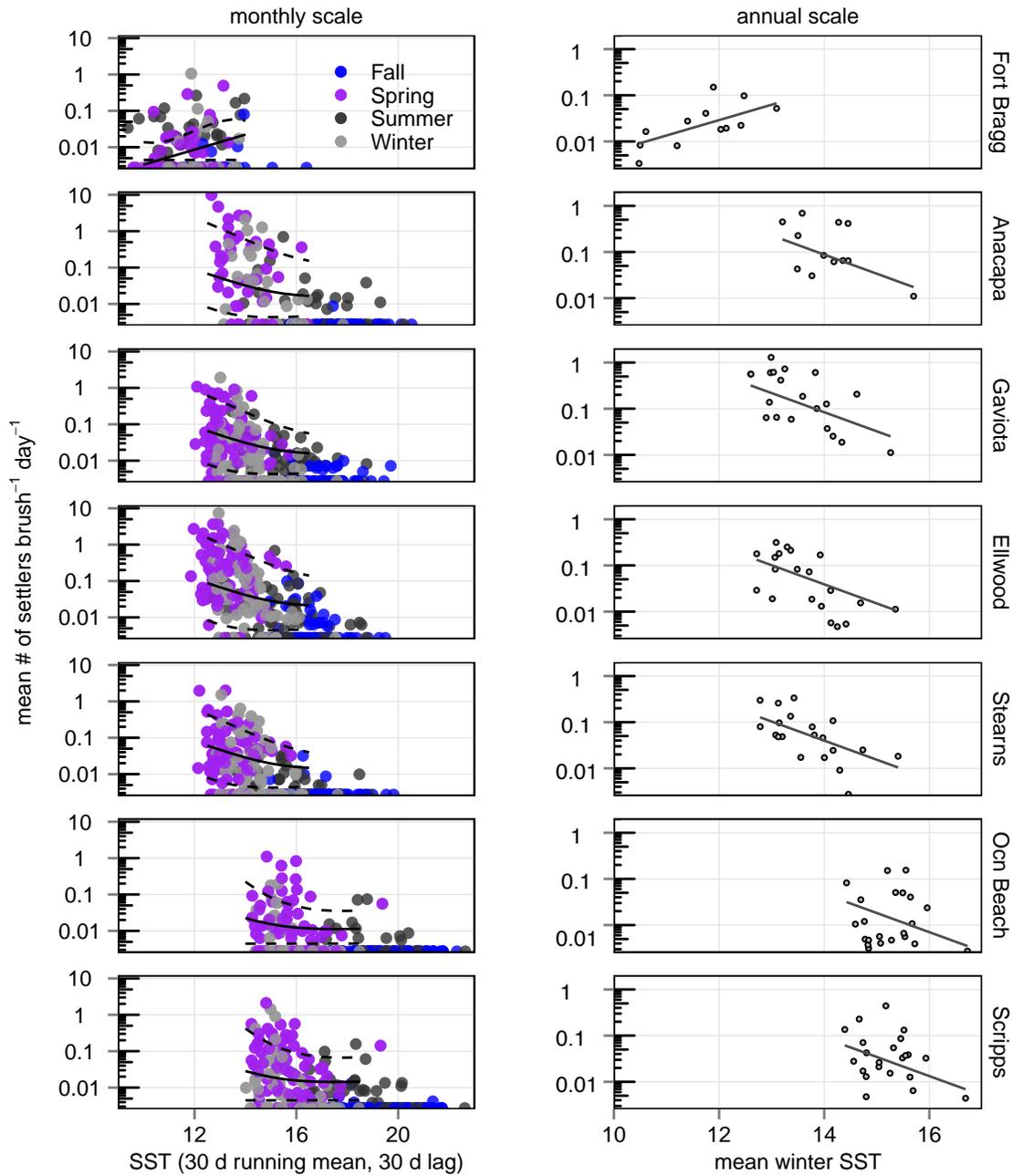
Figure 4.6: Monthly scale: Monthly mean settlement versus spatially averaged sea surface temperature (SST). Solid lines represent the GAMM prediction of the mean while dashed lines represent the 20th and 80th quantile from quantile regressions. Both the model forms directly account for the seasonal trend (Figure 4.3). Predictions shown are for the month of March. **Annual scale:** Annual mean settlement at each collection location versus the mean SST composite from December through April. Lines represent the predictions from the linear mixed effects model with regional interactions.
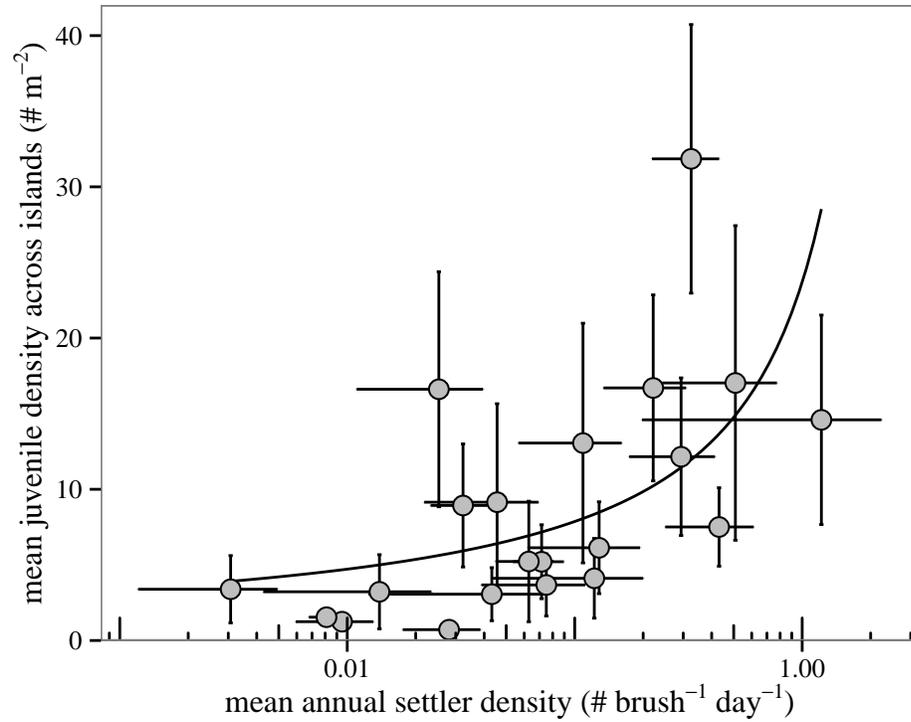
Figure 4.7: Mean summer juvenile urchin density (<2 cm test diameter) across the Channel Islands versus mean density of settlers in the preceding winter season (December through April) in the Santa Barbara Channel (mean of settlement at Gaviota Pier, Stearns Wharf, Ellwood Pier and Anacapa Pier) from 1992 through 2011.

Appendix D

Experimental comparison of reproductive capacity of barren versus kelp forest urchins

I conducted three studies to evaluate the impacts of urchin barrens and malnourishment on reproductive capacity in the purple urchin *Strongylocentrotus purpuratus*. First I collected urchins from one barren and one nearby healthy kelp forest through time to illustrate the persistence of reproductive depression in barrens in comparison to the seasonal changes in reproductive mass in kelp forests. Second, I estimated total fecundity in female urchins from several urchin barrens and several kelp forests by inducing them to spawn. Finally, I conducted an experiment in which I fed urchins from barrens and starved urchins from healthy kelp forests to ascertain the approximate length of time required for kelp forest urchins to resemble barren urchins (in terms of gonad index) and visa versa.

Methods

Time series of gonad index in a healthy kelp forest and an urchin barren

I monitored urchin gonad mass from one barren (Carpinteria reef) and one kelp forest site (Mohawk reef) with the help of the Santa Barbara Coastal Long Term Ecological Research (SBC LTER) program approximately every two months from mid-2011 to early 2014. I collected ≈ 20 urchins from each site, measured test diameter and test height, and measured dry mass of one intact gonad. I dried gonads in a drying oven at 60 for three to five days (until the mass leveled off at a constant value) and weighed each to the nearest 0.01 gram. I used dry mass because replicate wet mass measurements were highly variable (and likely overestimates) due to associated seawater content and blotting techniques during the reproductive period tended to remove copious amounts of gamete material. I only removed one gonad because of the challenge in acquiring more than a single gonad before the tissue oozed substantial gamete material. I multiplied the dry mass of the single intact gonad by 5 (the number of gonads per individual) to estimate the total dry gonad mass of that individual. I calculated the gonad index as the total dry mass divided by adjusted test volume (the volume minus the baseline volume

associated with size at first reproduction which [diameter $= 2.5$ cm, volume ≈ 32.7 cm^3).

Urchin test volume was calculated via the formula for a spheroid:

$$\text{test volume} = \frac{4\pi}{3}r^2h \tag{D.1}$$

where r is the maximum longitudinal test diameter and h is the test height (anus to peristomal opening)

Female fecundity in healthy kelp forests and urchin barrens

To evaluate size specific fecundity of urchins in barrens vs. urchins in kelp forests, I collected urchins and induced them to release their eggs. I collected urchins from a range of sizes at 7 locations: 4 kelp forest and 3 barrens near those kelp forests in January of 2012. The three urchin barrens had nearby kelp forests available for sampling, but were still hundreds of meters away (i.e. distinct but adjacent sets of reefs). Once colliected, urchins were held in flow through seawater tables for 24 hours and monitored for egg release. Any female that extruded eggs prior to artificial spawning (either in transit or in the lab) was not a candidate for sampling.

Fecundity was estimated by inducing egg extrusion until urchins released no more eggs. Induction of egg extrusion was accomplished via serial injection of 1 ml 0.55 M KCl into the body cavity. Once a pulse of egg release ceased, I waited approximately 20 minutes and injected another 1 ml of KCl. I repeated this process until injection yielded no further egg extrusion from live urchins. While extruding eggs, urchins were

submerged in containers filled with seawater that were themselves partly submerged in a flow through seawater table to maintain adequate temperature. I replaced seawater periodically by carefully decanting the container (eggs are visible and negatively buoyant and thus remain on the container bottom if undisturbed). Once all egg release had ceased and injections of KCl into live urchins no longer induced further egg extrusion, I removed each urchin and immediately dissected it for gonad sampling. I then carefully decanted water from the container and poured the concentrated egg solution into a graduated cylinder and diluted to 100 ml. I homogenized the solution was homogenized and removed a 1ml subsample and placed it into a 1.75 ml microcentrifuge tube with 0.5 ml of 2% formaline to preserve the sample for quantitative microscopy.

I compared egg extrusion of females by size in urchin barrens vs in kelp forests using a two step process. First I fit a logistic regression to estimate probability of releasing eggs in urchins from barrens (100% of urchins from kelp forests released eggs) and if this probability varied by test volume. Second I used mixed effects models to estimate the effect of reef state (kelp forests vs barren) while controlling for urchin size (test volume). I allowed the intercepts to vary by site, and checked to make sure that the x-intercept in the fecundity-test volume relationship roughly agreed with the minimum reproductive size (see above).

Impact of starvation or re-nourishment on urchin gonads

In order to evaluate the time required for a "healthy" kelp forest urchin to become similar in reproductive capacity to emaciated urchins from urchin barrens, I conducted an experiment in which I starved healthy urchins for variable time periods leading up to mid December and compared those to barren and kelp forest urchins that were fed for the same period of time as well as urchins freshly collected from both barrens and kelp forests. The experiment was stopped in mid-December because urchins tend to reach a maximum gonad size at approximately this time.

Treatments included A) urchins from kelp forests that were starved for 24, 18, 12, or 6 weeks before mid December, B) urchins from kelp forests that were fed two uniformly cut 10 cm diameter discs of Macrocystis twice per week for the same time periods as A, and C) urchins from barrens that were fed the same rations and frequency as A. The feeding rations were initially chosen according to the slowest consuming urchins. Thus most urchins consumed their individual ration by the next feeding period but some urchins were still consuming the previous ration at this point.

Urchins for each period were collected from the field, and test height and width measurements were taken, and only 8 urchins ranging from approximately 4.5 to 5.5 cm in test diameter were used for each treatment in each period. Once urchins were measured, I placed each within an individual 1 liter ventilated cell within a flow through seawater table. Cells were porous such that only very small (<2 cm) particles were capable of escaping the container and would sink if they escaped. To ensure that urchins

were not consuming fecal matter, the floor of the cells were lined with plastic light diffuser ("egg crate") that effectively trapped and isolated all feces from urchin grazing. The trapped feces was cleaned 1-2 times per week. Each cell had its own individual water source piped in but shared a common sea table and set of drains with all urchins. Urchins were monitored and if any urchin died within 1 week of being placed in the experiment, it was replaced with reserve urchins collected form the same location at the same site that kelp in an adjacent holding tank and had been provided the same rations. Any urchin dying after 1 week was not replaced.

At the end of the experiment, all urchins were remeasured (height and diameter), and one gonad extracted to measure dry mass and the gonad index defined above. In addition to urchins for the experiment, 15 additional reference urchins from each location were collected during each period (24, 18, 12, 6, and 0 weeks). These urchins were measured, dissected and one gonad was weighed for dry mass.

Results

Time series of gonad index in a healthy kelp forest and an urchin barren

Gonad index at Mohawk kelp forest always exceeded those in the Carpinteria barren (Figure D.1). Urchins from Carpinteria on average had 0.13 g total dry gonad mass while urchins from Mohawk had on average 1.57 g total gonad mass. Urchins from Mohawk showed clear seasonal patterns of reproductive allocation, with an obvious decline in

gonad size in the spring. In contrast, urchins from Carpinteria barrens showed little seasonal change in gonad index or gonad size.

Female fecundity in healthy kelp forests and urchin barrens

100% of individuals from kelp forest areas extruded eggs in contrast to only 33% of urchins from barren grounds. The fraction of adults that extruded eggs in the Carpinteria barrens did not appear to change in test volume (χ^2 = 0.78, p = 0.38) . With respect to total egg extrusion, on average urchins in barrens that extruded eggs produced 95.9% (95% CI = 86.6-98.7%) fewer than those from kelp forest sites for a given size (i.e., a 95.9% reduction in the fecundity-size relationship) which was a significant decline in the slope of the fecundity relationship (χ^2 = 47.0, P <0.001). When combined with the extrusion probability the cost of being in an urchin barren for an extended period of time is close to a 99% reduction in expected fecundity (if urchins that did not extrude eggs are considered to have fecundity of 0). Egg extrusion-size relationships and data are displayed in Figure D.2. Urchins from kelp forests that were induced to extrude eggs appeared to release the majority of their gametes. Inspection of the gonads showed very few eggs remaining and the gonad index was on average reduced to that of the pre-reproductive period (black dots, Figure D.1)

Impact of starvation or re-nourishment on urchin gonads

On average, healthy urchins that were then starved for four months had gonad indices indistinguishable from the mean gonad index of urchins in the Carpinteria barrens. In contrast the healthy urchins that were fed modest rations maintained a gonad index similar to individuals on their collection date (blue points versus grey points to which they connect, Figure D.3), though it was lower than that of the urchins freshly collected in December (last grey point versus blue points, Figure D.3).

Starved urchins that were fed modest rations required approximately several months to achieve a gonad index similar to the kelp forest urchins in the experiment, while those fed for two months showed only a small recovery in this time period.

Figures
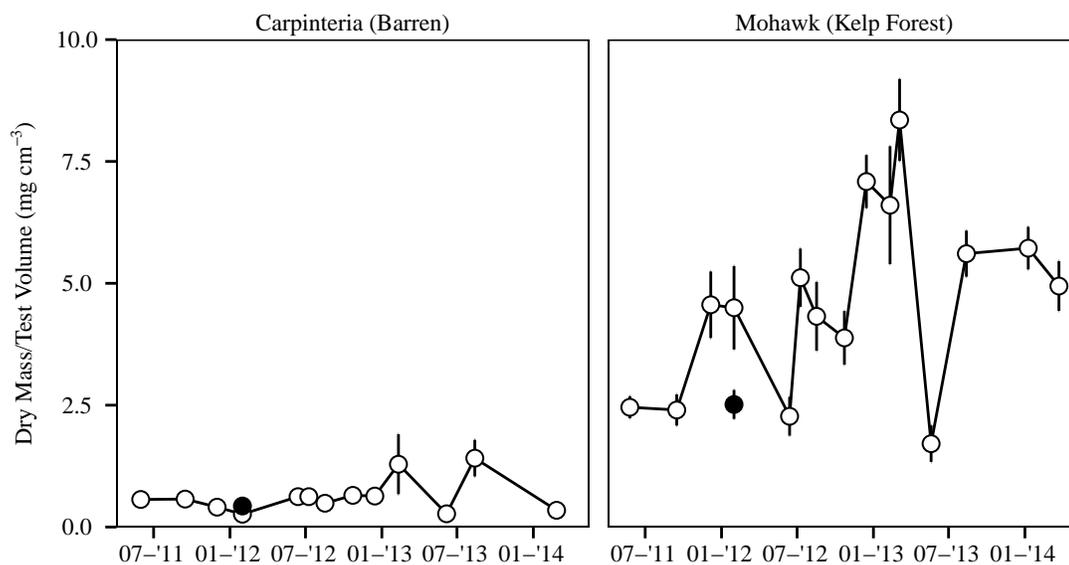
Figure D.1: Time series of gonad indices from barren and kelp forest urchins. The solid black points represent the spawned out gonads from Carpinteria and Mohawk, respectively, from the spawning experiment.
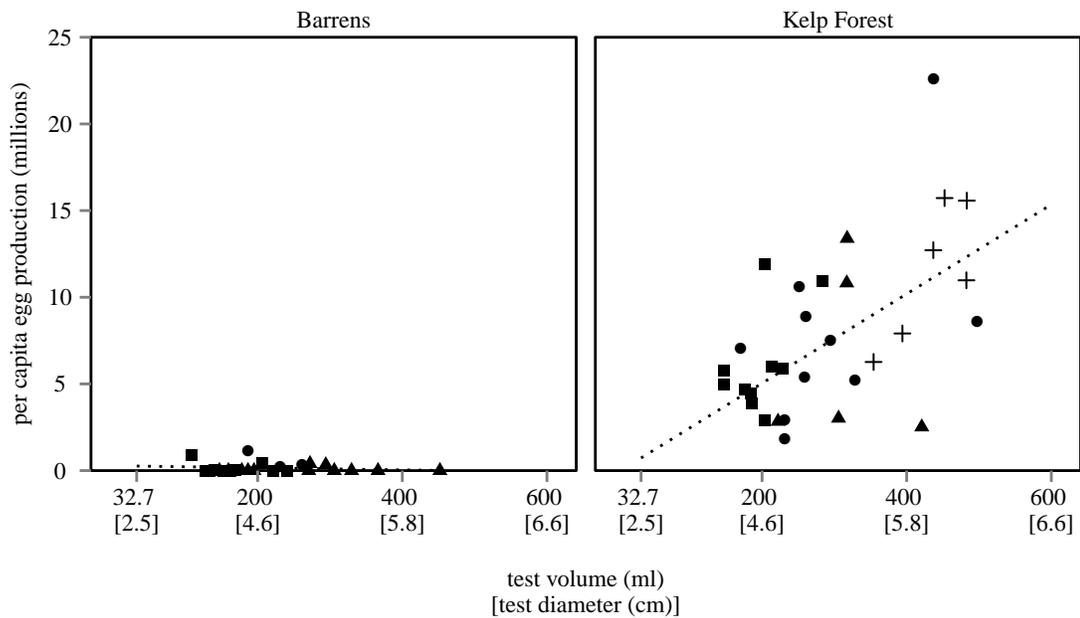
Figure D.2: Relationship between test volume (with associated diameter displayed in brackets) and estimated fecundity (in millions) for females from urchin barrens and kelp forests in January 2012. The dotted line represents the mean estimated relationship (fixed effects) for each reef state. The line in the barrens panel includes the estimated 33% probability of extruding eggs and is thus the product of this probability and the estimated relationship when eggs are extruded. Symbols denote the four different reefs, including Arroyo Quemado, Carpinteria, Isla Vista and Mohawk (note: Mohawk reef had no barren areas at the time of collection). Note that the x-intercept for for Mohawk is near 2.5 cm, the approximate minimum size for reproduction.
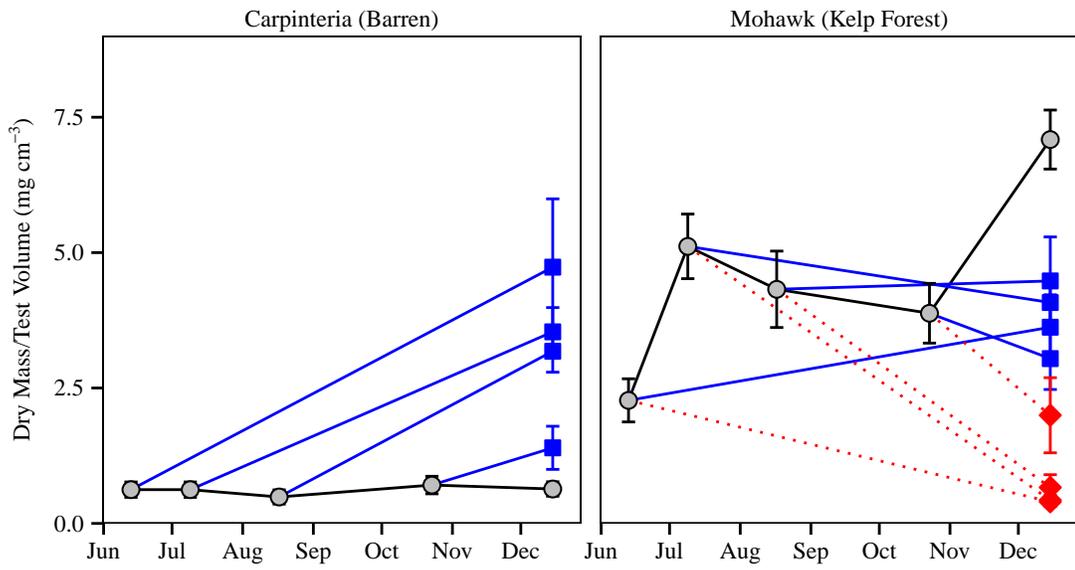
Figure D.3: Urchin gonad indices under different experimental treatments (blue = fed, red= starved) or from reference individuals dissected directly after collection. Lines connected to the grey points indicates the length of time for which the urchins were fed or starved (i.e. the grey point is the original reference on the day the urchins were collected and treatments initiated. The blue or red points indicated the final value at the end of the experiment when urchins were dissected.